UNCLASSIFIED

AD NUMBER
AD063446
CLASSIFICATION CHANGES

TO: **unclassified**

FROM: **confidential**

LIMITATION CHANGES

TO:

Approved for public release, distribution unlimited

FROM:

Distribution authorized to U.S. Gov't. agencies and their contractors; Administrative/Operational Use; 20 MAY 1955. Other requests shall be referred to Bureau of Naval Weapons, Washington, DC.

AUTHORITY

USNWL notice, 19 Jan 1971; USNWL notice, 19 Jan 1971

THIS PAGE IS UNCLASSIFIED

AD 63446

Armed Services Technical Information Agency

NPG Report No. 1351

NAVORD REPORT NO.1340

PREPARATION OF

ANTI-AIRCRAFT RANGE TABLE FOR

2.75 GUN-FIRED ROCKET T-132

U. S. NAVAL PROVING GROUND
DAHLGREN, VIRGINIA

55AA 24924

Copy No. 14

JUN 10 1955 Date 20 May 1955

CONFIDENTIAL

U. S. Naval Proving Ground
Dahlgren, Virginia

Preparation of

Anti-Aircraft Range Table for

2V75 Gun-Fired Rocket T-132

by

C. J. Cohen
D. R. Brown, Jr.
H. M. Lieberstein
Computation and Ballistics Department

APPROVED: J. F. BYRNE
            Captain, USN
            Commander, Naval Proving Ground

E. A. Ruckner

E. A. RUCKNER
Captain, USN
Ordnance Officer
By direction

CONFIDENTIAL

55AA   24924

CONTENTS

CONTENTS (Continued)

- -

1. ABSTRACT

The Naval Proving Ground was directed by the Bureau of Ordnance to prepare an interim anti-aircraft range table for the 2775 gun-fired rocket T-131 from data obtained by firing inert-loaded rounds designated T-132. This report contains a description of the firing program and measurement methods, together with a listing of firing data. It also contains a description of the ballistic analysis of the firing data employed in preparation of the anti-aircraft range table, which is included as an appendix.

Acceptable dispersion patterns were obtained for the rounds tested. This, along with other phenomena, indicated a consistency of performance that was exceptionally good considering previous experiences with other lots of T-132 ammunition. Excellent Sperry Doppler Radio Chronograph records were obtained, revealing spin and unexpected thrust characteristics. It was established that burning in flight is very progressive and is inconsistent with the relatively uniform burning observed in static tests.

In the analysis of firing data necessary to produce the range table, unconventional procedures were used to determine thrust acceleration as well as drag parameters. To allow for the effects of yaw during burning, some rigid body trajectories were integrated, subject to a rather comprehensive aerodynamic force system. The derivation of deflection and wind effects formulas used for the range table, exhibiting the assumptions necessary to obtain them, are also included in this report.

It is recommended that: (a) an appropriate drag function be obtained for use in future ballistic programs involving the T-132 rocket; (b) studies be undertaken to determine the causes of the difference between the static burning rate and the dynamic burning rate; (c) upon production of the service mount, several be sent to the Naval Proving Ground for measurement of jump at launch; and (d) in view of the difficulty encountered in observing the inherently small splash on water impact, live-loaded T-131 rounds or T-132 rounds loaded with spotting charges be used in future range table firings.

- -

2. FOREWORD

This is the final report on the preparation of an
Anti-Aircraft Range Table for the 2.75 Rocket T-132. The
project was requested by references (a) and (b) and was
carried out under Task Assignments NPG-Re3d-417-2-53,
NPG-Re3d-439-2-53 and NPG-B-2d-439-2-54. The firings upon
which the range table was based were conducted in the
period from 22 January to 6 March 1953. The anti-aircraft
range table, which is included in this report as Appen-
dix (G), was forwarded to the Bureau of Ordnance on 10 June
1953 by reference (c). Subsequently, air-to-air firing
tables were computed and transmitted to the Bureau of
Ordnance by reference (d).

Unconventional methods of ballistic analysis reported
herein were developed by a team consisting of C. J. Cohen,
W. E. Barnes, and H. M. Lieberstein.

The report in large part has been revised and edited
by C. H. Frick and J. E. Mulligan. It has been reviewed
for technical accuracy by:

        W. E. BARNES, Head, Ballistic and
                  Statistical Theory Branch
                Theory and Analysis Division
                Computation and Ballistics Department
        C. J. COHEN, Chief, Theory and Analysis Division
                Computation and Ballistics Department
        W. A. KEMPER, Chief, Ballistics Division
                Computation and Ballistics Department
        R. H. LYDDANE, Assistant Director of Research
        N. A. M. RIFFOLT, Director of Research

- -

3. INTRODUCTION

The 2¾75 rocket T-132 is an inert-loaded practice round for the 2¾75 HE rocket T-131. The T-131 rocket is a gun-fired, spin-stabilized rocket projectile designed for air-to-air, ground-to-air, and ground-to-ground firings. When ground fired, it has a maximum range of approximately 6000 yards. Both the T-131 and the T-132 rockets are fired from the 2¾75 Antomatic Rocket Launcher T-110. The launcher-missile system is capable of cyclic rates of approximately 900 rounds per minute. With a propellant temperature of 70°F, the muzzle velocity is approximately 1200 feet per second and the rocket is accelerated to about 2700 feet per second during a burning period of approximately 0.6 second. The spin is imparted by rifling with progressive twist in the launcher barrel and by the torque component of the thrust resulting from the cant of the two rocket motor nozzles.

The original projects for the design and development of the ammunition and the associated launcher were carried out by the Armour Research Foundation of the Illinois Institute of Technology. These development projects for the rocket and launcher are described in references (e) and (f), respectively. The development of the rocket propellant now being used was undertaken by the Thiokol Corporation.

During development of the missile, preliminary flight tests were conducted at Fort Sheridan, Illinois, and at Aberdeen Proving Ground. The purpose of these tests was to determine the feasibility of the various design proposals with regard to the structural strength of the rocket, the launching and ignition systems, and the propulsion characteristics. Provisional ballistic tables for aircraft firings were computed by the Ballistic Research Laboratories, Aberdeen Proving Ground, in March 1949 and revised in February 1952.

- -

The object of this project was to prepare an anti-
aircraft range table for the 2"75 rocket T-132 to be used
as an interim anti-aircraft range table for the 2"75 rocket
T-131. Work done under the project included performing the
necessary firings, ballistic measurements, ballistic
analyses, and computations.

4. DESCRIPTION OF MATERIAL

The 2"75 rocket T-132 and the 2"75 HE rocket T-131 are
identical except that the T-131 round has a live-loaded
head and fuze whereas the T-132 round has an inert-loaded
head and a dummy fuze. Figure 1, Appendix (A), is a photo-
graph of a T-132 round with the cartridge case and igniter
tube removed; this particular round was from the ammunition
lot used for the range table firings. Table 1, Appen-
dix (B), contains representative physical data on the
rounds fired.

The ammunition components of the rounds used for the
range table firings are identified below:

	Desig-nation	Lot No.	Drawing No.
Assembled Ammunition	T-132	PA-E-11499	P-8206-8B
Cartridge Case		111	23D-1-200
Head, Inert Loaded		PA-E-11107 PA-E-10073	P-81909B
Igniter	T-25	PA-E-11226	P-82070
Fuse, Dummy	M50B1	None	72-5-4
Rocket Propellant (see reference (g))	T-10E1	Mix H-1050 loaded by Thiokol Corporation	
Launcher Propelling Charge	T-302	PA-E-715	P-82071
Gas Seal		2	23D-1-201

2

- -

The cartridge case and gas seal were manufactured by Reo Motors; the head, igniter, fuze, and launcher propelling charge were manufactured by Picatinny Arsenal. The rocket propellant was manufactured by Thiokol Corporation. The components listed above were manufactured in 1952 and were assembled by Picatinny Arsenal in December 1952.

5. DESCRIPTION OF TEST EQUIPMENT

a. Launcher and Mounts

All rounds in the range table program were fired singly from a 2"75 Automatic Rocket Launcher T-110-E2B. Although this is an aircraft type launcher, it was used because the anti-aircraft launcher type T-110-E2C was unavailable at the Naval Proving Ground at the time of the range table firings. The two launcher types have identical recoilless barrels.

The firings were conducted in two phases. The firings of the first phase were conducted at a low elevation angle to establish the trajectory parameters during burning; the firings of the second phase were conducted at higher angles to obtain data at longer times of flight. For the first phase, the launcher was installed on a rigid, box type mount. A fixed angle of elevation was obtained by means of wedge-shaped mounting shims. The second phase of the firings was conducted with the launcher installed on a modified 4-inch gun mount as shown in Figure 2, Appendix A. The launcher could be trained and elevated by means of the handwheels; because of the backlash in the gear trains and the non-rigidity of the mount, however, it was not possible to assure a fixed launching angle during firings. (This did not hinder the determination of drag parameters, since data on distance versus time rather than distance versus launcher angle were employed.) It should be noted in Figure 2 that the launcher bore axis is above the trunnion axis of the mount, thus creating a source of positive vertical jump; such jump was observed in the second phase of the firings.

The firing current for all rounds was supplied by a 16 microfarad condenser charged to 250 volts. The pressure bleed-off system for automatic cycling of the launcher loading sprocket was connected in such a manner that rapid fire service conditions were approximated. The launcher was loaded, however, with only one round at a time; therefore, no work was

- -

done by the launcher sprocket other than in ejecting the
case of the round fired. While no direct measurements of
the effects of this loading difference have been made, it
is believed that the effect on the initial conditions of
the rocket flight is insignificant.

b.   **Ballistic Instrumentation**

     The following items of equipment were used for ballistic
measurements (see Figure 3, Appendix A, for a schematic layout
of the cameras and the Sperry Radio Doppler Chronograph):

     (1) A Sperry Radio Doppler Chronograph provided
measurements of velocity and slant range versus time on a
majority of the rounds fired. Velocity measurements were
obtained over intervals of approximately 75 feet in range
from about 0.05 second beyond the muzzle to about 0.3 second
beyond burn-out (or about 1800 feet in range). The antenna
of the equipment was located as close as practicable to the
launcher in order to minimize the geometric errors incurred
in measurements of the rocket motion. A drum camera used
with this instrument recorded the Doppler signal and also t
firing signal marking the initial current flow to the prope
ling charge igniter; this firing signal was used as a time
reference. A photocell sky screen was located on the line
fire, approximately 100 feet down range from the muzzle, in
order to detect the passage of the missile and to provide a
reference value of range.

     (2) A 35mm Fastax camera equipped with a lens of 35mm
focal length and operated at a rate of approximately 3000
frames per second was located 12 feet down range and 50 feet
off range. It photographed the first 25 feet of rocket flight.
The optic axis of the camera was horizontal and perpendicular
to the line of fire. The actual frame rate of the camera was
determined by means of a thousand-cycle pulse recorded on the
edge of the film. Two reference targets in the field of view
of the camera and in the plane of fire served as a scale.

     (3) A Bowen camera equipped with a lens of 12-inch focal
length and operated at a rate of 60 frames per second was
located 1100 feet down range and 850 feet off range from the
launcher. It was used during the first phase of the range
table firings to photograph the rocket flight at the end of

- -

burning. The camera was aimed so that its optic axis was at a known elevation angle and perpendicular to the line of fire. Reference targets erected in the field of view of the camera defined the horizontal and served as references for measurements of range.

(4) A 35mm Mitchell chronograph camera equipped with a lens of 6-inch focal length and operated at a rate of 100 frames per second was located 1100 feet down range and 600 feet off range from the launcher. It was used during the second phase of firings to photograph the rocket at the end of burning. The camera was aimed perpendicularly to the line of fire and was elevated to a known angle by means of a gunner's quadrant.

(5) Three 35mm Mitchell chronograph cameras, one equipped with a lens of 10-inch focal length and two with lenses of 6-inch focal length, were operated at a rate of 100 frames per second. The camera with the 10-inch focal length lens was located 200 feet off range and 50 feet behind the launcher, and the two cameras with 6-inch focal length lenses were located at down range stations. All three cameras photographed the impact splashes; in addition, the camera with 10-inch focal length lens photographed a reference target in the field of view.

(6) A Bowen camera equipped with a lens of 12-inch focal length and operated at a rate of 90 frames per second was located at a down range station. It was used to photograph the impact splashes and a reference target. The camera was used at a different location in the second phase of the firings.

(7) An Askania cine-theodolite equipped with a lens of 60cm focal length and operated at a rate of four pictures per second was located at a down range station. It was used in conjunction with the above cameras to determine the impact locations.

(8) Associated equipment, including radio and electronic equipment and lamps for registering master timing impulses on the Mitchell and Bowen camera film, was used. The timing and firing signals were recorded on an oscillogram, thereby making it possible to reference the camera time measurements to the origin of the trajectory.

- -

(9) A modified Gunner's Quadrant Mk 3 was used to
measure the angle of elevation of the launcher barrel. This
modified quadrant has two parallel cylinders, each about
eight inches long and approximately three-quarters of an
inch in diameter, attached to the base to ensure a more
accurate fit of the quadrant on a cylindrical barrel.

(10) An optical boresight tool from an Aircraft Machine
Gun Boresight Kit Mk 1 was used to determine the line of
fire. A 2⅞75 bore adapter, manufactured by the Naval Gun
Factory (piece sketches 507398-A-4, 230083-1, and 230083-2)
permits the use of this boresight tool with the 2⅞75 Auto-
matic Rocket Launchers T-110-E2B and T-110-E2C.

(11) A test stand of special design was constructed for
use in local static firing tests of two rounds. The rocket
was mounted vertically downward in the test stand and the
thrust was directed against a strain gauge plate. In order
to mount the rocket in the test stand, the nose fuse was
replaced by a cylindrical adapter about six inches long and
one inch in diameter. The adapter was fitted into a sup-
porting block which permitted movement in the vertical direc-
tion only. Rotation about the long axis of the rocket was
restrained by an arm welded perpendicularly to the adapter;
the arm bore against a second strain gauge plate, thereby
providing a measure of the rocket motor torque.

6. FIRING AND MEASUREMENTS PROCEDURE

a. Description of Firings

(1) Range Table Firings

Ninety-eight rounds from a single ammunition lot
were fired to obtain the information needed for the prepa-
ration of the range table. Data on the number of rounds
fired at each angle of elevation and propellant temperature
are contained in Table 2, Appendix B. In addition, five
rounds were fired to obtain information on the jump of the
launcher and two rounds were fired for the determination of
spin.

- -

The firings were conducted at three rocket propellant temperatures: 30, 70, and 110°F. The rounds were conditioned at the desired temperature, with a tolerance of about 3°F, for at least 48 hours prior to firing. Since only one round at a time was removed from the temperature conditioning facilities, the time of exposure to ambient temperatures was minimized and was generally less than three minutes.

A wind measuring set was placed about 100 feet down range and 20 feet off range from the muzzle, and about 10 feet above the ground to record the direction and velocity of the surface wind during burning of the rocket. In addition, the surface pressure and temperature (dry and wet bulb), which are required for the determination of surface density, were recorded every thirty minutes. Measurements of wind and density structures aloft were obtained hourly from pilot balloon and radiosonde observations. No rounds were fired when the surface winds were in excess of 13 knots, most rounds being fired with surface winds of less than 9 knots.

Individual values of rocket weights could not be obtained directly since to do so would have required disassembly of the rocket from the cartridge case. However, each assembled round was weighed prior to firing and each cartridge case with igniter tube was weighed after firing; the difference between these two weights equaled the weight of the unburnt rocket and the propelling charge. The weight of the propelling charge (6-1/2 ounces) was included in information supplied with the ammunition; subtracting this value left the weight of the unburnt rocket. To obtain the weight of the burnt rocket, the weight of the rocket propellant, including the inhibitor, was obtained from information in reference (h) and subtracted from the weight of the unburnt rocket.

During the first phase of the range table firings, a launcher mount with a fixed angle of elevation was used. The desired angle of elevation was set by means of the gunner's quadrant when the launcher was installed. During the second phase of the range table firings, the angles of elevation were set by means of the quadrant placed on the launcher barrel just forward of the receiver. This procedure, which could be used since the barrel is not tapered, minimized the deflection of the barrel due to the weight of the quadrant.

- -

The angles were checked by a boresight and differential leveling technique, in which the difference in heights between two points on the boresight line, one at the muzzle and the other at a known distance from it, was used to compute the angle of elevation. For both phases of the firings, the bore axis was set in the horizontal direction by means of the boresight tool and the 2475 bore adapter.

The launcher barrel was cleaned and lubricated after each day's firing. It was the practice to fire a slug round (T-217) prior to the range table firings each day in order to clear the bore of lubricant and to approximate the service condition of the barrel. The existence of an effect on the muzzle velocity of a round fired from an oiled barrel was reported in reference (e).

The firings of the first phase were conducted primarily to establish the trajectory characteristics and parameters during burning and to obtain ranging data at a short time of flight. A launcher elevation of 1°30' was used for the firings. Since the muzzle of the launcher was approximately 24 feet above the impact point, a time of flight of about four seconds was obtained. Eleven rounds were fired at a propellant temperature of 70°F, ten rounds at 30°F, and ten rounds at 110°F. Measurements of velocity and slant range versus time during the burning period were obtained by means of the Sperry Radio Doppler Chronograph. The velocity of the rocket at the muzzle was determined photographically, as were the time and position of impact. During this phase of the firings, measurements of trajectory angle in the vertical plane at the end of burning were also obtained photographically. The low angle of fire was particularly convenient for these measurements.

The purpose of the second phase of the firings, consisting of 67 rounds, was to obtain ranging data at times of flight longer than those of the first phase, and to determine the free flight ballistic coefficient of the rocket. The launcher elevations used were 1°30', 2°45', 5°30', and 10°00'; the times of flight corresponding to these launcher elevations were approximately 4, 8, 12, and 16 seconds, respectively.

- -

The propellant temperatures used were 30, 70, and 110°F; however, a greater number of rounds were fired at 70°F than at either of the other temperatures (see Table 2, Appendix B). The types of data obtained in this phase of the firings were the same as those obtained in the first phase, except that measurements of rocket height rather than of trajectory angle at the end of burning were obtained.

(2) Launcher Jump Test

The ranges and times of flight to impact and rocket heights measured at the end of burning during the second phase of the firings, with the launcher installed on the modified 4-inch gun mount, were greater than had been expected. It was considered desirable to investigate the possibility of the existence of launcher jump since the discrepancies could be explained if the effective launcher angle, in the vertical plane, was approximately one degree greater than that preset using the gunner's quadrant. In this investigation it was necessary to determine the rocket coordinates and the direction of the rocket velocity at the end of burning, and to determine whether the magnitude and direction of the jump were consistent. For this purpose two jump cards were erected on the line of fire and perpendicular to it, in order to bracket the end of burning. These jump cards, with the centers of the cards about the same height as the launcher muzzle, were located 850 feet and 1300 feet down range from the muzzle. Negative launcher angles were selected prior to firing on the basis of an estimated one degree of jump, as indicated by the results of the range table firings. Measurements were made on five rounds, all of which were fired at a propellant temperature of 70°F. Measurements of the surface wind at the time of firing of each round were made in order to correct the target impact coordinates to the standard condition of no wind.

(3) Static Firing Test

Two rounds, which had been conditioned at a temperature of 70°F, were fired statically in a test stand in order to provide measures of rocket thrust, torque, and impulse for comparison with values computed with the use of the in-flight accelerations derived from the velocity records. Both rounds

- -

contained propellant from Mix H-1050, but only one round was
from the range table ammunition lot. The outputs of the
strain gauges of the test stand, together with a timing sig-
nal, were recorded on an oscillogram. Ignition of the pro-
pellant grain was accomplished by directing an oxy-acetylene
torch into one of the nozzles, the seals of both nozzles
having been removed prior to firing.

b. Reduction of Test Data

(1) Muzzle Velocity

Muzzle velocities were determined for a total of
17 rounds by means of the Fastax camera installation de-
scribed above. Four of the rounds had propellant tempera-
tures at 30°F, nine rounds at 70°F, and four rounds at 110°F.
Although camera records for a considerably larger number of
rounds were available, muzzle velocities were calculated only
for the number of rounds needed to determine the burning
period parameters for the three temperatures. Individual
values of velocity are given in Table 3, Appendix B. It is
estimated that the computed velocities are accurate to within
two feet per second.

(2) Velocity and Slant Range During Burning

Measurements of radial velocity and slant range
versus time during burning and for a fraction of a second
after burning, were obtained from the Sperry Radio Doppler
Chronograph records. Individual values of maximum velocity
of the rounds used in the ballistic analysis and the corre-
sponding times and slant ranges are contained in Table 4,
Appendix B.

(3) Trajectory Coordinates and Angle at Burnout

The ballistic analysis required that measurements
be made of the trajectory angle and trajectory drop at the
end of burning resulting from gravity, thrust, and aerody-
namic forces. Trajectory angle measurements were made only
on the firings conducted at an elevation angle of 1°30' by
means of a Bowen camera. Measurements were made on four
rounds fired with propellant temperatures at 70°F, three
rounds at 30°F, and three rounds at 110°F. The individual

- -

values of trajectory angle computed from these measurements
are given in Table 5, Appendix B. It is estimated that the
angles obtained are accurate to within 0.5 minute.

For firings at elevation angles greater than 1°30',
the height of the rocket near burnout was obtained from
photographs taken by a Mitchell camera.

(4) Range and Deflection

The ranges and deflections of the rockets at impact
were computed using information from the photographs of the
impacts. The individual values of the uncorrected ranges and
deflections used for the range table computations are listed
in Table 6, Appendix B. It is estimated that these values
are accurate to within two yards.

(5) Time of Flight

Measurements of times of flight were obtained from
the records of the chronograph cameras which photographed the
impact splashes and the oscillograph which recorded the
firing signals and the radio-transmitted timing signals. The
individual values of the uncorrected times of flight used for
the range table computations are also listed in Table 6,
Appendix B. It is estimated that these values are accurate
to within 0.01 second.

(6) Spin

A knowledge of the spin during burning was required
for the integration of rigid-body trajectories. At the muzzle,
the spin is determined from the known twist of the rifling and
the muzzle velocity, zero slippage being assumed. Extensive
firings to measure the spin of the rocket during burning were
found unnecessary since two independent measurements of the
spin were readily available from the records of instruments
used for other measurements during the tests.

One source of measurement of spin was the oscillo-
gram of the drum camera used with the Sperry Radio Doppler
Chronograph, on which was recorded the Doppler signal. The
amplitude of the Doppler signal was observed to be modulated
both during and after burning without discontinuity. The

- -

frequency of this modulation was approximately twice the
expected frequency of the rocket rotation. Since the wave
length (2.4 inches) of the radiation is comparable with the
diameter of the rocket base (2.75 inches), and since this
radiation is largely plane polarized, the reflectivity of
the rocket base is changed as that diameter of the base
containing the two nozzles is rotated with respect to the
plane of polarization. The rotation of the rocket about its
longitudinal axis is, therefore, considered to be the cause
of the observed modulation of the amplitude of the Doppler
signal. In addition to the modulation as a result of the
spin described above, a second amplitude modulation of the
Doppler signal was observed which had a frequency in close
agreement with the theoretical frequency of nutation of the
rocket.

        The other source of measurement of spin was the
film records of the Bowen and Mitchell cameras which photo-
graphed the rocket trajectory near the end of burning.
Since the vertical width of the trail of propellant gases
is also modulated as a result of the rotation of the diameter
containing the two nozzles, the distance traveled between
alternate maxima of the trail width corresponds to one revo-
lution of the rocket. This distance was obtained from com-
parator measurements on the film and converted to travel in
feet.

        The two methods described above gave results which
were in excellent agreement. Figure 4, Appendix B, is a
print of portions of the test records showing the modulation
of the amplitude of the Doppler signal and the modulation of
the width of the propellant gas trail.

7. BALLISTIC ANALYSIS

Introduction

        The basic trajectories for the T-132 rocket were computed
using a mathematical model in which perfect trailing is
assumed. The methods used in obtaining parameters for this
mathematical model, making allowances for deviations from
perfect trailing, and determining the effects of wind are the
principal subjects of this section. Various unconventional
techniques of ballistic analysis employed in this work require

- -

detailed discussion. A more concise summary of numerical
results can be found in section 8. A retrospective dis-
cussion of these techniques and the conclusions reached are
contained in section 9, Discussion and Conclusions. Organi-
zation of the Ballistic Analysis Section is as follows:

a.   The Perfect Trailing Model

b.   Thrust Parameters and Mozzle Velocity
      (1)   Description of Thrust Parameters
      (2)   Method of Optimizing Thrust Parameters
      (3)   Muzzle Velocity and Treatment of Non-Standard
            Propellant Temperatures

c.   Drag Parameters
      (1)   After Burning
      (2)   During Burning

d.   Motion During Burning with Yaw
      (1)   The Yawing Model of Motion
      (2)   Thrust as a Function of Time
      (3)   Deflection of Velocity Vector at End of Burning

e.   Range Table Formulas with Allowances for Yawing Motion
      (1)   Allowances for Yaw with No Wind
            (a)   Drift
            (b)   Effect of Yaw on Range and Altitude
      (2)   Effects of Range Wind
            (a)   Effect on Range and Altitude
            (b)   Effect on Deflection
      (3)   Effects of Cross Wind
            (a)   Effect on Deflection
            (b)   Effect on Range and Altitude
      (4)   Range Table Allowance for Non-Uniform Wind

f.   Dispersion

g.   Jump

- -

a.   The Perfect Trailing Model

The idealization in the perfect trailing mathematical model of motion is the assumption that there is no yaw and, further, that the thrust, the aerodynamic force, and the velocity relative to the air mass are aligned. Initial alignment, i.e., alignment at launch, is accomplished in this model by supposing that the axis of the round and the direction of application of the thrust are changed so as to lie along the direction of the actual initial velocity relative to the air mass rather than along the launcher line.

The general equations of motion for this model are:

$$(7.01) \qquad \ddot{x} = (\frac{A}{v_a} - E_a)(\dot{x} - w_x) + a_y\dot{z} - a_z\dot{y}$$

$$(7.02) \qquad \ddot{y} = (\frac{A}{v_a} - E_a)\dot{y} - g + a_z\dot{x} - a_x\dot{z}$$

$$(7.03) \qquad \ddot{z} = (\frac{A}{v_a} - E_a)(\dot{z} - w_z) + a_x\dot{y} - a_y\dot{x}$$

where

x is horizontal range (yds),

w_x is range wind (yds/sec),

w_s is cross wind (yds/sec),

y is altitude (yds),

s is deflection (yds),

w_s is cross wind (yds/sec),

A is acceleration (yds/sec^2) resulting from thrust,

- -

v_a is velocity (yds/sec) of the rocket measured with respect to the air mass,

$\dot{x}$, $\dot{y}$, $\dot{z}$ are the components (yds/sec) of the velocity of the rocket with respect to the ground,

g is acceleration resulting from gravity (yds/sec^2),

$\ddot{x}$, $\ddot{y}$, $\ddot{z}$ are the components (yds/sec^2) of the acceleration of the rocket with respect to the ground, and

$$E_a = \frac{\rho g v_a K_D(M_a)}{C}$$, in which ρg is atmospheric density (lbs wt/yd-in^2),

$K_D(M_a)$ is the drag coefficient for the projectile type 6.1 expressed as a function of Mach number, M_a, measured with respect to the air mass, and C is the ballistic coefficient (lbs/in^2) with respect to the drag function for projectile type 6.1.

The terms containing a_x, a_y, and a_z are Coriolis terms and the a's are minus twice the components of the earth's angular velocity. The components depend on the latitude and line of fire. Specifically,

$$a_x = - 1.4584(10^{-4})\cos L \cos \overline{LOF}$$

$$a_y = - 1.4584(10^{-4})\sin L$$

$$a_z = 1.4584(10^{-4})\cos L \sin \overline{LOF}$$

These formulas give a_x, a_y, a_z in radians/second. In them L represents the latitude and $\overline{LOF}$ represents the angle between true north and the line of fire measured in a clockwise direction.

The basic trajectories for range tables are integrated under the conditions of no wind and no Coriolis force and with atmospheric density and velocity of sound specified by arbitrary, so-called "standard" functions of altitude. The general

- -

equations then reduce to

(7.04)
$$\ddot{x} = (\frac{A}{v} - E)\dot{x}$$

(7.05)
$$\ddot{y} = (\frac{A}{v} - E)\dot{y} - g$$

(7.06)
$$\ddot{z} = 0$$

with $\rho = \rho_0 e^{-hy}$, $\rho_0 = 0.7513(\frac{3}{144})$lbs/yd-in^2, $h = 0.0000947469$

per yd, and the velocity of sound = 1120 $\sqrt{1 - \alpha y}$ ft/sec,

$\alpha = \frac{0.0065}{288}(\frac{36}{39.37})$ per yd. The representation of the density

and velocity of sound specified above is the one which defines
what is known as the present Navy ballistic standard atmosphere.

b. __Thrust Parameters and Muzzle Velocity__

   (1) Description of Thrust Parameters

        A constant acceleration during burning was found to
be unrealistic. Doppler records established that the accelera-
tion versus time curve rises almost linearly with time to a
peak near burn-out, and then the acceleration decreases very
rapidly. The corresponding thrust was obtained from these
records rather precisely as a function of time for use in evalu-
ating the effects of yaw during burning. The thrust data are
described below in section 7d(2). For the perfect trailing
model, however, an acceleration of the simple form,

$$A = C_1 t + C_2 \text{ for } t \leq t_b$$

and

$$A = 0 \qquad \text{for } t > t_b$$

was chosen. The values of C_1, C_2, and t_b were determined for

- -

each propellant temperature, 30, 70, and 110°F, so as to make
the calculated radial velocity and slant range at some selected
time, t_c, beyond the end of burning, match the observed radial
velocity and slant range at t_c, as determined from the Doppler
records. The time t_c is measured from ignition. In the two
tables below are listed, for various propellant temperatures
and days of firing, the values at time t_c of

$\overline{R}$, mean slant range (ft),

σ_R, standard deviation of an individual measurement of
slant range (ft),

$\overline{\dot{R}}$, mean radial velocity (ft/sec), and

$\sigma_{\dot{R}}$, standard deviation of an individual measurement of
radial velocity (ft/sec).

Doppler Data at Time t_c

Slant Range and Dispersion in Slant Range

| | Propellant Temperature | | | | | |
| | 30°F (t_c = .80) | | 70°F (t_c = .88) | | 110°F (t_c = .92) | |
Date of Fire	$\overline{R}$(ft)	σ_R(ft)	$\overline{R}$(ft)	σ_R(ft)	$\overline{R}$(ft)	σ_R(ft)
2-16-53			1842	39	1750	18
2-18-53			1812	23		
2-19-53	1819	18				

Radial Velocity and Dispersion in Radial Velocity

| | Propellant Temperature | | | | | |
| | 30°F (t_c = .80) | | 70°F (t_c = .88) | | 110°F (t_c = .92) | |
Date of Fire	$\overline{\dot{R}}$(ft/sec)	$\sigma_{\dot{R}}$(ft/sec)	$\overline{\dot{R}}$(ft/sec)	$\sigma_{\dot{R}}$(ft/sec)	$\overline{\dot{R}}$(ft/sec)	$\sigma_{\dot{R}}$(ft/sec)
2-16-53			2445	22	2538	12
2-18-53			2454	6		
2-19-53	2371	25				

- -

(2) Method of Optimizing Thrust Parameters

The rounds fired at each propellant temperature were grouped according to the day of firing (same weather conditions) and angle of elevation, and within one group a first approximation to the linear acceleration was statistically obtained. The intercept with the t axis of the function $C_1 t + C_2$ was obtained from this analysis and fixed. It was necessary then to evaluate only C_1 (slope) and t_b.

For this purpose a grid of three values of C_1 and three values of t_b (bracketing first approximations) were chosen. Trajectories (one for each round) using actual atmospheric conditions and actual rocket weights were computed for each combination of the parameters C_1, C_2, and t_b. In these integrations the average initial velocity for all rounds fired at the given propellant temperature, not the average initial velocity of the group, was used. Interpolation produced, for each round, a locus of points, (t_b, C_1), for which the calculated radial velocity was matched with the radial velocity observed with the Doppler equipment. Another locus was obtained for which the calculated slant range was matched with the Doppler observation of slant range. Intersection of these loci produced the desired value of t_b and C_1 for each round. For the analysis of a typical group of rounds with a 70°F propellant temperature see Figure 5, Appendix C.

A group to group dispersion of points (t_b, C_1) occurred, presumably resulting from dispersion in ammunition and errors in measurements. This dispersion pattern, for 70°F propellant temperature, is given in Figure 6, Appendix C. The computed statistical range of the quantity t_b was approximately that of the range of the time of peak velocity as read from the Doppler data. Average values of t_b and C_1 were chosen. The values of acceleration (yd/sec^2) used were:

30°F propellant temperature, $A = 3293t$, $0 \leq t \leq 0.6147$

70°F propellant temperature, $A = 2302t + 345.3$,
$$0 \leq t \leq 0.6037$$

110°F propellant temperature, $A = 2739t + 410.8$,
$$0 \leq t \leq 0.5450$$

CONFIDENTIAL
- -

For the reciprocal of the ballistic coefficient a value of
1.94 was used during burning (see section 7c(2)). (A measure
of time of burning more generally used than the above opti-
mized values is time to maximum velocity, the observed values
of which are given in Table 4, Appendix B.)

The use of these acceleration parameters resulted
in computed trajectories having range and radial velocity
after burning, at the time, t_c, from ignition, which agree
with the values observed. However, the parameters are not
realistic representations of accelerations and care must be
exercised in their use. In particular, trajectories were
integrated assuming the round leaves the muzzle at the time
of ignition. Actually there is an interval of approximately
0.013 second between the time of ignition and the instant the
round leaves the muzzle. The effect, then, is the absorption
in the acceleration parameters of the delay between ignition
and ejection. In the consideration of air-to-air firings,
where the drag is significantly different from that at ground
level, the above acceleration parameters may prove inaccurate.
In fact, a redetermination of the acceleration parameters was
made for the later computation of the air-to-air trajectory
tables for the T-132 rocket.

(3) Muzzle Velocity and Treatment of Non-Standard
Propellant Temperatures

The average of the observed muzzle velocities, $\bar{v}_o$,
and the standard deviation of an individual measurement of
muzzle velocity, σ_{v_o}, are given for each propellant tempera-
ture in the following table:

Muzzle Velocity and Dispersion in Muzzle Velocity

Propellant Temperature	$\bar{v}_o$ (yd/sec)	σ_{v_o} (yd/sec)
30°F	$\dfrac{1112}{3}$	$\dfrac{13.7}{3}$
70°F	$\dfrac{1188}{3}$	$\dfrac{8.7}{3}$
110°F	$\dfrac{1234}{3}$	$\dfrac{5.8}{3}$

CONFIDENTIAL

- -

The preceding values of average muzzle velocities were used in computing the required anti-aircraft range table. The individual observed values are given in Table 3, Appendix B.

The standard propellant temperature is 70°F. An attempt was made to simplify the fire control problem by treating non-standard propellant temperatures as perturbations in the muzzle velocity for the 70°F propellant. It was felt at the outset of this experimental calculation that such a procedure would be acceptable only if an increment in muzzle velocity of the same magnitude as required to pass from 70°F propellant to 110°F propellant could be used to pass from the 70°F propellant to the 30°F propellant. The best such increment was $\Delta v_o = \pm 71.6$ ft/sec for $\pm 40°$F change in propellant temperature. This value was determined by minimizing the sums of the squares of the departures, ε , of x and y (which were computed using the 70°F propellant parameters except that v_o was replaced by $v_o \pm \Delta v_o$) from the 30°F and the 110°F range table values ($\varphi \leq t \leq 20$ sec). The resulting values of ε are displayed below, ε being positive when the value based on $v_o \pm \Delta v_o$ is in excess of the 30 or 110°F range table value.

Propellant Temperature

t (sec)	30°F		110°F	
	$\varepsilon(x)$ (yds)	$\varepsilon(y)$ (yds)	$\varepsilon(x)$ (yds)	$\varepsilon(y)$ (yds)
1	22.3	2.3	-14.6	- 1.3
2	18.3	2.6	- 5.8	- 1.0
3	15.3	2.9	0.7	- 0.5
4	13.5	3.1	3.9	- 0.4
5	12.5	3.3	5.7	- 0.2
6	11.6	3.5	7.2	- 0.2
7	11.1	3.6	8.3	0
8	10.6	3.6	9.3	0.1
9	10.0	3.8	10.2	0.3
10	9.6	3.8	11.0	0.4
11	9.3	4.0	11.5	0.5
12	9.1	4.0	12.1	0.6
13	8.8	4.1	12.5	0.8

- -

Propellant Temperature (Continued)

t	30°F		110°F	
(sec)	$\varepsilon(x)$ (yds)	$\varepsilon(y)$ (yds)	$\varepsilon(x)$ (yds)	$\varepsilon(y)$ (yds)
14	8.6	4.1	13.0	0.9
15	8.5	4.1	13.4	1.0
16	8.3	4.1	13.8	1.1
17	8.2	4.1	14.0	1.3
18	8.0	4.2	14.4	1.3
19	7.9	4.2	14.7	1.5
20	7.9	4.2	14.9	1.6

Weighting the ε's for the first six seconds in time of flight twenty to one over the ε's for times of flight of seven to twenty seconds produced a value of $\Delta v_0 = \pm 78.1$ ft/sec for $\pm 40°F$ change in propellant temperature. The errors obtained using this value of Δv_0 are tabulated below.

Propellant Temperature

t	30°F		110°F	
(sec)	$\varepsilon(x)$ (yds)	$\varepsilon(y)$ (yds)	$\varepsilon(x)$ (yds)	$\varepsilon(y)$ (yds)
1	20.4	2.2	-12.7	- 1.2
2	14.7	2.3	- 2.2	- .7
3	10.6	2.5	5.4	- .1
4	8.1	2.6	9.3	0.1
5	6.8	2.7	11.4	0.4
6	5.7	2.8	13.1	0.5
7	4.9	2.9	14.5	0.7
8	4.3	2.9	15.6	0.8
9	3.6	3.0	16.6	1.1
10	3.1	3.0	17.5	1.2
11	2.6	3.1	18.2	1.4
12	2.3	3.1	18.9	1.5
13	1.9	3.2	19.4	1.7
14	1.7	3.1	19.9	1.9
15	1.4	3.1	20.5	2.0

- -

Propellant Temperature (Continued)

t (sec)	30°F		110°F	
	$\varepsilon(x)$ (yds)	$\varepsilon(y)$ (yds)	$\varepsilon(x)$ (yds)	$\varepsilon(y)$ (yds)
16	1.2	3.0	20.9	2.2
17	1.1	3.1	21.2	2.3
18	.8	3.1	21.6	2.5
19	.6	3.1	22.0	2.6
20	.5	3.0	22.3	2.8

In view of the large size of these errors, it was considered advisable to produce separate range tables for the 30 and 110°F propellant temperatures.

c.   Drag Parameters

(1)   After Burning

A ballistic coefficient, C, relative to the drag function $G_{6.1}$ was computed for the after burning period using the formulation for a ballistic coefficient for closest approach as given in reference (i), paragraph 9(a). The value obtained was

$$\gamma = \frac{1}{C} = 2.33$$

However, the pattern of discrepancies between the calculated range to impact time using $\gamma = 2.33$ and the observed range to impact time (as obtained by the Askania cine-theodolites, Bowen camera, Mitchell cameras, etc., and for non-standard atmospheric conditions and variations in the weights of the rounds before burning) was unacceptably large; the values are tabulated below.

φ	t (sec)	ε (yds)	Estimated per cent change in ballistic coefficient necessary to match observed ranges
1°30'	4.0	53	7.6
2°45'	7.5	33	2.6
5°30'	11.3	- 82	- 4.8
10°00'	15.4	-226	-10.3

- -

In the preceding table

$\varepsilon = \overline{R} - \overline{R}(2.33),$

$\overline{R}$ = average observed range corrected for non-standard
atmospheric conditions and variations in
weight, and

$\overline{R}(2.33)$ = calculated range, using $\gamma = 2.33$ and
φ = angle of elevation of launcher.

The last column of the preceding table indicates
a definite monotonic variation of ballistic coefficient with
time of flight. While such a wide range of variation had
not previously been observed, variation of ballistic coeffi-
cient with time of flight for other missiles has led to the
development at the Naval Proving Ground of methods for
resolving this type of difficulty. Specifically, where i is
the form factor, mg is weight in pounds, and d is diameter
in inches, the retardation function, E (see section 7a), can
be written as

$$(7.07) \qquad E = \frac{\rho g v K_D(M)}{C} = \frac{\rho g v K_D(M)}{\dfrac{mg}{id^2}} = \rho v \, \frac{d^2}{m} \, (i K_D(M))$$

Ordinarily, the form factor is a multiplicative constant, the
purpose of which is to generate the drag coefficient of a
specific projectile from the drag coefficient for a projectile
type. However, the above tabulation demonstrates that $i K_D(M)$,
where $K_D(M)$ is the drag coefficient for projectile type 6.1
and i is a constant, is not a sufficiently accurate approxi-
mation to the drag coefficient for the T-132 rocket.

A least squares iterative technique has been
developed at the Naval Proving Ground for obtaining a form
factor which is a polynomial in Mach number squared; this
technique was used to resolve the above difficulty encountered
in estimating the drag. A considerable amount of computation
is required to optimize each parameter of a polynomial form
factor and, because of time limitations, it was decided to use
a form factor which was linear in Mach number squared. Where

- -

M is Mach number, this form factor gives

$$\gamma = \frac{1}{C} = \frac{id^2}{m\varkappa}$$

the polynomial form

$$\gamma = a_0 + a_1 M^2$$

A value of γ was sought which would minimize the squares of the percentage errors in slant range. The longest time of flight for which observations had been taken, 15.4 seconds, is well outside the tactical range. Moreover, the accuracy of measurements at this condition (based only on fragmentary radar data) was questionable, so it was not known how much weight this condition should be given in the determination of γ. Thus, for purposes of an exploratory investigation, two γ's were obtained:

       (a) using observations of slant range at times of 4.0, 7.5, and 11.3 seconds, and

       (b) using observations of slant range at times of 4.0, 7.5, 11.3, and 15.4 seconds.

These are referred to as $\gamma^{(3)}$ and $\gamma^{(4)}$, respectively. Discrepancies associated with each are listed below:

$$\gamma^{(3)} = 3.025 - 0.233M^2 \qquad\qquad \gamma^{(4)} = 3.196 - 0.281M^2$$

t (sec)	$\varepsilon = \bar{R} - R_\gamma^{(3)}$	t (sec)	$\varepsilon = \bar{R} - R_\gamma^{(4)}$
4.0	− 7 yd (− 1.0%C)	4.0	−15 yd (− 2.1%C)
7.5	25 yd (2.0%C)	7.5	30 yd (2.5%C)
11.3	−15 yd (− 0.9%C)	11.3	9 yd (0.5%C)
15.4	−69 yd (− 3.2%C)	15.4	−25 yd (− 1.1%C)

(Numbers in parentheses indicate discrepancies in units of per cent change in ballistic coefficient.)

      While the use of $\gamma^{(3)}$ may be acceptable within the tactical range, the resulting error at t = 15.4 seconds is quite large. The use of $\gamma^{(4)}$, on the other hand, sacrifices too much in the tactical range in order to obtain a small

- -

error at $t = 15.4$ seconds. For these reasons, a compromise

$$\gamma = \frac{\gamma^{(3)} + \gamma^{(4)}}{2} = 3.11 - 0.257 M^2$$

was made; the discrepancies tabulated below resulted.

t (sec)	$\varepsilon = \bar{R} - R_\gamma$
4.0	-10 yd (- 1.4%C)
7.5	29 yd (2.3%C)
11.3	- 2 yd (- 0.1%C)
15.4	-45 yd (- 2.1%C)

This value of γ appears nearly as good as $\gamma^{(3)}$ in the tactical range and is considerably better than $\gamma^{(3)}$ for use in extrapolations to longer times of flight. This is the value of γ used in the after-burning portion of each trajectory in the range table computations.

The above optimization was carried out for the standard propellant temperature of 70°F. A study of non-standard propellant temperatures, 30 and 110°F, indicates that the optimum constant ballistic coefficient varied monotonically with propellant temperature (at least for the two times of flight at which data are available). The residuals, using γ defined as a linear function of M^2, also varied monotonically with propellant temperature but in reverse order from the variation for a constant γ for temperatures of 30 and 70°F. The residuals for both values of γ are shown below.

t (sec)	$\varepsilon = \bar{R} - R_{2.33}$			$\varepsilon = \bar{R} - R_{3.11-.257M^2}$		
	30°F	70°F	110°F	30°F	70°F	110°F
4.0	51 yd (7.3%C)	53 yd (7.6%C)	64 yd (9.1%C)	9 yd (1.3%C)	-10 yd (-1.4%C)	-15 yd (-2.1%C)
7.5	27 yd (2.2%C)	33 yd (2.6%C)	52 yd (4.2%C)	40 yd (3.2%C)	29 yd (2.3%C)	-22 yd (-1.8%C)

Since after burning, drag is not expected to vary with propellant temperature, the variation noted here is attributed to difficulties in obtaining the correct drag.

- -

(2) During Burning

The use of a γ , during burning, which is a linear
function of M^2, would be an unnecessary complication. Over
a short period of time a small error in drag has a very small
effect on the trajectory. Moreover, the u.e of a constant
value for γ simplifies the optimization of the acceleration
parameters (see section 7b(2)). In addition, the thrust data,
which were required before a linear form factor could be de-
termined, were not available. On the other hand, γ = 2.33,
the best constant after burning, is not the value best suited
for use during burning since it is based on the mass of the
rocket after burning. It was sufficient, however, to adjust
the value of 2.33 for the difference in the average of the
mass before and after burning. This gave a value of γ = 1.94
for use during burning.

d. **Motion During Burning with Yaw**

(1) The Yawing Model of Motion

The perfect trailing mathematical model of motion
as given in section 7a, using the parameters as described in
sections 7b and 7c, provided the basic trajectories needed
for the anti-aircraft range table. However, that model does
not adequately represent some of the aspects of the physical
motion. In particular, since thrust is directed along the
rocket axis, an accurate model for the burning period must
take full account of the angular motion of the rocket axis.
A mathematical model which takes into account such phenomena
is called a yawing model of motion. In such a model, a system
of differential equations in the translational and angular
coordinates of the rocket is integrated. The equations used
in this work take account of an aerodynamic force and moment
system dependent on yaw, and also take account of thrust as
a realistic function of time. The solutions of these equa-
tions of motion with yaw are referred to as rigid body trajec-
tories, as opposed to particle trajectories. The rigid body
trajectories integrated in this investigation were all termi-
nated at the end of burning since yaw after burn-out is of
less consequence. However, the effect of yawing motion during
burning on the remaining portion of the trajectory was computed
by formulas, described in section 7e, which use the differences,
given in section 7d(3), between the direction of the velocity
vector at burn-out in rigid body trajectories and the direction

of the velocity vector in perfect trailing trajectories.
The effect of yaw after burn-out on deflection, out of the
plane of the trajectory, was calculated for the range table
by the yaw of repose theory, as discussed in section 7e(1).

In the rigid body equations of motion, account was
taken of the following forces:

      (a)   thrust as a realistic function of time,

      (b)   axial drag,

      (c)   aerodynamic normal force, and

      (d)   gravity;

and of the following torques:

      (a)   axial torque resulting from the canted nozzles
           of the rocket motor,

      (b)   aerodynamic overturning torque,

      (c)   aerodynamic spin damping torque, and

      (d)   aerodynamic and jet cross-spin damping torques.

The equations are formulated so as to allow for variation
during burning of:

      (a)   mass,

      (b)   center of gravity, and

      (c)   transverse moment of inertia.

The axial moment of inertia is treated as constant.

It will be noted that the Magnus force and the
Magnus torque were neglected, indication being that large
yaws are not involved in actual flight. Cross-spin damping
is included in the torque equations though its associated
force, cross-spin force, was neglected in the force equa-
tions. Tip-off effects due to transverse components of
gravity and wind during the time in which only part of the
rocket is free of the launcher were neglected.

- -

Other than these exceptions, the equations used were essentially those developed at the Naval Ordnance Test Station and presented in reference (j). A list of the equations and further information about the symbols, coordinate system, and parameters used will be found in Tables 7, 8, and 9 and Figure 7, Appendix D. Any assumptions not specifically discussed above will be apparent upon consulting Tables 7 and 9.

(2)   Thrust as a Function of Time

The process of determining the rigid body motion required some searching for proper parameters. In particular, the deflection of the velocity vector during burning due to cross wind proved to be sensitive to the form of the thrust curve. The deflections were examined for a constant thrust, $T = 418.76$ lbs, and for a linear thrust, $T = 733t + 198.86$ lbs. The linear thrust was chosen so that the impulse resulting therefrom would match exactly the total impulse derived from the constant thrust and also so that the accelerations resulting therefrom would approximately match those determined from the Doppler data. However, the results obtained when using the two sets of thrust data were appreciably different (see Figure 8, Appendix E). This indicated the desirability of a more refined determination of the actual dynamic thrust.

Data from the Sperry Radic Doppler Chronograph were found to be adequate for this purpose. Data from four rounds (70°F propellant temperature) fired on 16 February 1953 appeared at first to vary radically (see Figure 9, Appendix E). However, when normalized, i.e., when velocities for each round were divided by the maximum velocity, and when times were divided by the time at maximum velocity, data for the four rounds matched quite well (see Figure 10, Appendix E). These normalized velocities were averaged and the original velocity and time units were restored by multiplying the normalized data by the average maximum velocity and the average time at maximum velocity.

Two basic formulas

(7.08) $T = m[\dot{v} + E(m)v + g \sin \varphi]$

- -

and

(7.09) $\qquad \dot{m} = - (1/v_g)T$

(where dots indicate differentiation with respect to time)
give the differential equation

(7.10) $\qquad \dot{m} + (\dfrac{\dot{v} + g \sin \varphi}{v_g})m = - \dfrac{m_o}{v_g} E(m_o)v$

where

$\qquad m_o$ = mass before burning, and

$\qquad v_g$ = gas velocity.

It is to be noted that $m_o E(m_o) = mE(m)$ because $mE(m)v$ = aero-
dynamic drag, which is independent of m. In fact, $mE(m)$
= $\rho d^2 v K_D$, using the notation of section 7(a) and using d
for the diameter of the rocket.

$\qquad$ The solution of equation (7.10) is

(7.11) $\qquad m = \dfrac{m_o}{e^{(v - v_o + g(\sin \varphi)/v_g}} [1 - (\int_o^t vE(m_o)e^{(v - v_o + g(\sin \varphi)/v_g} dt)/v_g]$

where

$\qquad$ T = the dynamic thrust (the function being sought),

$\qquad$ v = velocity of the average round after the averaging
$\qquad \qquad$ procedure discussed above,

$\qquad$ t = time measured from ignition,

$\qquad \dot{v}$ = acceleration obtained by a five point formula from
$\qquad \qquad$ Doppler velocity data,

$\qquad$ E(m) = E determined for mass m,

$\qquad$ g = acceleration of gravity at Dahlgren (32.154 ft/sec^2),
$\qquad \qquad$ and

$\qquad \varphi$ = angle of elevation.

- -

Upon substituting after-burning conditions in
equation (7.11), v_g was determined by successive approxi-
mations where a first approximation, $\bar{v}_g$, was available
from an approximate solution of equation (7.09). This
approximation is

$$\bar{v}_g = \frac{\frac{m_o + m_b}{2}\,(v_b - v_o)}{m_o - m_b}$$

where m_b is mass after burning, v_o and v_b are velocity before
and after burning, respectively. Knowing v_g, m versus time
was then computed using equation (7.11), and T versus time
was computed from equation (7.08). A fit was applied to T
using an eighth degree polynomial in time. The available
rigid body coding for the electronic calculators restricted
the degree to eight, though the accuracy could be slightly
improved by a higher degree fit. Comparisons of the constant,
linear, and dynamic thrusts used are given in Figure 11,
Appendix E. Comparisons of the difference in cross wind
effect using these thrust data are given in Figure 8, Appen-
dix E, though final values of wind effects were computed
using a more accurate (larger) value of spin than was avail-
able in the earlier work. A graph of mass versus time is
presented in Figure 12, Appendix E. Static thrust, including
data obtained from the Thiokol Corporation, reference (h),
are presented for comparison purposes in Figure 13, Appen-
dix E. Impulse from the static thrust was 263 lb-sec and
impulse from the dynamic thrust was 260 lb-sec, though times
of burning were considerably different.

It is believed that the equations used above account
for all variables which could appreciably influence the thrust
determination. In particular, variation of ballistic coeffi-
cient with mass is accounted for and the effect of gravity is
included. However, an average value of the term g sin φ was
used in analyzing the data on the four pertinent rounds, and
the ballistic coefficient was assumed to be constant with
respect to velocity, i.e., a form factor depending on Mach
number was not used. For times of flight greater than 0.58
second, the remaining thrust is extremely small. In the pro-
cess of curve fitting, the portion of the thrust curve beyond
t = 0.58 second was determined and the fitted value of thrust

- -

up to t = 0.58 second was scaled up to give a total impulse
equal to the observed impulse. The dynamic thrust curve
was taken to be this scaled value up to t = 0.58 second,
and as zero beyond t = 0.58 second. Rigid body trajectory
integrations were then continued with zero thrust from t
= 0.58 second to the range table time of burning for the
70°F propellant temperature, that is to 0.6037 second.

Determination of mass of the rocket at the muzzle
was not considered to be worth the effort required. The
thrust used in the computations is based upon the assumption
that no mass is expended in the barrel; the consequent error
in impulse has been estimated to be less than 0.3%. The
rigid body solutions are not sensitive to such a small error
of this type, and in any case the thrust is believed to be
much more accurate than many of the other rigid body para-
meters used in the calculations. The dynamic thrust must
be used and interpreted in the same manner as the acceler-
ation parameters (see section 7b(2)) in that the times are
interpreted as times from ignition, while for the purpose
of computation, it is assumed that the rocket leaves the
muzzle of the launcher when time equals zero.

The rigid body parameters in Table 9, Appendix D,
are those used with the dynamic thrust.

(3) Deflection of Velocity Vector at End of Burning

As indicated in section 7d(1), rigid body trajec-
tories were integrated to take proper account of the angular
motion of the rocket axis during burning and, in particular,
to obtain corrections at the end of burning to the direction
of motion as computed from the perfect trailing model. The
corrections were obtained at the cost of only two rigid body
integrations. This will now be explained.

First, it is noted that if there were no launching
disturbance (and therefore no jump) and if there were no com-
ponents of wind and gravity normal to the launcher line, there
would be no initial yaw, no initial yaw rate, and no forces
or torques to produce yaw. The yawing and perfect trailing
models of motion would then be identical. For present purposes
jump is assumed to be zero, the problem of correcting for jump
being discussed later in section 7g. In this section, it is

- -

assumed that corrections to the direction of motion at the
end of burning, in the perfect trailing model of motion, are
needed only as a result of (1) the normal component (g cos φ)
of gravity and (2) the normal components (w_x sin φ and w_z)
of wind. The direction angles to be corrected are the
inclination

$$\theta_b = \tan^{-1} (\frac{\dot{y}}{\dot{x}})_b$$

of the tangent at the end of burning, and the lateral deflec-
tion, $(\dot{z}/v)_b$, of the tangent at the end of burning.

If a function F_b of g cos φ, w_x sin φ, and w_z be
represented by a truncated Taylor series, one has approximately

$$(7.12) \quad F_b(g \sin \varphi = w_x \sin \varphi = w_z = 0) + (\frac{\partial F_b}{\partial g \cos \varphi})g \cos \varphi$$

$$+ (\frac{\partial F_b}{\partial w_x \sin \varphi})w_x \sin \varphi + (\frac{F_b}{\partial w_z})w_z$$

Here the various derivatives are evaluated for g cos φ = w_x
sin φ = w_z = 0, and any dependence on g sin φ and w_x cos φ is
neglected. There is a similar equation for $F_{b, Tr}$ where Tr
stands for the trailing model of motion. Inserting $\dot{z}/v$ in
the parentheses of equation (7.12) and the corresponding
trailing equation and repeating with θ inserted in the
parentheses, one has

$$(\frac{\dot{z}}{v})_b - (\frac{\dot{z}}{v})_{b, Tr} = [\frac{\partial (\frac{\dot{z}}{v})_b}{\partial g \cos \varphi} - (\frac{\partial (\frac{\dot{z}}{v})_b}{\partial g \cos \varphi})_{Tr}]g \cos \varphi$$

$$+ [\frac{\partial (\frac{\dot{z}}{v})_b}{\partial w_x \sin \varphi} - (\frac{\partial (\frac{\dot{z}}{v})_b}{\partial w_x \sin \varphi})_{Tr}]w_x \sin \varphi$$

$$+ [\frac{\partial (\frac{\dot{z}}{v})_b}{\partial w_z} - (\frac{\partial (\frac{\dot{z}}{v})_b}{\partial w_z})_{Tr}]w_z$$

- -

$$(7.13) \quad \theta_b - \theta_{b,Tr} = [\frac{\partial \theta_b}{\partial g \cos \varphi} - (\frac{\partial \theta_b}{\partial g \cos \varphi})_{Tr}] g \cos \varphi$$

$$+ [\frac{\partial \theta_b}{\partial w_x \sin \varphi} - (\frac{\partial \theta_b}{\partial w_x \sin \varphi})_{Tr}] w_x \sin \varphi$$

$$+ [\frac{\partial \theta_b}{\partial w_z} - (\frac{\partial \theta_b}{\partial w_z})_{Tr}] w_z$$

The six bracketed expressions in equations 7.13 are not all different since, as will be shown below,

$$\frac{\partial \theta_b}{\partial w_x \sin \varphi} = - \frac{\partial (\frac{\dot{z}}{v})_b}{\partial w_z} \quad \text{and} \quad \frac{\partial \theta_b}{\partial w_z} = \frac{\partial (\frac{\dot{z}}{v})_b}{\partial w_x \sin \varphi}$$

Using these relationships and defining

$$C_1 = [\frac{\partial (\frac{\dot{z}}{v})_b}{\partial g \cos \varphi} - (\frac{\partial (\frac{\dot{z}}{v})_b}{\partial g \cos \varphi})_{Tr}] g$$

$$C_3 = -[\frac{\partial (\frac{\dot{z}}{v})_b}{\partial w_z} - (\frac{\partial (\frac{\dot{z}}{v})_b}{\partial w_z})_{Tr}]$$

$$= [\frac{\partial \theta_b}{\partial w_x \sin \varphi} - (\frac{\partial \theta_b}{\partial w_x \sin \varphi})_{Tr}]$$

$$C_4 = - [\frac{\partial (\frac{\dot{z}}{v})_b}{\partial w_x \sin \varphi} - (\frac{\partial (\frac{\dot{z}}{v})_b}{\partial w_x \sin \varphi})_{Tr}] = - \frac{\partial (\frac{\dot{z}}{v})_b}{\partial w_x \sin \varphi}$$

$$= - [\frac{\partial \theta_b}{\partial w_z} - (\frac{\partial \theta_b}{\partial w_z})_{Tr}] = - \frac{\partial \theta_b}{\partial w_z}$$

- -

and using the fact that

$$\frac{\partial \theta_b}{\partial_R \cos \varphi} - \left(\frac{\partial \theta_b}{\partial_R \cos \varphi}\right)_{Tr}$$

is negligible (see equation (7.17) and section 7e(1)(b)), it is possible to write equations (7.13) in the form

$$\left(\frac{\dot{z}}{v}\right)_b - \left(\frac{\dot{z}}{v}\right)_{b, Tr} = C_1 \cos \varphi - C_4 w_x \sin \varphi - C_3 w_x$$

(7.14) $\qquad \theta_b - \beta_{b, Tr} = C_3 w_x \sin \varphi - C_4 w_z$

The validity of

$$\frac{\partial \theta_b}{\partial w_x \sin \varphi} = - \frac{\partial \left(\frac{\dot{z}}{v}\right)_b}{\partial w_z}$$

can be seen by observing that both

$$\frac{\partial \theta_b}{\partial (- w_x \sin \varphi)} \quad \text{and} \quad \frac{\partial \left(\frac{\dot{z}}{v}\right)_b}{\partial w_z}$$

are the derivatives with respect to a normal component of wind, of the angle through which the tangent to the trajectory is deflected in the direction of the normal component of wind. Similarly,

$$\frac{\partial \theta_b}{\partial w_z} \quad \text{and} \quad \frac{\partial \left(\frac{\dot{z}}{v}\right)_b}{\partial w_x \sin \varphi}$$

are both the derivatives of the angle through which the tangent to the trajectory is deflected in the direction of the vector product of the launcher line vector times the wind vector. To evaluate the C's, one rigid body trajectory

- -

was integrated with gravity and no wind for $\varphi = 0$, and
another was integrated with cross wind ($w_z = 40$ knots) and
no gravity for $\varphi = 0$. The corresponding trailing solutions
were readily obtained by integration of the much simpler
equations of the trailing model, which were adjusted to pro-
duce the same velocity at end of burning (v_b) as the yawing
model. The trailing trajectory with cross wind was computed
for $\varphi = 90°$ instead of $0°$, so that y in the trailing tra-
jectory corresponded to x in the rigid body trajectory, and
also w_x rather than w_z was made equal to 40 knots so that x
in the trailing trajectory corresponded to z in the rigid
body trajectory. Actually, there is a simple analytic ex-
pression in the perfect trailing model for deflection in the
case of cross wind. Thus, the general equations of section
7a without the Coriolis terms yield

$$(7.15) \qquad \frac{\ddot{z}}{\dot{z} - w_z} = \frac{A}{v_a} - E_a = \frac{\ddot{x}}{\dot{x}}$$

Integrating, one obtains

$$\frac{\dot{z} - w_z}{- w_z} = \frac{\dot{x}}{\dot{x}_o}$$

and therefore

$$(7.16) \qquad (\dot{z}/v)_{b,Tr} = w_z(\frac{1}{v_b} - \frac{\dot{x}_b}{v_b \dot{x}_o}) \doteq w_z(\frac{1}{v_b} - \frac{1}{v_o})$$

        Results obtained by the application of this formula
were in good agreement with the results of the trajectories
integrated for perfect trailing with cross wind considered.

- -

It was found that

$$(7.17) \quad g\left[\frac{\partial \theta_b}{\partial g \cos \varphi} - \left(\frac{\partial \theta_b}{\partial g \cos \varphi}\right)_{Tr}\right] \doteq \left(\frac{\dot{y}}{\dot{x}}\right)_{b \atop \varphi=0} - \left(\frac{\dot{y}}{\dot{x}}\right)_{b, Tr \atop \varphi=0} = -0.66° + 0.63° = -0.03 \text{ degree}$$

$$= -0.0005 \text{ radian}$$

$$(7.18) \quad C_1 = g\left[\frac{\partial(\dot{z}/v)_b}{\partial g \cos \varphi} - \left(\frac{\partial(\dot{z}/v)_b}{\partial g \cos \varphi}\right)_{Tr}\right] \doteq \left(\frac{\dot{z}}{\dot{x}}\right)_{b \atop \varphi=0} - \left(\frac{\dot{z}}{\dot{x}}\right)_{b, Tr \atop \varphi=0} = 0.0017 \text{ radian} - 0 \text{ radian}$$

$$= 0.0017 \text{ radian}$$

$$(7.19) \quad C_3 = -\left[\frac{\partial(\dot{z}/v)_b}{\partial w_z} - \left(\frac{\partial(\dot{z}/v)_b}{\partial w_z}\right)_{Tr}\right] \doteq -\frac{100}{40}\left[\left(\frac{\dot{z}}{\dot{x}}\right)_{b \atop \varphi=0 \atop w_z=40} - 40\left(\frac{1}{v_b} - \frac{1}{v_0}\right)\right] = 0.0821 - 0.0793$$

$$= 0.0028 \text{ rad/100 kts}$$

$$(7.20) \quad C_4 = -\left[\frac{\partial \theta_b}{\partial w_z} - \left(\frac{\partial \theta_b}{\partial w_z}\right)_{Tr}\right] \doteq -\frac{100}{40}\left(\frac{\dot{y}}{\dot{x}}\right)_{b \atop \varphi=0 \atop w_z=40} = 0.0146 \text{ radian/100 knots}$$

(An equal sign with a dot over it means "approximately equals.")

Two other C's are also used in the range table formulas of section 7e. They are

$$C_2 = \text{drift coefficient after burning}$$

(see section 7e(1)), and

$$(7.21) \quad C_5 = -\frac{\partial\left(\frac{\dot{z}}{v}\right)_b}{\partial w_z} = \frac{\partial \theta_b}{\partial w_x \sin \varphi} = 0.085 \text{ radian/100 knots}$$

- -

e.   Range Table Formulas with Allowances for Yawing Motion

   (1)   Allowances for Yaw with No Wind

      (a)   Drift

            Under no wind conditions, there is at the end
of burning a small lateral deflection of the direction of
motion as noted above in section 7d(3), which results from
yawing motion. After burning, still under no wind conditions,
there is also a yawing motion which leads to forces normal
to the trajectory. Since in the after burning period there
is no thrust and the spin is more nearly constant, the motion
is estimated using classical theory without rigid body inte-
grations. The average aerodynamic normal force is directed
t the right of the plane of fire if the spin is right-handed
and the moment of the normal forces is overturning. This
produces a right drift. The theory of drift has been given
by McShane, Kelley, and Reno (reference (k)), by Moulton
(reference (l)), and by Fowler, Gallop, Lock, and Richmond
(reference (m)). In their various developments of the theory
simplifying assumptions are made after very complex analyses.
It perhaps gives more insight into the theory if the simpli-
fying assumptions are made at the outset, as will now be done.

            Instead of considering the actual oscillatory
yaw, one considers the mean yaw estimated using the yaw of
repose theory. The latter is a yaw of such amplitude and
orientation as to be aerodynamically compatible with the time
rate of change, $\dot{\theta}$, of the inclination of the trajectory.
For constant $\dot{\theta}$, consider a reference frame turning with an
angular velocity, $\dot{\theta}$, about the z axis. The shell axis and
the angular momentum vector, H, would be invariant in this
frame. The time rate of change, $\dot{H}$, of H with respect to an
inertial frame, would then be the vector product of the
angular velocity vector, $\dot{\theta}e_z$, of the reference frame and
the vector H, e_z being a unit vector parallel to the z axis.
Thus,

(7.22) $\dot{H} = \dot{\theta}e_z \times H$

Since the z axis is approximately normal to the shell axis,
one has approximately

(7.23) $H = ANe_1 + B\dot{\theta}e_z$

- -

e_1 being a unit vector parallel to the shell axis, N being the spin, and A and B being moments of inertia about the longitudinal and transverse axes. Whence

(7.24) $$\dot{H} = \dot{\theta}e_z \times H = AN\dot{\theta}e_z \times e_1$$

This equals the torque on the shell due to the aerodynamic normal forces. If the only aerodynamic torque considered to be acting is the overturning torque, the axis of this moment must be normal to the z axis since it lies along the vector $e_z \times e_1$. The plane of yaw, which is normal to the axis of the overturning moment, must accordingly contain the z axis. Thus the yaw of repose is to the right or left. Resolving the moment vector along $e_z \times e_1$, one finds

(7.25) $$AN\dot{\theta} = - \rho v^2 d^3 K_M \sin \delta_r$$

where K_M is the overturning moment coefficient and δ_r is the yaw of repose, being positive to the right. The effect of this lateral yaw on the deflection of the trajectory is given by the differential equation

(7.26) $$\ddot{z} = - E\dot{z} + \frac{1}{m} \rho v^2 d^2 K_L \sin \delta_r$$

K_L being the aerodynamic lift coefficient. Eliminating $\sin \delta_r$ from these two equations and replacing $-E$ with $\ddot{x}/\dot{x}$ (see section 7.4), the differential equation for z becomes

(7.27) $$\ddot{z} - \frac{\ddot{x}}{\dot{x}} \dot{z} = \frac{AN\dot{\theta}K_L}{mdK_M}$$

Considering x, $\dot{x}$, and $\ddot{x}$ to be known functions of time and remembering that $\tan \theta = \dot{y}/\dot{x}$ and therefore $\theta = - g\dot{x}/v^2$, this differential equation has the solution

(7.28) $$z = z_b + \frac{\dot{z}_b}{\dot{x}_b} (x - x_b) + \frac{Ag}{md} \int_{t_b}^{t} \dot{x} \int_{t_b}^{t} \frac{NK_L}{v^2 K_M} dt dt$$

----

the subscripts "b" indicating evaluation at the end of
burning. Essentially this result is attributed to Mayevski
by Fowler, Gallop, Lock, and Richmond. It is also the last
equation of the Kelley-McShane report of reference (n).

Upon integration by parts, assuming the spin
N and the ratio K_L/K_M of aerodynamic coefficients do not
vary and that

$$z_b - \frac{\dot{z}_b}{\dot{x}_b} x_b$$

is negligible, and noting that

$$\frac{\dot{z}_b}{\dot{x}_b} = \frac{\dot{z}_b}{v_b \cos \varphi} = C_1$$

the equation for drift becomes

(7.29) $$z = C_1 x + C_2 \left(x \int_{t_b}^{t} \frac{dt}{v^2} - \int_{t_b}^{t} \frac{x}{v^2} dt \right)$$

which is the formula by which drift was computed for the
T-132 range table. Here C_2, the drift constant, is theo-
retically an average value of

$$\frac{A\alpha N K_L}{m d K_M}$$

Actually, C_2 was determined from observed values of drift
since, as with many projectiles, the observations were not
consistent with the theoretical value of C_2. By observed
values of drift is meant observed deflections corrected for
wind, Coriolis force, and lateral jump. The lateral jump,
however, was negligible in the data used (see section 7g).
Since dispersion of the observed drift was large, as can be
seen in the table below, a value

$$C_2 = 286.5 \text{ yd}^2/\text{sec}^3$$

----

which minimizes the sum of the squares of the differences
between the measured and computed values of drift (expressed
as a percentage of horizontal range) was used in preparing
the range table. In this computation the observed values
of drift at four seconds time of flight were neglected.
These values were obtained in the firings of the first phase
(described in section 5a), which gave an unexplained lateral
displacement as compared with results obtained in the second
phase of firing. The theoretical value of C_2, indicated
above, is 554 yd^2/sec^3.

Drift was required in the range table only for
the 70°F propellant temperature; therefore, only 70°F obser-
vations were used to obtain C_2. However, drift for 30 and
110°F propellant temperatures was obtained from observed and
corrected deflections and there may be interest in the dis-
crepancies between these values and the computed values for
the propellant temperature of 70°F. Using the notation

ϵ_z = z (observed, corrected) - z (range table)

the following is a table of z, the mean measured value of
drift for each condition, σ_z, the standard deviation of the
measured drift, and ϵ_z, the mean discrepancy in drift.

Drift of the T-132 Rocket

Approximate Time of Flight sec	Propellant Temperature °F	$\bar{z}$ yds	σ_z yds	$\bar{\epsilon}_z$ yds
4	70	1.3	±1.6	-4.7
7.5	70	19.0	±4.6	1.8
11.5	70	39.1	±9.2	-1.6
4	30	0.5	±2.9	-5.8
7.5	30	14.2	±2.7	-3.2
11.5		NOT OBSERVED		
4	110	1.6	±2.1	-4.6
7.5	110	25.4	±4.3	6.8
11.5		NOT OBSERVED		

(b) Effect of Yaw on Range and Altitude

The rigid body trajectory integrated with no wind, g = 32.2 ft/sec^2, and φ = 0, yielded a value of

$$\theta_b \doteq \dot{y}_b/\dot{x}_b = -0.66°$$

The perfect trailing trajectory integrated for the same conditions yielded a value of

$$\theta_b = -0.63°$$

The difference between these quantities is much smaller than the dispersion in θ_b from round to round. For other values of φ, the component of g, normal to the launcher line, would be smaller and the difference between values of θ_b yawing and θ_b trailing would be less than 0.03 degree. Thus, no correction of the perfect trailing trajectories was necessary to take account of the effect of gravity on θ_b. This result was anticipated.

(2) Effects of Range Wind

(a) Effect on Range and Altitude

Let φ_a be the inclination at the muzzle of the trajectory relative to the air mass, and let x_a be the horizontal distance in the moving air along the line of fire. Then

$$x_a = x - w_x t$$

and

$$\left(\frac{\partial x_a}{\partial w_x}\right)_{Tr} = \left(\frac{\partial x_a}{\partial \varphi_a}\frac{\partial \varphi_a}{\partial w_x} + \frac{\partial x_a}{\partial v_{0,a}}\frac{\partial v_{0,a}}{\partial w_x}\right)_{Tr}$$

For the model which yaws during burning, it is assumed that the effective φ_a is the true $\varphi_a + (\theta_{a,b}) - (\theta_{a,b})_{Tr}$.

Thus

$$(7.30) \quad \frac{\partial x_a}{\partial w_x} = \frac{\partial x_a}{\partial \varphi_a} \left[\frac{\partial \varphi_a}{\partial w_x} + \left(\frac{\partial \theta_{a,b}}{\partial w_x} \right) - \left(\frac{\partial \theta_{a,b}}{\partial w_x} \right)_{Tr} \right] + \frac{\partial x_a}{\partial v_{o,a}} \frac{\partial v_{o,a}}{\partial w_x}$$

But

$$\left(\frac{\partial \theta_a}{\partial w_x} \right)_{w=0} = \left(\frac{\partial \theta}{\partial w_x} + \frac{\sin \theta}{v} \right)_{w=0}$$

which can be verified by differentiating

$$\dot{x} \tan \theta = \dot{y}$$

and

$$(\dot{x} - w_x) \tan \theta_a = \dot{y}$$

with respect to w_x, taking into account that $\dot{x}$ and $\dot{y}$ depend on w_x. In particular,

$$\frac{\partial \varphi_a}{\partial w_x} = \frac{\sin \varphi}{v_o}$$

since $\theta = \varphi$ at $t = 0$. Similarly,

$$\frac{\partial v_{o,a}}{\partial w_x} = - \cos \varphi$$

is verified by differentiating

$$v_{o,a}^2 = (\dot{x}_o - w_x)^2 + \dot{y}_o^2$$

Substituting from equation (7.30) for $\dfrac{\partial x_a}{\partial w_x}$

$$\frac{\partial x}{\partial w_x} = \frac{\partial x_a}{\partial w_x} + t = \frac{\partial x_a}{\partial \varphi_a}\left[\frac{\sin\varphi}{v_0} + \left(\frac{\partial \theta_b}{\partial w_x}\right) - \left(\frac{\partial \theta_b}{\partial w_x}\right)_{Tr} + \frac{\sin\theta_b - \sin\theta_{b,Tr}}{v_b}\right] - \frac{\partial x_a}{\partial v_{0,a}}\cos\varphi + t$$

or

(7.31) $\qquad \dfrac{\partial x}{\partial w_x} \doteq \dfrac{\partial x}{\partial \varphi}\left(\dfrac{1}{v_0} + C_3\right)\sin\varphi - \dfrac{\partial x}{\partial v_0}\cos\varphi + t$

Here $\sin\theta_b - \sin\theta_{b,Tr}$ is negligible for $\varphi = 0$, as noted in section 7e(1)(b). Also, all derivatives are evaluated at $w = 0$, where $x_a = x$, and $\varphi_a = \varphi$. Similarly,

(7.32) $\qquad \dfrac{\partial y}{\partial w_x} = -\dfrac{\partial y}{\partial v_0}\cos\varphi + \dfrac{\partial y}{\partial \varphi}\left(\dfrac{1}{v_0} + C_3\right)\sin\theta$

These two equations, appropriately modified for the units of the range table, are those used to tabulate

$$\frac{\partial x}{\partial w_x} \quad \text{and} \quad \frac{\partial y}{\partial w_x}$$

(see Appendix G).

(b) Effect on Deflection

The azimuth of motion at the end of burning is the azimuth of the line of fire plus

$$\tan^{-1}\frac{\dot{z}_b}{\dot{x}_b}$$

For the rate of change of azimuth with respect to w_x, one

----

has then, since φ is independent of w_x,

$$(7.33) \quad \frac{\partial(\tan^{-1} \frac{\dot{z}_b}{\dot{x}_b})}{\partial w_x} = \frac{1}{1 + (\frac{\dot{z}}{\dot{x}})^2_b} \frac{\partial (\frac{\dot{z}}{v})_b}{\partial(w_x \sin \varphi)} \tan \varphi = - \frac{1}{1 + (\frac{\dot{z}}{\dot{x}})^2_b} C_4 \tan \varphi$$

C_4 having the definition given in section 7d(3). The value of C_4 is 0.0146 radians/100 knots. Since the derivative indicated on the left-hand side of equation (7.33) is to be evaluated at $w_x \approx 0$, the right-hand side becomes $- C_4 \tan \varphi$, if $\varphi < 90°$. Therefore, to correct for deflection resulting from range wind, the azimuth of the line of fire must be increased by an amount 0.0146 $w_x \tan \varphi$ radians, w_x being in hundreds of knots and φ having a value such as to make $\tan \varphi$ finite. This correction appears as a note accompanying the range table (Appendix G).

   (3)   Effects of Cross Wind

      (a)   Effect on Deflection

         As previously discussed (section 7d(1)), motion during burning is sensitive to the yaw. When there is no thrust, a perfect trailing model trajectory is adequate for computing the effects of cross wind. For the T-132 rocket, the effect of a cross wind on deflection is computed therefore from the particle trajectory from the end of burning, the conditions at the end of burning having been computed by rigid body integrations.

         The perfect trailing differential equation for z with cross wind w_z is

$$(7.34) \qquad \ddot{z} = (\frac{A}{v_a} - E_a)(\dot{z} - w_z) = \frac{\ddot{x}}{\dot{x}} (\dot{z} - w_z)$$

The solution for $z_0 = \dot{z}_0 = 0$ is

$$\dot{z}_{Tr} = w_z(1 - \frac{\dot{x}}{x_0})$$

and

$$z_{Tr} = w_z(t - \frac{x}{x_0})$$

To obtain z based on yawing motion during burning and perfect trailing thereafter, consider the expansion for $z - z_{Tr}$ as a power series in $x - x_b$. It is first noted that, for $x > x_b$,

$$\frac{d^2 z}{dx^2} \equiv \frac{\ddot{z}\dot{x} - \dot{z}\ddot{x}}{\dot{x}^3} = \frac{\ddot{x}(\dot{z} - w_z) - \dot{z}\ddot{x}}{\dot{x}^3}$$

$$\sim = - \frac{\ddot{x}}{\dot{x}^3} w_z = (\frac{d^2 z}{dx^2})_{Tr}$$

assuming that, for $t > t_b$, $\dot{x}$ and $\ddot{x}$ are not appreciably affected by yawing when $t < t_b$. Therefore, the higher derivatives of $z - z_{Tr}$ with respect to x are considered to vanish. The expansion is then

$$z - z_{Tr} = z_b - z_{b,Tr} + (x - x_b)[(\frac{dz}{dx})_b - (\frac{dz}{dx})_{b,Tr}]$$

Whence, after dropping $z_b - x_b(\frac{dz}{dx})_b$ and $z_{b,Tr} - x_b(\frac{dz}{dx})_{b,Tr}$

$$z \doteq z_{Tr} + x[(\frac{\dot{z}}{\dot{x}})_b - (\frac{\dot{z}}{\dot{x}})_{b,Tr}]$$

Differentiating

$$\frac{\partial z}{\partial w_z} = t - \frac{x}{\dot{x}_o} + x \frac{\partial}{\partial w_z} \left[(\frac{\dot{z}}{\dot{x}})_b - (\frac{\dot{z}}{\dot{x}})_{b, \text{Tr}} \right]$$

or

(7.35)
$$\frac{\partial z}{\partial w_z} = t - (\frac{1}{v_o} + C_3)x \sec \varphi$$

using

$$C_3 = \left[(\frac{\partial \dot{z}/\dot{x}}{\partial w_z})_{b, \text{Tr}} - (\frac{\partial \dot{z}/\dot{x}}{\partial w_z})_b \right] \cos \varphi$$

as defined in section 7d(3), and assuming $\frac{\partial x}{\partial w_z}$ to be
negligible. This formula, properly modified to yield z in
yards where the w_z unit is 100 knots, is used to compute
deflection due to cross wind for range tables (see
Appendix G).

The perfect trailing term in C_3, when deter-
mined in closed form from the equation

$$\dot{z}_{\text{Tr}} = w_z (1 - \frac{\dot{x}}{\dot{x}_o})$$

agreed quite satisfactorily with the value obtained from an
integrated trajectory; in units used for the range table
$C_3 = 0.0028$ radian/100 knots.

(b) Effect on Range and Altitude

The deflection effect given in equation (7.35)
is the only effect of a cross wind tabulated in the range
table. However, a cross wind during burning (whether a uni-
form wind or one applicable only during burning) will, because
of the spinning of the rocket and the consequent precessional
motion, cause a windage jump and therefore affect x and y.

Continued cross wind after the end of burning has negligible effect on x and y. Thus, the windage jump (effect on angle of departure) can be generated by multiplying

$$\frac{\partial \theta_b}{\partial w_z}$$

by the indicated wind. This value, since it does not involve the effects of gravity, is independent of the angle of elevation. Therefore, with C_4 defined to be

$$\left(\frac{\partial \theta_b}{\partial w_z}\right)_{\varphi=0} = -\left(\frac{\dot{y}_b/\dot{x}_b}{w_z}\right)_{\substack{R=0 \\ \varphi=0}} = 0.0146 \text{ radian}/100 \text{ knots}$$

(computed from a rigid body trajectory, section 7d(3)), one must correct for this effect of a cross wind by increasing the angle of elevation by the amount $C_4 w_z$ radians, where the w_z unit is 100 knots. This correction appears as a note accompanying the range table (see Appendix C).

(4) Range Table Allowance for Non-Uniform Wind

The formulas given in sections 7e(2) and 7e(3) for range wind effect on x and y and for cross wind effect on deflection assume that the wind is uniform. A uniform wind should be interpreted to represent some type of average of the actual winds prevailing, and it must be noted that no specification is made as to how a uniform wind is to be computed. (To do so, weighting factors would be needed.) But if wind after burning differs from wind during burning (which plays the more important role), the two must be treated separately, as suggested in the notes to the tables (Appendix G). This case may easily occur if wind varies markedly with the altitude of the rocket. Note also that formulas given in sections 7e(2) and 7e(3) for range wind effect on deflection and for cross wind effect on x and y involve only wind during burning. Consequently, non-uniform winds do not affect these formulas.

The notes accompanying the range table (Appendix G) recommend that in the event the rocket trajectory is subjected to a non-uniform wind, the wind effects be obtained from the tables (which employed the formulas of sections 7e(2) and 7e(3)) using the ballistic wind determined from the wind acting during the after-burning portion of the trajectory.

In addition, the angle of elevation and azimuth angle should
be corrected for the effect of the differential wind during
burning, i.e., the wind whose range component is range wind
during burning minus ballistic range wind after burning, and
whose cross component is cross wind during burning minus
ballistic cross wind after burning. The effect of the dif-
ferential range wind component on angle of elevation can be
obtained immediately assuming that

$$\frac{\partial \varphi}{\partial w_x} = \frac{\partial \theta_b}{\partial w_x}$$

It is seen that this can be expressed in terms of C_5 as
defined in section 7d(3)

$$C_5 = \frac{\partial \theta_b}{\partial w_x \sin \varphi} = - \frac{\partial (\frac{\dot{z}}{v})_b}{\partial w_z}$$

Giving

(7.36)
$$\frac{\partial \theta}{\partial w_x} = C_5 \sin \varphi$$

$C_5 = 0.084$ radian per 100 knots. Hence, the effect of each
100 knots of range wind during burning in excess of ballistic
range wind after burning is to increase the angle of elevation
by the amount $C_5 \sin \varphi$ radians or $180/\pi \; C_5 \sin \varphi$ degrees. The
correction to the sight angle necessary to score a hit is the
negative of this quantity. This formula is quoted in the
notes to the range table incorrectly as $180/\pi \; C_3 \sin \varphi$. A
"Change 1" to the range table, correcting the formula to read

$$\frac{180}{\pi} C_5 \sin \varphi$$

is being prepared by the Bureau of Ordnance in accordance
with reference (o) which corrects a similar error in the
formula for the effect of differential cross wind on deflec-
tion. This latter formula can be obtained immediately.

From

$$C_5 = - \frac{\partial (\frac{\dot{z}}{v})_b}{\partial w_z}$$

as given above, and from

$$v_b = \dot{x}_b (\sec \theta)_b \doteq \dot{x}_b \sec \varphi$$

it follows that

(7.37)
$$\frac{\partial (\frac{\dot{z}}{\dot{x}})_b}{\partial w_z} = - C_5 \sec \varphi$$

Hence, the effect of each 100 knots of cross wind (blowing from left to right) during burning, in excess of ballistic cross wind after burning, is to decrease the azimuth of the launcher by the amount

$$C_5 \sec \varphi \text{ radians}$$

This formula will be given in the notes accompanying the range table after Change 1 is entered in the form indicated in Appendix G.

The adjustment of v_o necessary to compensate for a range wind during burning, in excess of ballistic range wind, has also been examined. Using

$$v_{ab}^2 = (\dot{x}_b - w)^2 + \dot{y}_b^2 \qquad\qquad v_b^2 = \dot{x}_b^2 + \dot{y}_b^2$$

$$\left(\frac{\partial v_b}{\partial w_x}\right)_{w=0} = \left(\frac{\partial v_{ab}}{\partial w_x}\right)_{w=0} + \left(\frac{\dot{x}_b}{v_b}\right)_{w=0} = \left(\frac{\partial v_{ab}}{\partial v_{oa}} \frac{\partial v_{oa}}{\partial w_x} + \frac{\partial v_{ab}}{\partial \varphi_a} \frac{\partial \varphi_a}{\partial w_x}\right)_{w=0} + \left(\cos \theta_b\right)_{w=0}$$

and

$$\frac{\partial v_{ab}}{\partial \varphi_a} \doteq 0 \doteq (\cos \theta_b)_{w_x=0} - \cos\varphi$$

----

the formula

$$\frac{\partial v_0(\text{effective})}{\partial w_x} = \frac{\dfrac{\partial v_b}{\partial w_x}}{\dfrac{\partial v_b}{\partial v_0}} = \frac{(1 - \dfrac{\partial v_b}{\partial v_0})\cos \varphi}{\dfrac{\partial v_b}{\partial v_0}}$$

was derived. This formula, properly modified for range table
units, can be applied to assess the necessary correction to
initial velocity for a wind during burning in excess of the
uniform wind. However, consideration of extreme plausible
differences between the burning and after burning winds has
indicated that the correction is an insignificant one. A ten
knot difference, for example, at $\varphi = 0$, would result in a
correction to velocity at the end of burning of about four
feet per second and this is hardly significant considering
observed dispersions in maximum velocity (see Table 4,
Appendix B).

It should be noted that all wind effects quoted
here and in the range table, as well as all other effects due
to non-standard ballistic conditions, are given for 70°F
propellant temperature only, although the basic AA trajectory
data (sight angle and time of flight versus slant range and
position angle) were determined for 30, 70, and 110°F propel-
lant temperatures.

f. Dispersion

The total number of rounds fired at any given angle of
elevation and propellant temperature was not sufficiently
large to afford reliable dispersion data; available measure-
ments indicate a dispersion in range to surface which is
monotonic decreasing with time of flight (Figures 14-21,
Appendix F). While it is not impossible that at burn-out
the velocity, ballistic coefficient, range, and their re-
spective dispersions could be so related as to produce such
a result, no reasonable explanation withstood numerical
investigation.

Observed impact patterns, corrected for atmospheric
conditions and projectile mass before burning, for each angle
of elevation and propellant temperature fired are given in
Figures 14-21, Appendix F. For evaluation purposes, the
effect of 1% change in density and of 0.1 second change in

----

time of flight, as well as other differential effects, are included for 70°F propellant temperature. In Figure 17, Appendix F, slant range is used instead of x and y coordinates because the observations consisted only of radar range versus time.

Examination of the scatter diagrams will show that two rounds fell far outside any reasonable limits in horizontal range. These rounds are marked "mavericks" and were considered too wild for use in the basic range table analysis. They were Round 2, 70°F propellant temperature, $\varphi = 5°30'$, fired 20 February 1953; and Round 4, 30°F propellant temperature, $\varphi = 1°30'$, fired 26 January 1953.

Rounds 2, 3, and 5, 70°F propellant temperature, $\varphi = 5°30'$, fired 20 February 1953, fell outside any reasonable limits in deflection and were excluded from the drift analysis. For reasons indicated in paragraph 7e(1)(a), nonstandard propellant temperatures and short times of flight ($\varphi = 1°30'$) were not used in the drift analysis. For drift dispersion figures see section 7e(1)(a). See Table 6, Appendix B, for a summary of observed data.

The bias in y shown in Figures 15, 16, 19, and 21, Appendix F, is attributable to jump which is discussed in the following paragraphs.

g.   Jump

It should be noted that the observed impact positions, when firing from the launcher installed on the modified 4-inch gun mount (Figure 2, Appendix A), were about 15 mils above the range table trajectories for the actual elevation angles of the launcher. This is shown in Figures 15, 16, 19, and 21, Appendix F. The discrepancies are attributable to jump, which was confirmed by data showing the rocket height at the end of burning and also by special jump firings. These results are described below. Such discrepancies at impact did not arise when firing from the launcher installed on the box mount and in that case more complete data obtained at the end of burning (section 6b(3) and Table 5, Appendix B) indicated that jump was not in excess of five minutes (compare Table 5, Appendix B, with values in equation (7.17)). For the service mount, the determination of jump must, of course, await development of the mount.

The usual definition of jump means little for this weapon. As with other rockets, the complex helical motion during burning focuses attention not upon the angle at which the rocket leaves the barrel but upon the direction of the velocity vector at the end of burning. If this direction (and, of course, position of the rocket at burn-out) is well determined, motion after burning is predictable.

Let $(\theta_y, \theta_z)_b$ represent the angles which the velocity vector at the end of burning makes with the xz and xy planes, respectively, the y-axis being upward and the z-axis to the right. Jump, then, is defined as $(\theta_y, \theta_z)_b$, observed, minus the value of $(\theta_y, \theta_z)_b$ which would occur if there were no launching disturbance.

In the special jump test (section 6a(2)) of the modified 4-inch gun mount, measurements of altitude and deflection were taken from two targets bracketing the end of burning in order to estimate the direction of the velocity vector at end of burning. Because the angles involved are small, let

$\left(\dfrac{dy}{dx}\right)_{obs}$ = inclination of the velocity vector with respect to the launcher line, observed by means of the two target impacts;

$\left(\dfrac{dy}{dx}\right)_{std}$ = inclination of the velocity vector with respect to the launcher line, determined from a rigid body trajectory with no wind and no jump;

$\left(\delta \dfrac{dy}{dx}\right)_{wind}$ = inclination of the velocity vector with respect to the launcher line, scaled to the observed wind from a rigid body trajectory integrated with 40 knots cross wind and g = 0 (this definition implies that

$$\left(\delta \dfrac{dy}{dx}\right)_{wind}$$

is the change in dy/dx due to cross wind); and

$\theta_y = \left(\delta \dfrac{dy}{dx}\right)_{jump}$ = vertical component of jump.

Then

$$(7.38) \qquad \left(\frac{dy}{dx}\right)_{obs} = \left(\frac{dy}{dx}\right)_{std} + \left(\delta\,\frac{dy}{dx}\right)_{wind} + \left(\delta\,\frac{dy}{dx}\right)_{jump}$$

if linearity is assumed. Prevalent range components of wind were too small to have an appreciable effect.

$$\left(\delta\,\frac{dy}{dx}\right)_{jump}$$

was determined from this equation, and

$$\left(\delta\,\frac{dz}{dx}\right)_{jump}$$

defined as the lateral component of jump was found in a similar manner.

Unfortunately, varying cross winds plagued the test and only two out of five rounds hit both targets. All five rounds, however, hit the second target. The angles which the lines, connecting the points of impact on this target with the muzzle, made with the launcher line were observed. An analysis of these data similar to the above analysis produced the portion of these angles, $(\delta\,y/x)_{jump}$ and $(\delta\,z/x)_{jump}$, due to jump.

Results of the analysis are:

Round No.	$(\delta\,y/x)_{jump}$	$(\delta\,z/x)_{jump}$	$\left(\delta\,\frac{dy}{dx}\right)_{jump}$	$\left(\delta\,\frac{dz}{dx}\right)_{jump}$
1	50.1'	-3.6'	---	---
2	50.6'	-1.6'	---	---
3	59.3'	3.1'	---	---
4	52.4'	1.3'	50.4'	2.1'
5	52.3'	3.2'	57.0'	.4'

It was concluded that the lateral jump of the launcher as shown in Figure 2, Appendix A, is negligible, while vertical jump is of the order of one degree. The former conclusion was used in determination of the drift coefficient since observed deflections were not corrected for lateral jump (see section 7e(1)). In the regular firings for the range table,

----

measurements of rocket height at the end of burning
(section 6b(3)) also indicated a vertical jump of the same
order of magnitude as that found in the special jump test.
On several rounds the rocket was observed to be about 7.4
feet above the boresight line. This additional height,
when combined with the expected trajectory drop due to
gravity and thrust, yielded a jump of about 47 minutes.
Although the heights were not measured on all rounds fired,
the data records showed qualitatively that this jump was
incurred for each round fired.

There is ample evidence, therefore, to indicate that
the range table trajectories for any launcher elevation
should be well below the observed impact positions (shown
in Figures 15, 16, 19, and 21, Appendix F) when firing
from the modified 4-inch mount, and the discrepancies are
a result of jump.

8. SUMMARY OF NUMERICAL RESULTS

a. Thrust parameters used in the range table are for

30°F propellant temperature, $A = 3293t$, $t_b = 0.6147$,

70°F propellant temperature, $A = 2302t + 345.3$, $t_b = 0.6307$,

and

110°F propellant temperature, $A = 2739t + 410.8$, $t_b = 0.5450$,

where associated initial velocities are $\frac{1112}{3}$ yd/sec,

$\frac{1188}{3}$ yd/sec, and $\frac{1234}{3}$ yd/sec, respectively.

b. (1) To account for drag after burning, a polynomial in
Mach number for $\gamma = 1/C$ was obtained which minimized per -
centage errors in range. The minimizing polynomial was
$\gamma = 3.11 - 0.257 M^2$, where M is Mach number. The pattern
of range discrepancies (computed values minus mean corrected
observed values) in yards are listed below for four observed
times of flight and three propellant temperatures. For evalu-
ation purposes, discrepancies corresponding to the constant
ballistic coefficient $\gamma = 1/C = 2.33$ at 70°F propellant
temperature are included.

----

t (Seconds)	Discrepancies (yds)			
	$\gamma = 3.11 - .257\ M^2$			$\gamma = 2.33$
	30°F Propellant Temperature	70°F Propellant Temperature	110°F Propellant Temperature	70°F Propellant Temperature
4.0	9	-10	-15	53
7.5	40	29	-22	33
11.3	--	- 2	--	- 82
15.4	--	-45	--	-226

(2) To account for drag during burning, the constant $\gamma = 2.33$ was adjusted to the average mass during burning, giving $\gamma = 1.94.$

c. The dynamic thrust curve, represented by an eighth degree polynomial, is given in Figure 11, Appendix E; for comparison with static thrust data see Figure 13, Appendix E. Other rigid body parameters are given in Table 7, Appendix D.

d. The values

$$C_1 = 0.0017 \text{ radians}$$

$$C_2 = 286.5 \text{ yd}^2/\text{sec}^3$$

$$C_3 = 0.0028 \text{ radians}/100 \text{ kts}$$

$$C_4 = 0.0146 \text{ radians}/100 \text{ kts}$$

$$C_5 = 0.084 \text{ radians}/100 \text{ kts}$$

when used in the proper formulas generate all yawing motion effects for the conditions of

   (i) no wind

  (ii) uniform range wind

 (iii) uniform cross wind

 (iv) wind during burning in excess of the uniform wind.

The necessary formulas and instructions for their use are included in the Range Table, Appendix G, as revised by Change 1 (recommended in reference (o)).

e. (1)   The rounds fired at any given angle of elevation and propellant temperature were not of sufficient number to establish reliable quantitative dispersion data. However, corrected observed impact patterns for each angle of elevation and propellant temperature fired are given in Figures 14 through 21, Appendix F; differential effects for $70^{\circ}F$ propellant temperature are included.

(2)   For the launcher, as installed on the modified 4-inch gun mount (see Figure 2, Appendix A), it was concluded that lateral jump was negligible while vertical jump was of the order of one degree.

9. DISCUSSION AND CONCLUSIONS

The rocket T-132 (T-131), though perhaps not an entirely new concept in ballistics, provided a decidedly new type of problem in the production of a range table. To some extent this report is directed toward the exhibiting of the unconventional exterior ballistic methods used in preparing the range table.

Although quantitative dispersion measures were not found, acceptable magnitudes of dispersion were obtained in the tests. This, and other phenomena, indicated a consistency of performance of the rounds tested that was exceptionally good considering previous experiences with other lots of T-132 ammunition. The principal cause of the loss of ranging data during the Naval Proving Ground firings was not a result of poor performance of the round, but was a result of the inability to observe the inherently small splash on impact.

One of the methods used in analysis of firing data was the determination of thrust parameters in such a manner as to allow the matching of observed slant ranges and radial velocities with the computed values at a selected time shortly after burn-out. This method, generally, offers advantage in range table production over methods which use directly measured (static or dynamic) accelerations, since this method is focused on accurately obtaining those quantities which determine the after-burning trajectory. The method had previously been successfully applied in determining thrust parameters for the 2\#75 FFAR Aircraft Firing Table, OP 1998.

Originally, it was assumed (as indicated by static tests) that acceleration due to thrust could be treated as constant. Sperry Radio Doppler Chronograph instrumentation, however, gave clear and accurate information on this point; it showed, beyond reasonable doubt, that the acceleration increased markedly with time. The formulation for obtaining acceleration parameters due to thrust was then revised to allow for linear variation with time of flight.

It was discovered that the drag function for the projectile type 6.1 planned for use with the T-132 rocket was a poor estimate of the true drag function. Rather than delay production of the range table while wind tunnel or other studies produced an "ad hoc" drag coefficient, a form factor expressed as a polynomial in Mach number was determined. This type of polynomial form factor had been previously developed and tested for use in such situations; it is obtained by application of a least squares iterative technique.

Insofar as horizontal range and altitude under no wind conditions are concerned, it was found that the perfect trailing model computations would have been sufficient. Of course, the range table could not be useful without assessment of deflection or of wind effects, and any accurate assessment of deflection or of wind effects must take account of the angular motion during burning. The rigid body formulation used for this purpose is possibly more comprehensive than generally applied in the actual production of range tables. Even so, it is far from being complete. Magnus torque, for example, was neglected because indications are that large yaws are not involved in actual flight.

It was shown that the required rigid body values (especially under wind conditions) were sensitive to the form of the thrust. A cross wind (or normal component of a range wind) causes a large initial yaw, and the extent to which the thrust quickly damps this initial yaw is dependent upon the form of the thrust versus time function. A method was devised which generated the dynamic thrust from the Sperry Radio Doppler Chronograph data. This dynamic thrust agreed well with the static thrust insofar as total impulse is concerned but exhibited a progressive burning rate which could not be inferred from data obtained statically.

Derivations of deflection and wind effects formulas for rocket tables are not always easily available in the literature. Formulas of this type necessary for the T-132 rocket table are derived here for convenience of the reader and in order to exhibit the assumptions necessary to obtain them.

10. RECOMMENDATIONS

a. Drag

Discrepancies listed in the section "Ballistic Analysis" between observed slant ranges and those computed using either $\gamma = 2.33$ or $\gamma = 3.11 - 0.257 M^2$ are proof of a poor drag determination. Time limitations and ammunition requirements were such as to prevent further firings or tests to be conducted for this program, but it is recommended that for future ballistic programs involving the T-132 rocket a drag coefficient be obtained specifically for the purpose.

----

b.   Thrust

The form of the dynamic thrust curve is curious. It shows a high degree of progressive burning (rapidly increasing thrust) which contrasts with the rather uniform thrust found in static tests (see Figure 11, Appendix E). It is recommended that studies be undertaken to determine the cause and design consequences of this phenomenon.

c.   Jump

Upon production of the service mount, it is recommended that several mounts be sent to the Naval Proving Ground for jump determination. The technique employed should be that used for the test mount; i.e., two targets should be used which bracket the end of burning. From the vertical jump (end of burning) the necessary correction to angle of elevation can be computed. Also, if a non-zero lateral jump θ_z (in radians) is observed, then, where x is horizontal range, the term $\theta_z x$ must be added to the deflection obtained from the drift quoted in the range table.

d.   Range Table Ammunition and Launcher

Successful ranging measurements were not obtained on a considerable number of rounds fired as a result of the difficulty encountered in observing the small splash of the T-132 rocket on impact. Therefore, it is recommended that live-loaded T-131 rounds or T-132 rounds loaded with spotting charges be used in future range table firings of this missile.

In order to obtain jump and dispersion effects more consistent with service firings, it is recommended that future anti-aircraft range table programs be conducted with the service launcher.

----

11. REFERENCES

(a)   BUORD Conf ltr Re3d-WKB:hm S78-1(119) Ser 26269 of
      28 Sept 1951

(b)   BUORD Conf ltr Re3d-WKB:bc S78-1(119) Ser 50323 of
      12 Jan 1953

(c)   NAVPROV Conf ltr OK:ALJ:jlr All/3d439-2 Ser 32654 of
      10 June 1953

(d)   NAVPROV Conf ltr OK:ALJ:dmf All/3d439-2 Ser 35060 of
      31 Aug 1953

(e)   Final Report on Project 90-396D, Armour Research Foun-
      dation, Illinois Institute of Technology, of 31 Jul 1950

(f)   Final Report on Project 90-398D, Armour Research Foun-
      dation, Illinois Institute of Technology, of 31 Jul 1950

(g)   Redstone Arsenal Report No. 33, Project TU2-1005, of
      3 Jan 1953

(h)   Thiokol Corporation ltr Ser 53-3846 of 24 Mar 1953

(i)   NPG Conf Report No. 1216, "Ballistic Assessment of the
      AA Range Table for the 5"/38 Gun," of 15 Dec 1953

(j)   NOTS Conf Tech Memo RRB-45 of 30 Sept 1949

(k)   "Exterior Ballistics," by E. J. McShane, J. L. Kelley,
      and F. V. Reno, University of Denver Press, 1953

(l)   "New Methods in Exterior Ballistics," by Forrest Ray
      Moulton, University of Chicago Press, 1926

(m)   "The Aerodynamics of a Spinning Shell," by R. H. Fowler,
      E. G. Gallop, C. N. H. Lock, and H. W. Richmond, F. R. S.,
      Philosophical Transactions of the Royal Society of
      London, Series A, Vol. 221, pp. 295-387

(n)   Ballistic Research Laboratories Report No. 446, Aberdeen
      Proving Ground, Maryland, 29 Jan 1944 (Revised 2 Dec 1944)

(o)   NAVPROV Conf ltr OK:WEB:jlr All/3d439-2 Ser 37479 of
      29 Dec 1953
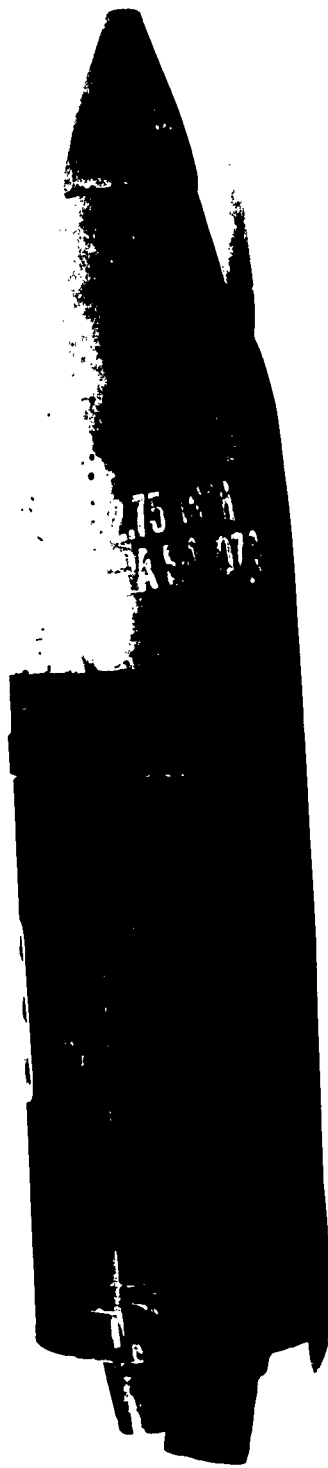
APPENDIX A

2.75-Inch Rocket, T-132, Removed from Cartridge Case.
Figure 1
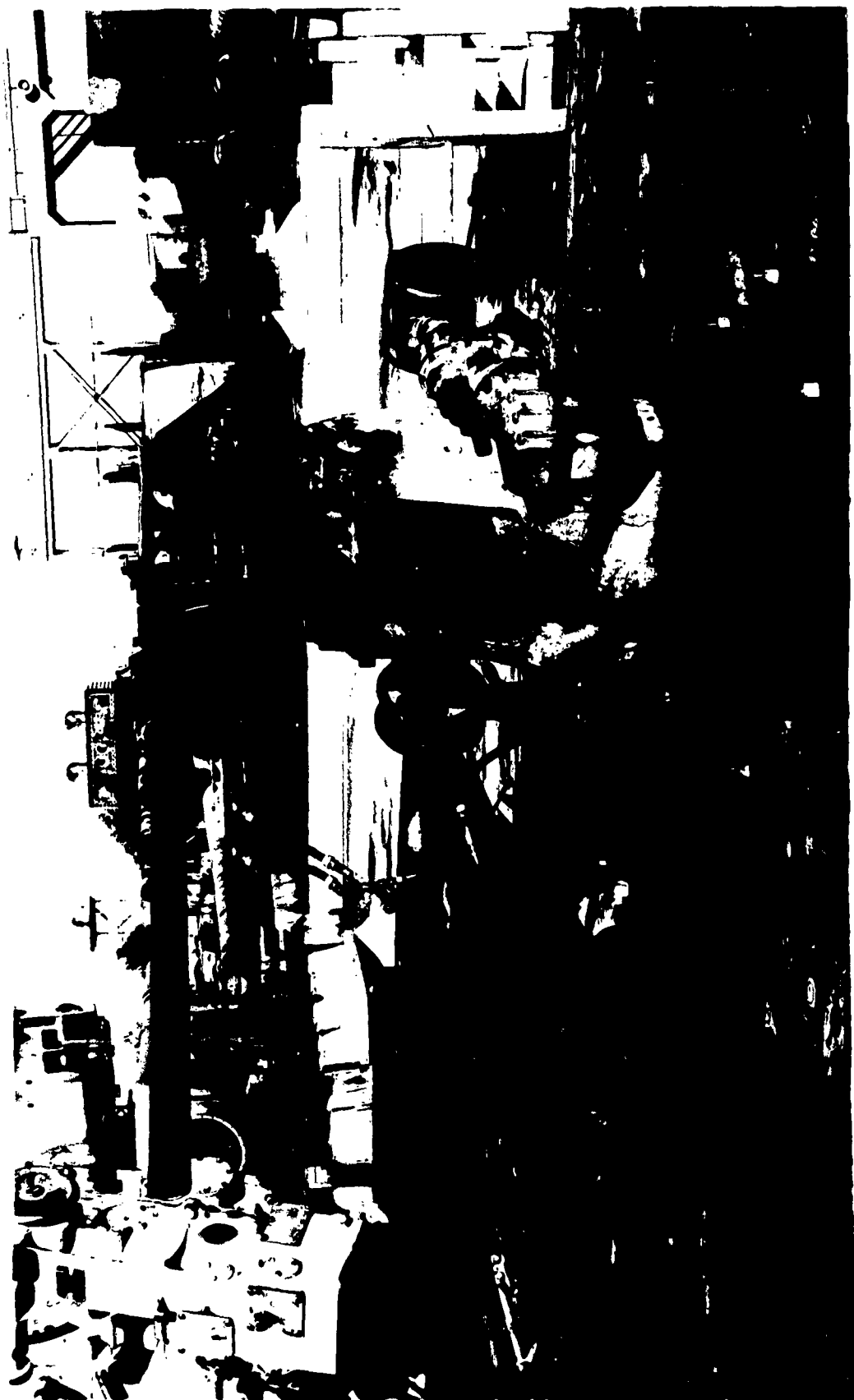
RP9-64130

Mitchell Camera, 10" lens
(impact position angle and
time of flight)

Wind Measuring Set

Launcher

End of Burning

Impact

Sperry Radio
Doppler
Chronograph
(velocity,
acceleration,
slant range and
time during burning)

Fastax Camera, 35mm lens
(muzzle velocity)

Bowen Camera, 12" lens
Mitchell Camera, 6" lens
(trajectory angle and
rocket height at
burnout)

Mitchell Camera, 6" lens
Bowen Camera, 12" lens
(impact position angle
and time of flight)

Askania Theodolite,
60 cm lens
Bowen Camera, 12"
lens,
Mitchell Camera,
6" lens
(impact position
angle and time of
flight)

SCHEMATIC LAYOUT OF BALLISTIC MEASUREMENTS EQUIPMENT

Figure 3
Appendix A

APPENDIX B
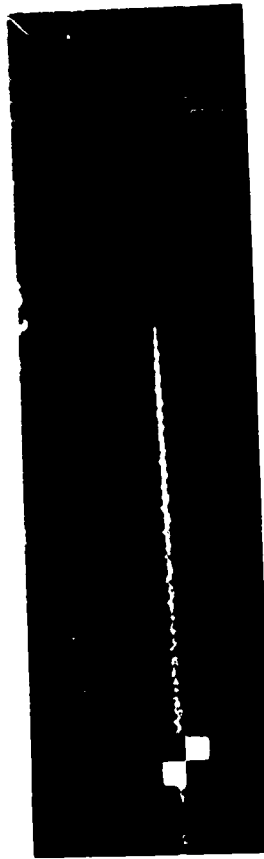
P9-6.395

Portions of Test Records Used for Spin Casing Gas Measur over a 2.47-ins 62.6s, 7-13.

Top: Doppler Signal Modulation, Drum Camera Oscillogra (1 in Dots are at intervals o one millisecond).

Bottom: Propellant Gas Trail Modulation, owed a era 11.

- -

TABLE 1   PHYSICAL MEASUREMENTS OF ROUNDS FIRED

	Unburnt Condition	Burnt Condition
Rocket Weight (pounds)	5.39	3.98
Center of gravity* (inches)	4.82	5.47
Axial Moment of Inertia (pound-inches-squared)	5.93	4.75
Transverse Moment of Inertia (pound-inches-squared)	57.2	46.9
Length (from base of motor to tip of nose fuze) (inches)	12.6	12.6

* The center of gravity position was measured from the base of the rocket motor.

The above data represent the average of measurements on two rounds for each condition. The rounds were from the lot of ammunition used for the ballistic firings.

- -

TABLE 2   RANGE TABLE FIRING CONDITIONS

Launcher Elevation Angle ° '	Propellant Temperature °F	Number of Rounds Fired
1 30	30	10
1 30	70	14
1 30	110	10
2 45	30	8
2 45	70	11
2 45	110	7
5 30	70	13
10 00	30	4
10 00	70	10
10 00	110	7
15 00	70	4

- -

TABLE 3   OBSERVED MUZZLE VELOCITIES

Date Fired	Round Number	Propellant Temperature °F	Launcher Elevation ° '	Muzzle Velocity feet/second
2-2-53	5	30	1 30	1092
2-2-53	6	30	1 30	1121
2-2-53	7	30	1 30	1121
2-2-53	8	30	1 30	1114
				1112 Average
2-2-53	1	70	1 30	1197
2-2-53	2	70	1 30	1173
2-2-53	3	70	1 30	1184
2-2-53	4	70	1 30	1187
2-16-53	1	70	2 45	1200
2-16-53	4	70	5 30	1180
2-16-53	6	70	5 30	1197
2-16-53	7	70	10 00	1188
2-16-53	8	70	10 00	1187
				1188 Average
2-16-53	10	110	10 00	1235
2-16-53	11	110	10 00	1226
2-16-53	12	110	10 00	1240
2-16-53	14	110	2 45	1234
				1234 Average

CONFIDENTIAL

TABLE 4

OBSERVED MAXIMUM VELOCITIES, WITH
CORRESPONDING SLANT RANGES AND TIMES

Date Fired	Round Number	Launcher Elevation ° '	Propellant Temperature °F	Maximum Velocity feet/second	Slant Range feet	Time** seconds
2-2-53	8	1 30	30	2642	1064	0.61
2-2-53	1	1 30	70	2617	1231	0.67
2-2-53	2	1 30	70	2702	1021	0.58
2-2-53	3	1 30	70	2576	1141	0.66
2-2-53	4	1 30	70	2687	1028	0.59
2-13-53	1	1 30	70	2675	1038	0.60
2-13-53	3	1 30	70	2670	1111	0.63
2-2-53	9	1 30	110	2769	1027	0.56
2-2-53	10	1 30	110	2581	1320	0.72
2-2-53	11	1 30	110	2669	1215	0.65
2-2-53	12	1 30	110	2645	1261	0.67
2-2-53	13	1 30	110	2815	873	0.49
2-2-53	15	1 30	110	2800	1091	0.56
2-18-53	1	2 45	30	2622	1038	0.63
2-18-53	2	2 45	30	2528	1116	0.66
2-18-53	3	2 45	30	2531	1267	0.74
2-18-53	4	2 45	30	2628	1041	0.63
2-19-53	1	2 45	30	2618	1119	0.66
2-19-53	2	2 45	30	2606	1122	0.65
2-19-53	3	2 45	30	2524	1197	0.67
2-13-53	6	2 45	70	2723	962	0.55
2-13-53	7	2 45	70	2737	1038	0.58
2-13-53	8	2 45	70	2709	1121	0.62
2-13-53	9	2 45	70	2612	1265	0.71
2-16-53	2	2 45	70	2681	1093	0.60
2-16-53	3	2 45	70	2692	1157	0.63
2-16-53	14	2 45	110	2750	1036	0.56
2-19-53	15	2 45	110	2698	1111	0.60
2-19-53	16	2 45	110	2732	1112	0.60

- -

TABLE 4 (Continued)

Date Fired	Round Number	Launcher Elevation ° '	Propellant Temperature °F	Maximum Velocity feet/second	Slant Range feet	Time** seconds
2-13-53	4	5 30	70	2749	1044	0.57
2-13-53	5	5 30	70	2739	967	0.55
2-16-53	4	5 30	70	2682	1119	0.63
2-16-53	5	5 30	70	2736	964	0.55
2-16-53	6	5 30	70	2686	976	0.55
2-18-53	9	5 30	70	2711	968	0.55
2-20-53	1	5 30	70	2648	1118	0.63
2-20-53	3	5 30	70	2694	1034	0.58
2-16-53	7	10 00	70	2738	1052	0.58
2-16-54	8	10 00	70	2761	965	0.54
2-16-53	9	10 00	70	2671	1124	0.63
3-6-53	1	10 00	70	2788	945	0.53
3-6-53	3	10 00	70	2761	947	0.52
3-6-53	4	10 00	70	2661	1213	0.66
2-16-53	10	10 00	110	2814	967	0.52
2-16-53	11	10 00	110	2784	965	0.53
2-16-53	12	10 00	110	2807	960	0.51
2-19-53	10	10 00	110	2789	960	0.52
2-19-53	11	10 00	110	2760	1040	0.56
2-19-53	12	10 00	110	2783	1034	0.56

Average values, without respect to elevation angle			30	2587(±50*)	1121(±79*)	0.66(±.04*)
			70	2697(±49*)	1063(±92*)	0.60(±.05*)
			110	2746(±69*)	1065(±117*)	0.57(±.06*)

* Standard deviation of a single observation.

** Measured from instant of current flow to the igniter.

TABLE 5

OBSERVED TRAJECTORY ANGLE AT END OF BURNING

Date Fired	Round Number	Propellant Temperature °F	Launcher Elevation ° '	Trajectory Angle At End of Burning ° '
2-2-53	5	30	1 30	0 48
2-2-53	6	30	1 30	0 52
2-2-53	8	30	1 30	0 52
				0 51 Average
2-2-53	1	70	1 30	0 52
2-2-53	2	70	1 30	0 59
2-2-53	3	70	1 30	0 54
2-2-53	4	70	1 30	0 54
				0 55 Average
2-2-53	10	110	1 30	0 58
2-2-53	11	110	1 30	0 57
2-2-53	12	110	1 30	1 00
				0 58 Average

OBSERVED IMPACT DATA

TABLE 6

Date Fired	Round Number	Launcher Elevation ° '	Propellant Temperature °F	Observed Range yds	Observed Deflection yds	Observed Time of Flight seconds	Surface Density % of Std	Surface Range Wind kts	Surface Cross Wind kts
1-26-53	5	1 30	30	2190	+3	4.07	106.83	-8.8	+2.3
1-26-53	6	1 30	30	2130	+2	3.96	106.83	-8.9	+1.3
2-2-53	5	1 30	30	2066	-5	3.81	107.53	-8.4	+2.6
2-2-53	6	1 30	30	2037	-4	3.67	107.51	-8.7	+0.3
2-2-53	7	1 30	30	2059	+4	3.73	107.50	-6.5	-0.3
2-2-53	8	1 30	30	2108	-2	3.86	107.50	-6.3	+1.7
1-22-53	1	1 30	70	2163	+1	3.92	104.63	-3.4	+0.5
1-22-53	2	1 30	70	2289	+3	4.19	104.82	-3.9	+0.5
1-22-53	3	1 30	70	2108	-1	3.76	104.88	-4.3	+0.6
1-26-53	1	1 30	70	2175	-1	4.09	106.89	-9.3	+2.8
1-26-53	2	1 30	70	2371	+2	4.38	106.87	-8.9	+2.8
1-26-53	3	1 30	70	2310	-8	4.24	106.84	-8.6	+5.1
2-2-53	1	1 30	70	2184	-2	3.94	106.84	-8.7	+3.4
2-2-53	2	1 30	70	2219	+2	4.11	107.79	-4.8	+1.3
2-2-53	3	1 30	70	2150	0	3.95	107.71	-7.2	+0.8
2-2-53	4	1 30	70	2183	0	3.95	107.66	-8.6	+1.7
1-26-53	7	1 30	110	2412	0	4.28	106.78	-8.9	+1.3
1-26-53	8	1 30	110	2415	+2	4.28	106.84	-9.4	+1.4
1-26-53	9	1 30	110	2276	-1	3.99	106.92	-10.2	+1.5
2-2-53	9	1 30	110	2249	-2	4.03	107.51	-10.0	+3.6
2-2-53	10	1 30	110	2222	+1	4.02	107.52	-9.3	+2.3
2-2-53	11	1 30	110	2276	0	4.11	107.53	-8.8	+1.7
2-2-53	12	1 30	110	2226	-1	3.97	107.53	-10.0	+0.5
2-2-53	13	1 30	110	2309	+6	4.17	107.53	-9.9	-1.0
2-2-53	14	1 30	110	2157	+4	3.92	107.53	-7.2	-0.3
2-2-53	15	1 30	110	2346	-2	4.14	107.53	-7.3	+1.7

TABLE 6 (Continued)

Date Fired	Round Number	Launcher Elevation ° '	Propellant Temperature °F	Observed Range yds	Observed Deflection yds	Observed Time of Flight seconds	Surface Density % of Std	Surface Range Wind kts	Surface Cross Wind kts
2-18-53	1	2 45	30	3051	+20	7.41	108.90	+8.6	=8.0
2-18-53	2	8 45	30	3066	+20	7.54	108.93	+8.6	=6.4
2-18-53	3	2 45	30	3062	+ 8	7.80	108.72	19.3	=3.9
2-18-53	4	2 45	30	3115	+13	7.56	108.66	+9.4	=3.1
2-18-53	5	2 45	30	3104	+14	7.40	108.03	=2.7	+7.8
2-18-53	6	2 45	30	3107	+12	7.46	106.94	-1.9	16.1
2-18-53	7	2 45	30	3047	+11	7.28	106.86	=2.2	14.4
2-18-53	8	2 45	30	3027	+11	7.27	106.79	=2.6	14.2
	1		70	3240	+19	7.60	104.96	-1.9	=5.7
	2		70	3201	+16	7.58	104.54	-1.9	=5.7
	3			3151	+11	7.49	105.06	+3.6	=2.2
	4			3174	+22	7.47	105.52	=3.4	=2.2
	5			3102	+21	7.32	107.02	=1.3	=3.1
	6			3157	+25	7.55	107.13	=3.4	=4.4

TABLE 6 (Continued)

Date Fired	Round Number	Launcher Elevation ° '	Propellant Temperature °F	Observed Range yds	Observed Deflection yds	Observed Time of Flight[2] seconds	Surface Density % of Std	Surface Range Wind kts	Surface Cross Wind kts
2-18-53	1	2 45	30	3051	+20	7.41	108.90	+8.5	-6.5
2-18-53	2	2 45	30	3066	+20	7.54	108.83	+8.8	-5.4
2-18-53	3	2 45	30	3062	+8	7.30	108.73	+9.3	-3.8
2-18-53	4	2 45	30	3115	+13	7.56	108.66	+9.4	-3.1
2-19-53	1	2 45	30	3104	+14	7.40	106.03	-2.7	+5.2
2-19-53	2	2 45	30	3107	+12	7.46	105.94	-1.9	+5.0
2-19-53	3	2 45	30	3047	+11	7.26	105.86	-2.3	+4.4
2-19-53	4	2 45	30	3027	+11	7.27	105.79	-2.6	+4.2
2-16-53	1	2 45	70	3240	+18	7.60	104.92	-1.9	-5.7
2-16-53	2	2 45	70	3201	+16	7.58	104.84	-1.9	-5.7
2-18-53	5	2 45	70	3151	+11	7.49	108.58	+9.0	-2.9
2-18-53	6	2 45	70	3174	+22	7.47	108.52	+8.8	-2.9
2-18-53	7	2 45	70	3102	+21	7.38	107.32	+0.3	-3.5
2-18-53	8	2 45	70	3187	+25	7.59	107.15	-0.6	-6.8
2-16-53	14	2 45	110	3200	+26	7.41	103.49	-5.2	-6.0
2-19-53	13	2 45	110	3121	+18	6.98	105.27	-5.2	+2.9
2-19-53	14	2 45	110	3134	+21	7.01	105.26	-5.8	+1.9
2-19-53	15	2 45	110	3160	+27	7.29	105.25	-6.6	+2.6
2-19-53	15	2 45	110	3210	+28	7.36	105.24	-7.3	+5.4
2-12-53	10	5 30	70	3842	+44	11.38	106.90	+1.4	-8.0
2-18-53	11	5 30	70	3874	+41	11.48	106.81	+2.7	-8.0
2-20-53	1	5 30	70	3885[1]	+38	11.53	105.23	-6.4	-1.4
2-20-53	2	5 30	70	3961[1]	+31	10.96	105.17	-4.4	-1.1
2-20-53	3	5 30	70	3848	+25[1]	--	105.10	-8.5	-2.0
2-20-53	4	5 30	70	3827	+26[1]	11.14	105.03	-8.5	-2.4
2-20-53	5	5 30	70	3844	+24[1]	--	104.93	-5.9	-0.5

[1]Excluded from range table analysis.
[2]Measured from the instant of current flow to the igniter to the instant of impact.

All impacts occurred approximately 24 feet below the launcher muzzle.
A positive range wind is a tail wind.
A positive cross wind is from left to right, looking down range.
A positive deflection is to the right of the line of fire, looking down range.

APPENDIX C

70°F PROPELLANT TEMPERATURE

Locus of Points for which Computed Slant Range Equals Average Observed Slant Range for Group.

Locus of Points for which Computed Radial Velocity Equals Average Observed Radial Velocity for Group.

X - Grid Points for which Trajectories Were Computed (See Paragraph 7b(1))

0 - Interpolated Points. These Points Define the Loci for which Observed and Computed Values Match.
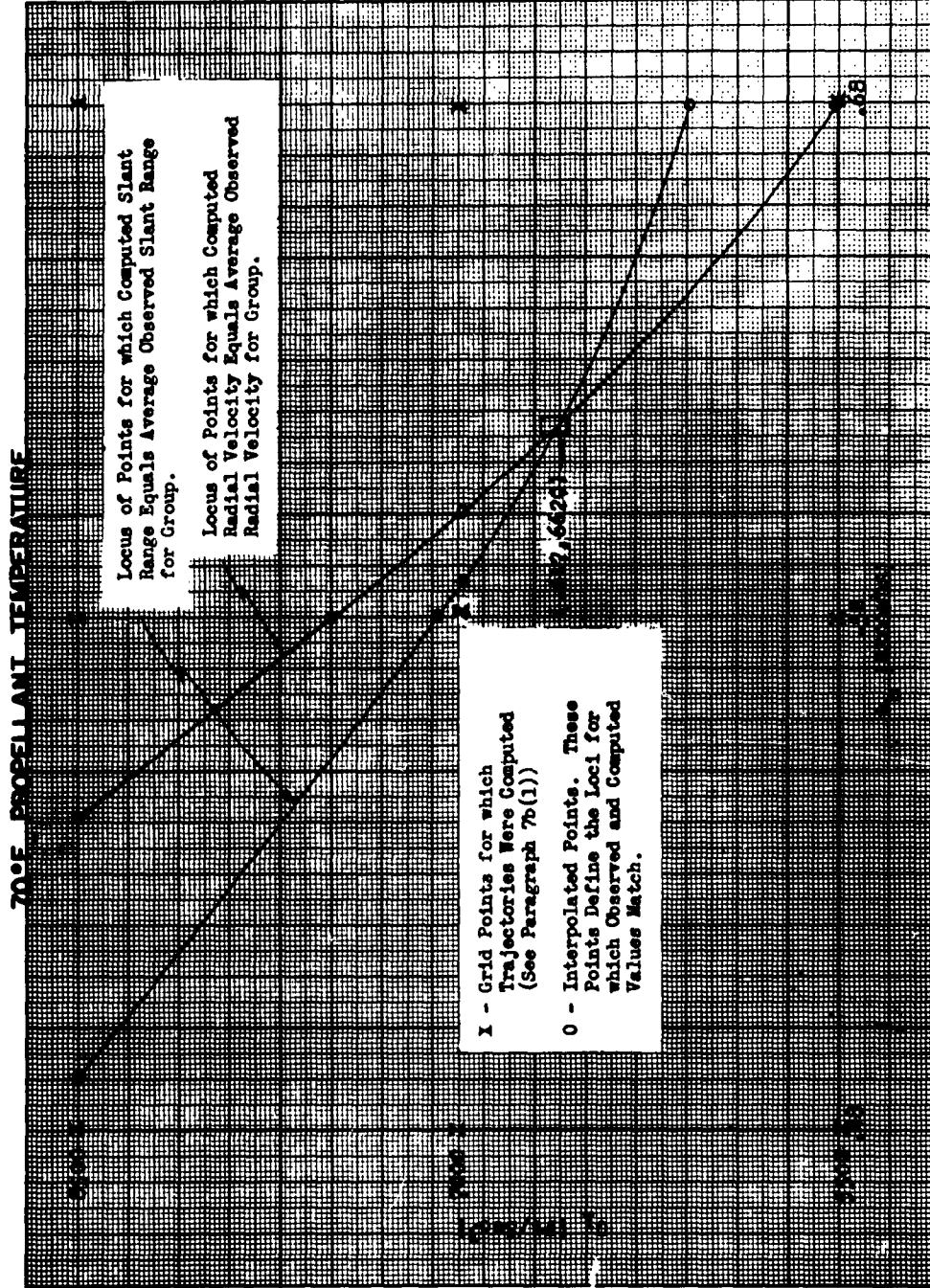
ANALYSIS OF A TYPICAL GROUP* FOR ACCELERATION PARAMETERS, t_b AND c_s

* Group Consisted of Four Rounds Fired on 13 February 1953 at Angle of Elevation of 2°45'
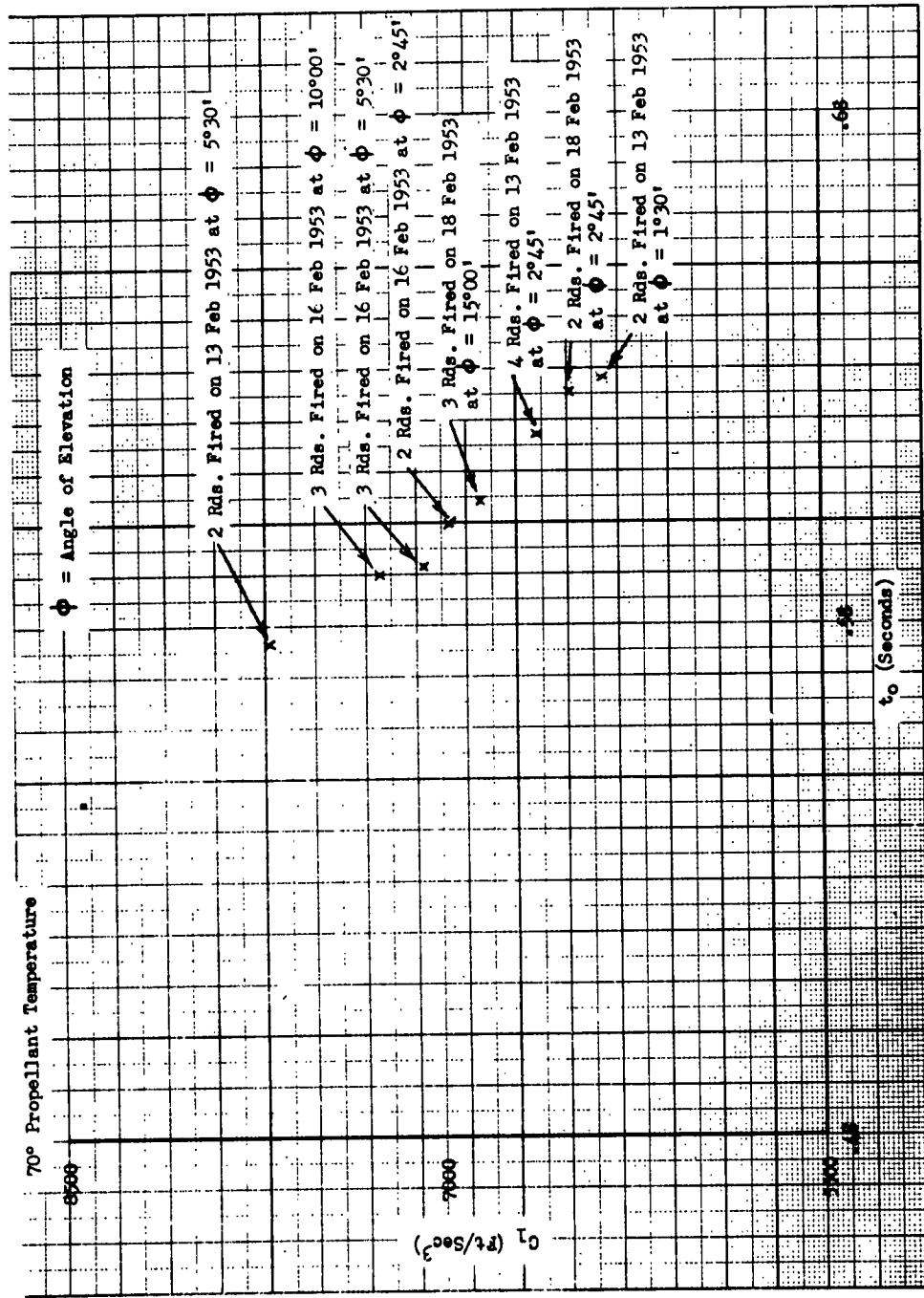
Figure 5

GROUP TO GROUP DISPERSION OF ACCELERATION PARAMETERS t_b AND c_i
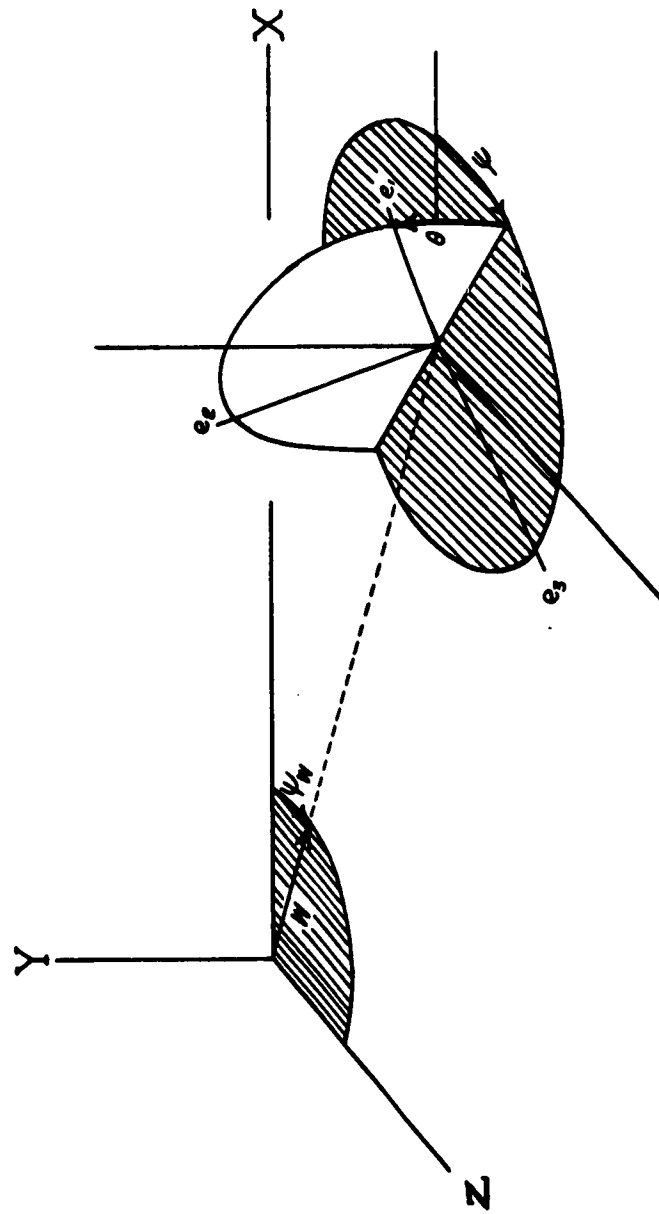
APPENDIX D

X, Y, Z - Rectangular System Fixed on the Earth.

e_1, e_2, e_3 - Right-handed System of Unit Vectors with e_1 along
Rocket Axis and e_3 in Horizontal Plane.

COÖRDINATE SYSTEM

(Rigid Body Integrations)

Figure 7
Appendix D

TABLE 7. RIGID BODY EQUATIONS OF MOTION

Force Equations:

$$\dot{v}_1 = \frac{1}{m}\left[T - \rho d^2 K_{DA} v^2\right] - g\sin\theta + v_2\omega_3 - v_3\omega_2$$

$$\dot{v}_2 = -\frac{1}{m}\rho d^2 K_N v v_2 - g\cos\theta - v_1\omega_3 + v_3\omega_2\tan\theta$$

$$\dot{v}_3 = -\frac{1}{m}\rho d^2 K_N v v_3 + v_1\omega_2 - v_2\omega_2\tan\theta$$

Torque Equations:

$$A\dot{\omega}_1 = KT + C_1\omega_1 v_1$$

$$B\dot{\omega}_2 = -(\lambda - r)\rho d^2 K_N v v_3 - (\rho d^4 K_H v - \dot{m}l^2)\omega_2$$

$$- A\omega_1\omega_3 + \omega_3\omega_2\tan\theta$$

$$B\dot{\omega}_3 = B\ddot{\theta} = (\lambda - r)\rho d^2 K_N v v_2 - (\rho d^4 K_H v - \dot{m}l^2)\omega_3$$

$$+ A\omega_1\omega_2 - B\dot{\omega}_3^2\tan\theta$$

$\dot{\theta}$ Equation:

$$\dot{\theta} = \omega_3$$

Equations for generating coordinates ψ, X, Y, and Z (see Figure 7) from solutions of the force, torque, and $\dot{\theta}$ equations are:

$$\dot{\psi} = - \omega_2 \sec \theta$$

$$\dot{X} = v_1 \cos \theta \cos \psi - v_2 \sin \theta \cos \psi - v_3 \sin \psi + W \cos \psi_W$$

$$\dot{Y} = v_1 \sin \theta + v_2 \cos \theta$$

$$\dot{Z} = v_1 \cos \theta \sin \psi - v_2 \sin \theta \sin \psi + v_3 \cos \psi + W \sin \psi_W$$

For parameters and for equations which generate B, m, r, and T as functions of t, see Table 9. For definition of symbols see Table 8.

TABLE 8. LIST OF SYMBOLS FOR RIGID BODY EQUATIONS

Moments of Inertia:

A	axial moment of inertia
B	instantaneous moment of inertia about a transverse axis through the instantaneous center of gravity

Force Parameters:

g	acceleration due to gravity
K_{DA}	axial drag coefficient
K_N	normal force coefficient
T	thrust resulting from jet action in direction of the rocket axis

Torque Parameters:

K	axial moment coefficient resulting from thrust of the rocket motor
C_1	coefficient associated with spin damping
K_H	cross-spin damping coefficient
λ	distance from nose to aerodynamic center of pressure
r	distance from nose to instantaneous center of gravity
l	length associated with jet damping

Velocities:

v	velocity of the particle at the instantaneous center of gravity, relative to the air mass
v_1, v_2, v_3	components of v resolved in the directions $\varepsilon_1, \varepsilon_2, \varepsilon_3$, respectively (see Figure 7)
$\omega_1, \omega_2, \omega_3$	components of angular velocity (as determined by motion of the rocket relative to the rectangular system x, y, z) resolved in the instantaneous direction $\varepsilon_1, \varepsilon_2, \varepsilon_3$ (see Figure 7)

Other Symbols:

t   time (t = 0 at ignition)

m   instantaneous mass of the rocket

ρ air density

d   diameter of rocket

θ inclination of rocket axis

ψ angle from line of fire to horizontal projection of rocket axis

W   magnitude of wind velocity relative to X, Y, Z axis system

ψ_W angle in X, Z plane specifying wind direction (see Figure 7) = arc tan $\dfrac{W_Z}{W_X}$

- -

TABLE 9   RIGID BODY PARAMETERS

(See Table 8 for definition of symbols)

Moments of inertia:

$$A = 0.001269 \text{ slug ft}^2$$

$$B = -0.006561 + 0.02634 \, m + 0.02237 \, r \text{ slug ft}^2$$

Mass:

$$m = -0.000182 \int_0^t T \, dt + 0.1685 \text{ slugs}$$

Air density:

$$\rho = \frac{.07513}{32.2} \text{ slugs/ft}^3$$

Force parameters:

$$g = 32.2 \text{ ft/sec}^2$$

$$K_{DA} = 0.15$$

$$K_N = 1.1$$

$$T = 16,655,218 \, t^8 - 33,058,162 \, t^7$$
$$+ 25,263,620 \, t^6 - 9,345,193.0 \, t^5$$
$$+ 1,692,133.9 \, t^4 - 122,782.69 \, t^3$$
$$- 1486.6128 \, t^2 + 1945.1327 \, t$$
$$+ 118.778372 \text{ lbs.}$$

- -

TABLE 9 (Continued)

Torque parameters:

$$K = 0.0167$$

$$C_1 = 3.55 \times 10^{-8}$$

$$K_H = 1.45$$

$$\lambda = 0.38 \text{ ft}$$

$$r = 0.7820 - \frac{0.02237}{m} \text{ ft}$$

$$l^2 = 1.05 \text{ ft}^2$$

Note: Overturning moment is formulated in terms of K_N and $(\lambda - r)$ so that a value of K_M is not given.

Initial conditions (propellant temperature of 70°F):

mass at muzzle	= 0.1685 slugs
initial velocity	- 1188 ft/sec
initial spin	= 2740 rad/sec
time at muzzle	= 0 sec

APPENDIX B

ẏ/ẋ vs ż/ẋ for 20 knot wind, g = 0, $\varphi = 0°$

ż/ẋ

ẏ/ẋ

$\frac{d}{dt}(\dot{z}/\dot{x}, \dot{y}/\dot{x})$ for perfect trailing at $t = t_0 = .50$

Constant Thrust, T = 418.76 lbs.
Linear Thrust, T = 733t + 198.86 lbs.
Dynamic Thrust Fit by an Eight Degree Polynomial

$T = 16,655,218\ t^8 - 33,058,162\ t^7 + 25,263,620\ t^6$
$- 9,345,193.0\ t^5 + 1,692,133.9\ t^4 - 122,782.69\ t^3$
$- 1486.6128\ t^2 + 1945.1327\ t + 118.778372$ lbs.
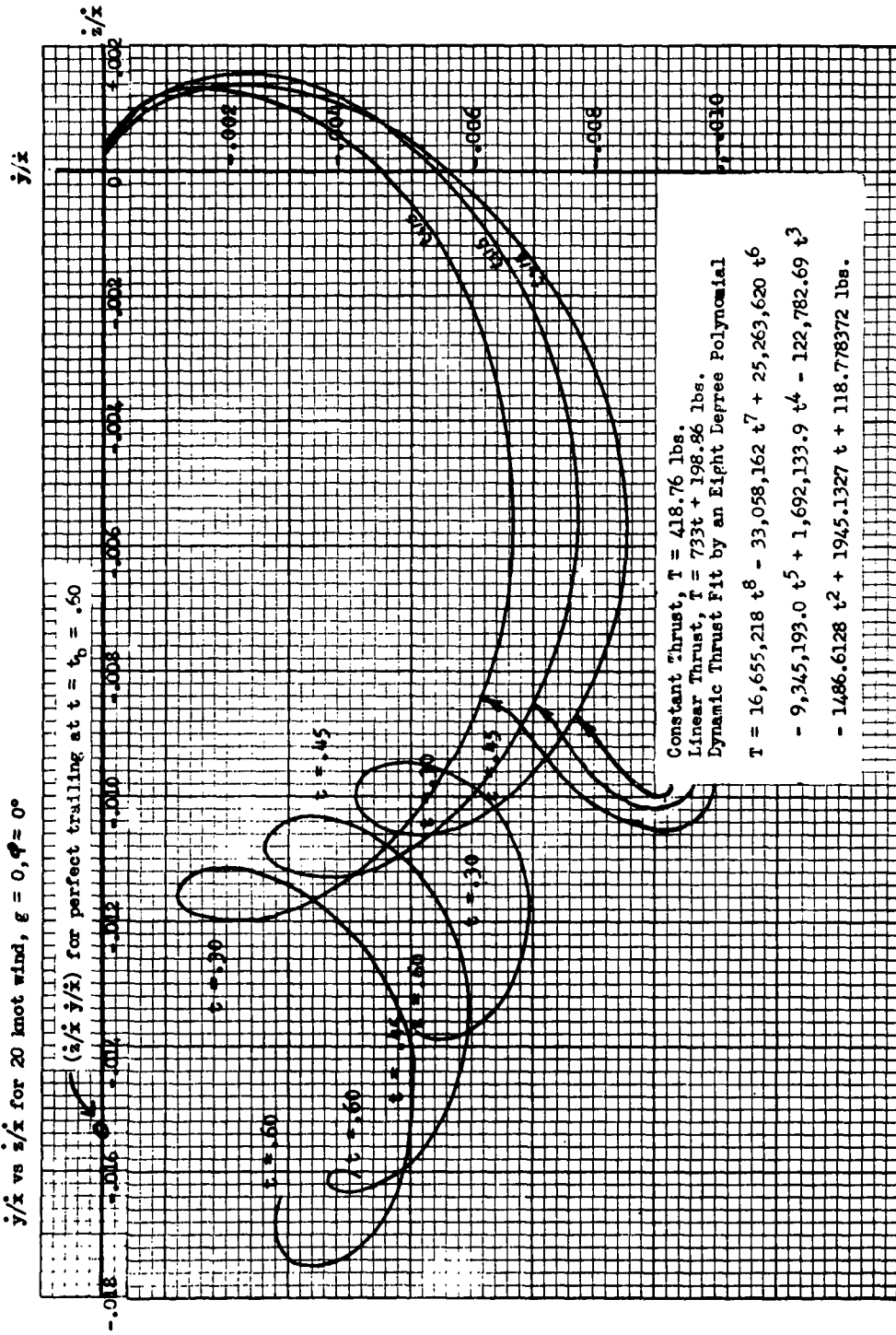
SENSITIVITY OF RIGID BODY SOLUTIONS TO FORM OF THE THRUST

Figure 8
Appendix E

Four Doppler Velocity Curves for Firing on 16 February 1953.
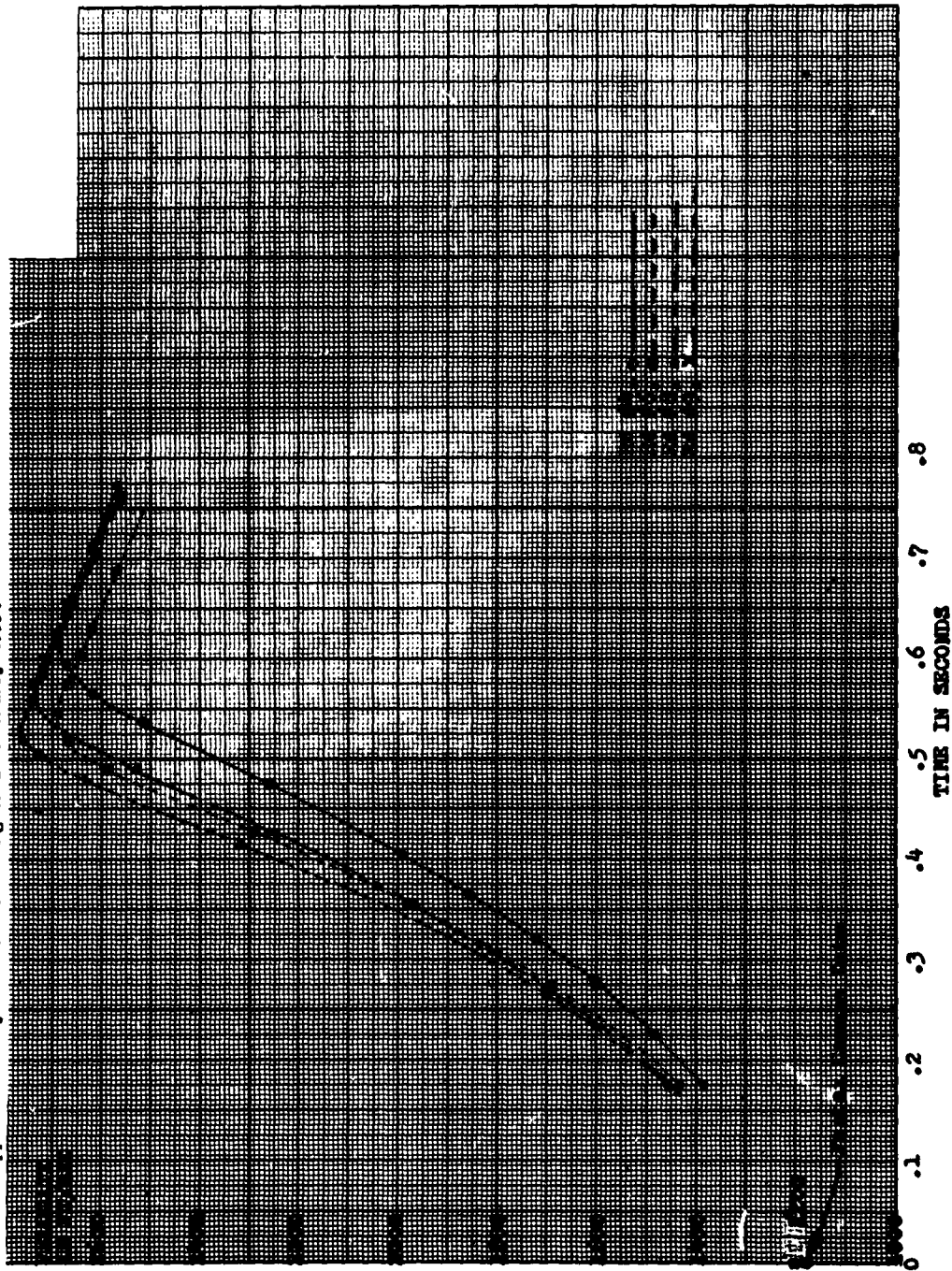
VELOCITY VS. TIME FOR DYNAMIC THRUST DETERMINATION

TIME IN SECONDS

Figure 9
Appendix E

Doppler Velocity Curves of Figure 9 Normalized with Respect to Maximum Velocity and Time to Maximum Velocity
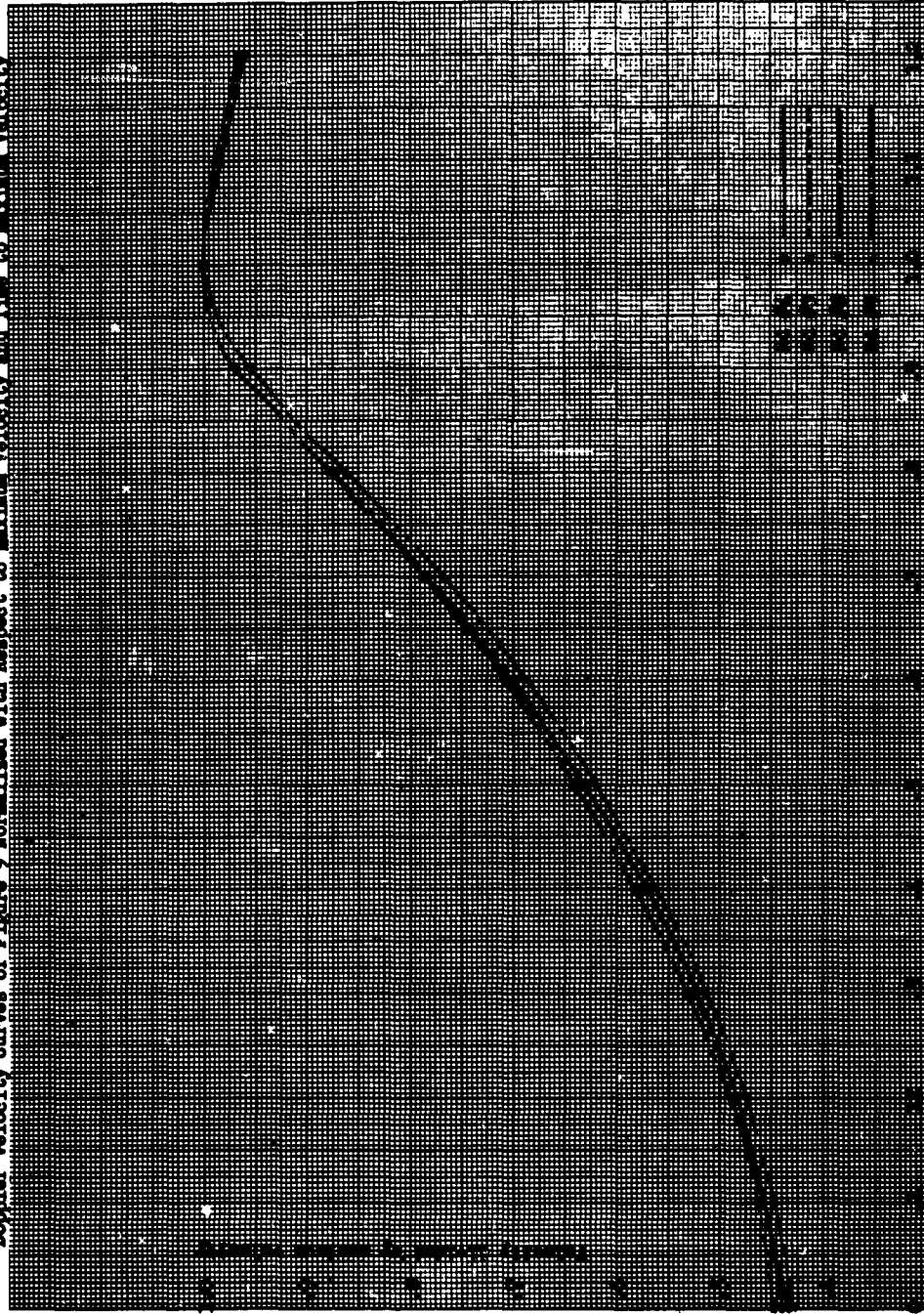
Time divided by time to maximum velocity

NORMALIZED VELOCITY VS. TIME FOR DYNAMIC THRUST DETERMINATION

Figure 10
Appendix B

Constant Thrust, T = 418.76

Linear Thrust, T = 733 t + 198.86

Dynamic Thrust Fit by an Eighth Degree Polynomial,

$T = 16,655,218\ t^8 - 33,058,162\ t^7 + 25,263,620\ t^6$
$- 9,345,193.0\ t^5 + 1,692,133.9\ t^4 - 122,782.69\ t^3$
$- 1486.6128\ t^2 + 1945.1327\ t + 118.778372$

Time in Seconds
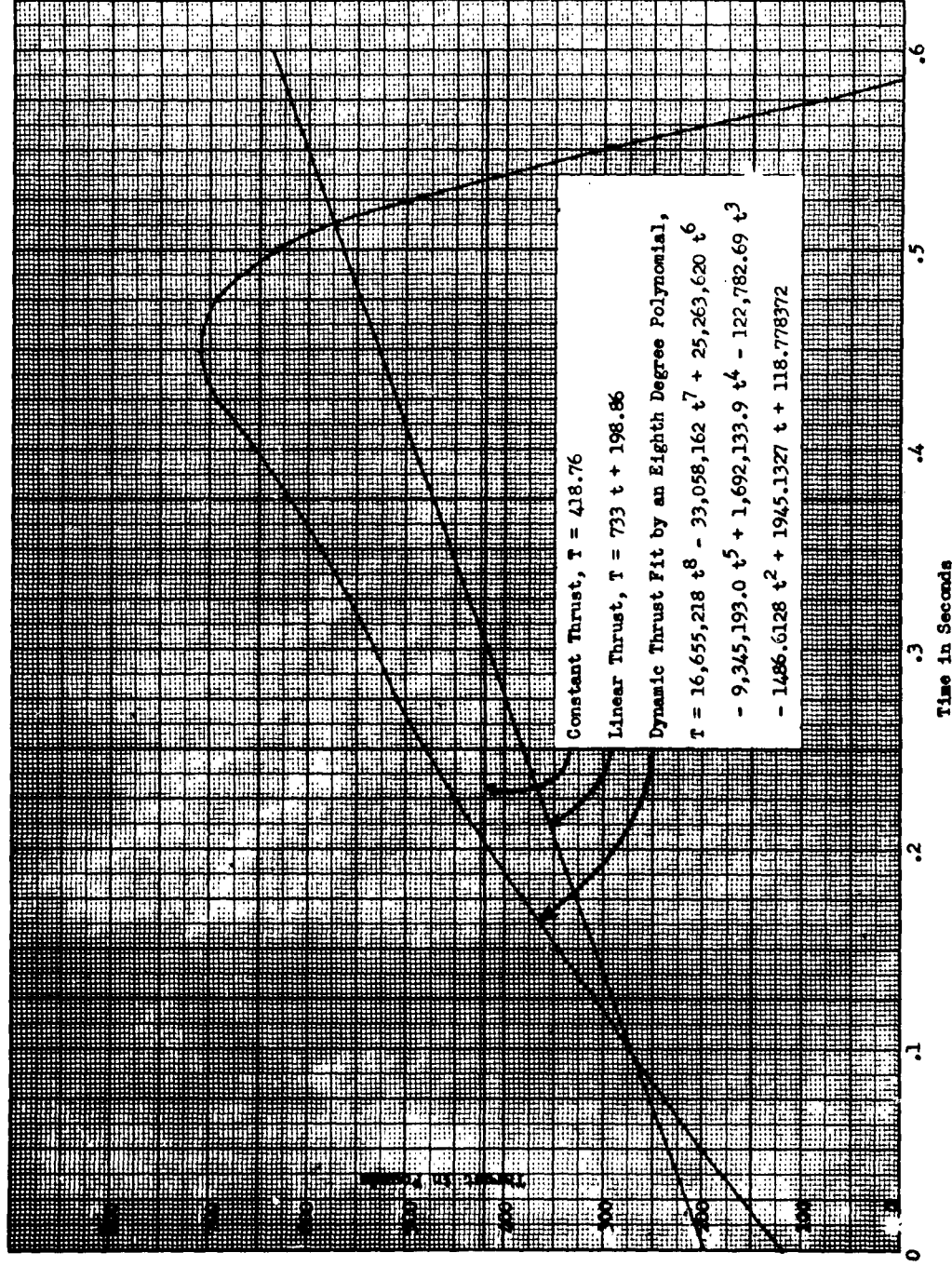
CURVES OF CONSTANT, LINEAR, AND DYNAMIC THRUST

CONFIDENTIAL

Figure 11
Appendix E
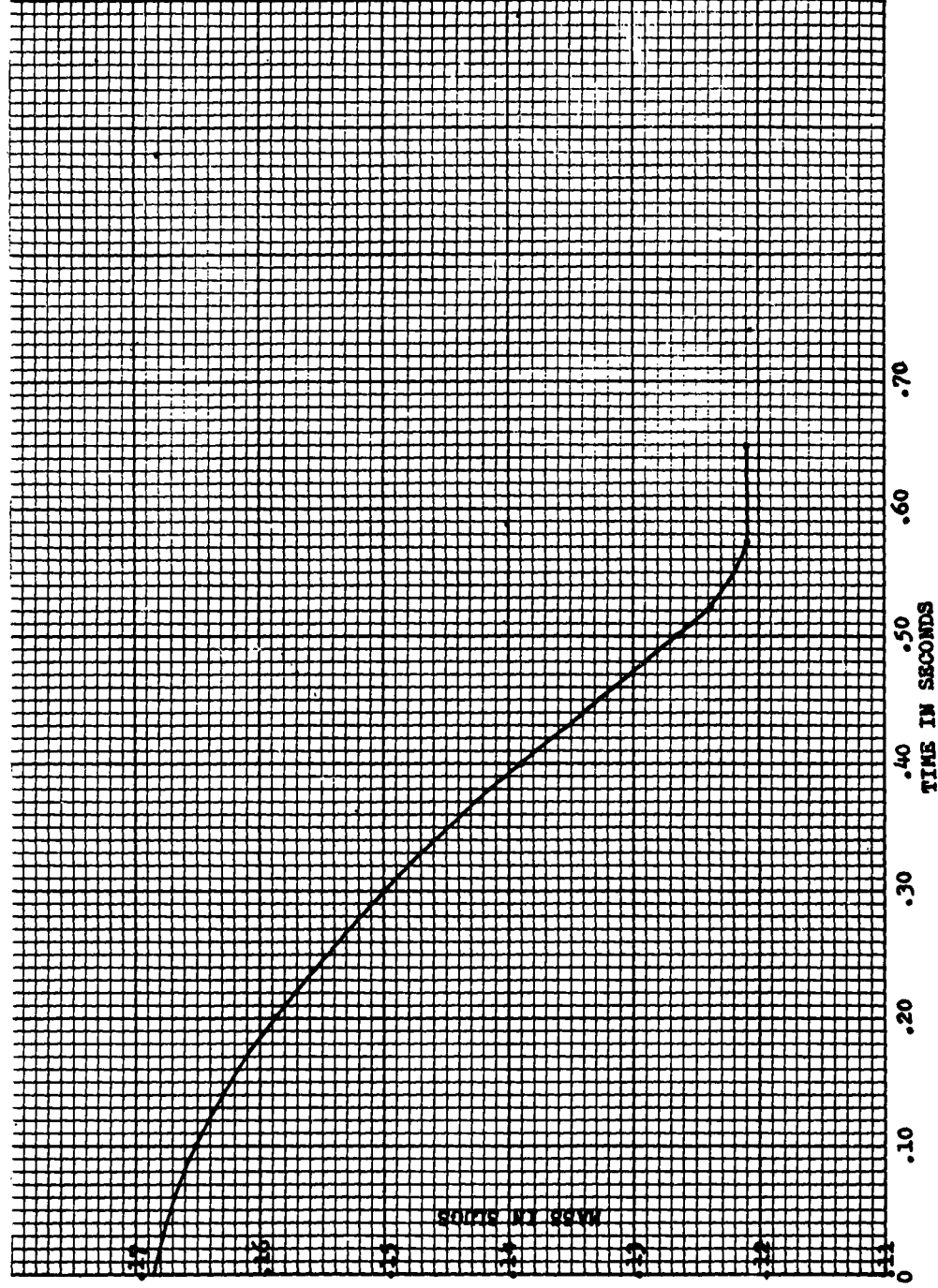
CURVE OF MASS VS. TIME ASSOCIATED WITH DYNAMIC THRUST

Figure 12
Appendix B

70°F PROPELLANT TEMPERATURE

(a) DATA OBTAINED BY THIOKOL CORPORATION, CONTAINED IN REFERENCE (h).

THRUST, LBS.

500

0

0   0.1   0.2   0.3   0.4   0.5   0.6   0.7   0.8

TIME IN SECONDS
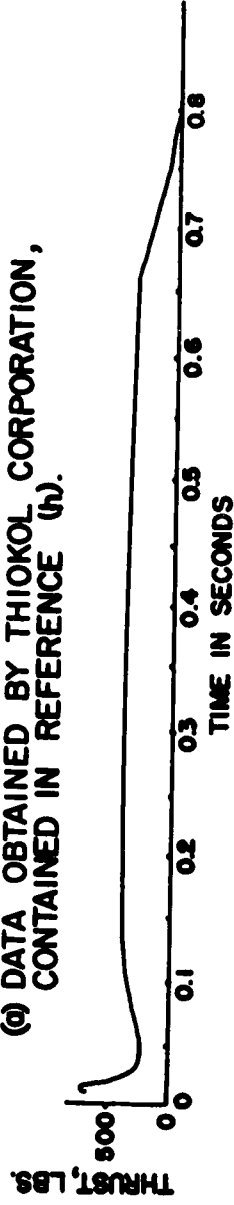
(b) DATA OBTAINED BY NAVAL PROVING GROUND

THRUST, LBS.

500

0

0   0.1   0.2   0.3   0.4   0.5   0.6   0.7   0.8   0.9

TIME IN SECONDS
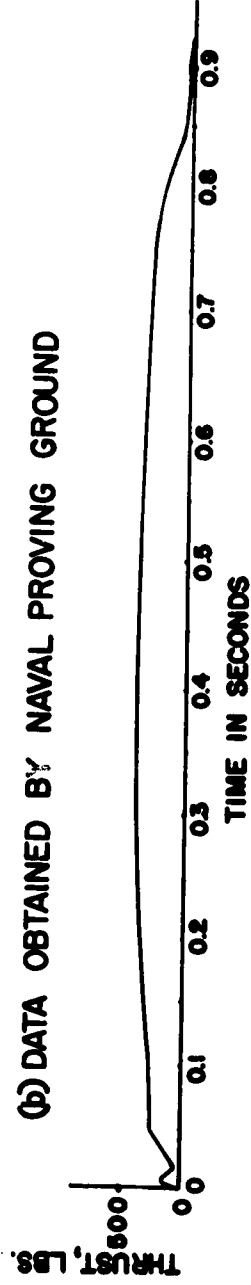
STATIC THRUST VERSUS TIME

Figure 13
Appendix E

APPENDIX F

1°30' QE Surface Firing

70° Propellant Temperature

   ⊙ 22 January 1953

   ⊟ 26 January 1953

   △ 2 February 1953

Departure in Yards
from Range Table Altitude

Departure in Yards from Range Table Range

Range Table Range 2282.3 yds

Range Table Altitude -6.5 yds

Range Table Time of Flight 4.0537 secs

A - Vector for 1%C

B - Vector for +10 min ∅

C - Vector for +10 ft/sec Initial Velocity

D - Vector for +10 kt Range Wind

E - Vector for 0.1 sec Time of Flight

F - Vector for +20°F Air Temperature

RANGE TABLE DIFFERENTIALS AND DEPARTURES FROM RANGE TABLE IN PLANE OF FIRE

FOR CORRECTED DATA

Figure 14
Appendix F

2°45' QE Surface Firing

70° Propellant Temperature

⊙ 16 February 1953

□ 18 February 1953

Departure in Yards
from Range Table Altitude

Departure in Yards from Range Table Range

Range Table Range 3227.3 yds

Range Table Altitude -52.2 yds

Range Table Time of Flight 7.5037 sec

A - Vector for 1%C

B - Vector for +10 min ∅

C - Vector for +10 ft/sec Initial Velocity

D - Vector for +10 kt Range Wind

E - Vector for 0.1 sec Time of Flight

F - Vector for +20°F Air Temperature

RANGE TABLE DIFFERENTIALS AND DEPARTURES FROM RANGE TABLE IN PLANE OF FIRE FOR CORRECTED DATA

Figure 15
Appendix F

5°30' QE Surface Firing

70° Propellant Temperature

18 February 1953

20 February 1953

Departure in Yards
from Range Table Altitude

x = +187.0 Maverick
y = + 40.2

Departure in Yards from Range Table Range

Range Table Range 3979.5 yds

Range Table Altitude -60.2 yds

Range Table Time of Flight 11.2987 sec

A - Vector for 1°C
B - Vector for 10 min ∅
C - Vector for +10 ft/sec
    Initial Velocity
D - Vector for +10 kt
    Range Wind
E - Vector for 0.1 sec
    Time of Flight
F - Vector for +20°F
    Air Temperature

RANGE TABLE DIFFERENTIALS AND DEPARTURES FROM RANGE TABLE IN PLANE OF FIRE FOR CORRECTED DATA

Figure 16
Appendix F

10° QE Surface Firing

70°F Propellant Temperature

⊕ 20 February 1953
    Observed Slant Ranges
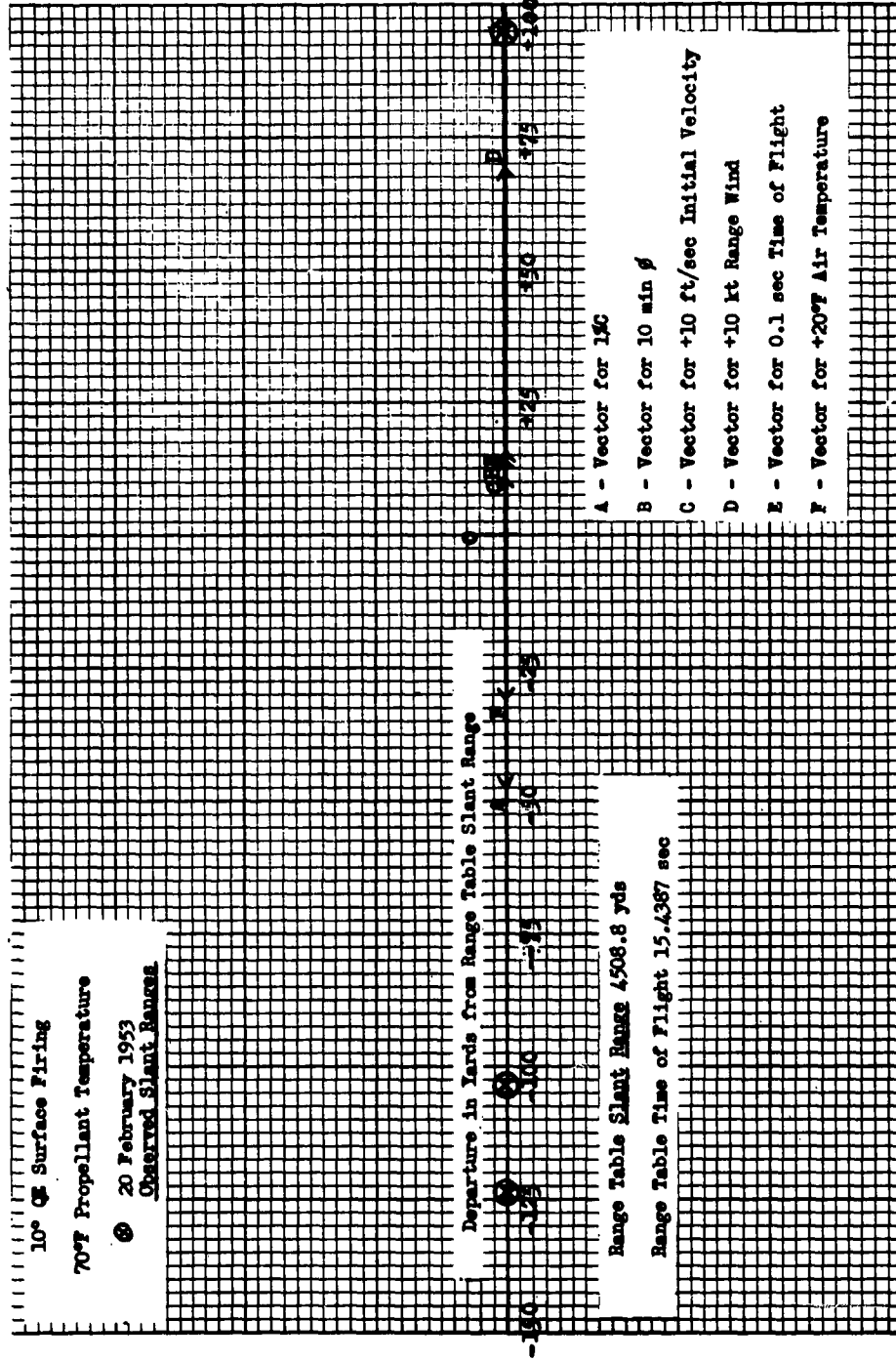
Departure in Yards from Range Table Slant Range

Range Table Slant Range 4508.8 yds

Range Table Time of Flight 15.4387 sec

A - Vector for 1%C

B - Vector for 10 min ∅

C - Vector for +10 ft/sec Initial Velocity

D - Vector for +10 kt Range Wind

E - Vector for 0.1 sec Time of Flight

F - Vector for +20°F Air Temperature

-150   -125   -100   -75   -50   -25   +25   +50   +75   +100

RANGE TABLE DIFFERENTIALS AND DEPARTURES FROM RANGE TABLE IN PLANE OF FIRE

FOR CORRECTED DATA

Figure 17
Appendix F

DEPARTURES FROM RANGE TABLE IN PLANE OF FIRE FOR CORRECTED DATA

Figure 18
Appendix F

CONFIDENTIAL

CONFIDENTIAL

DEPARTURES FROM RANGE TABLE IN PLANE OF FIRE FOR CORRECTED DATA

Figure 19
Appendix P

1°30' QE Surface Firing

110° Propellant Temperature

⊙ 26 January 1953

⊟ 2 February 1953

Departure in Yards
from Range Table Altitude

Departure in Yards from Range Table Range

Range Table Range 2318.0 yds

Range Table Altitude -5.4 yds

Range Table Time of Flight 3.995 sec

DEPARTURES FROM RANGE TABLE IN PLANE OF FIRE FOR CORRECTED DATA

Figure 20
Appendix F

2°45' QE Surface Firing

110° Propellant Temperature

16 February 1953

19 February 1953

Departure in Yards
from Range Table Altitude

Departure in Yards from Range Table Range

Range Table Range 3275.3 yds

Range Table Altitude -44.7 yds

Range Table Time of Flight 7.445 sec

DEPARTURES FROM RANGE TABLE IN PLANE OF FIRE FOR CORRECTED DATA

Figure 21
Appendix F

APPENDIX G

Tables of Ballistic Data for Anti-Aircraft Fire Control Equipment for 2.75-In. Rocket T-132

1. The tables of ballistic data for anti-aircraft fire control equipment for the 2.75-In. Rocket T-132 are presented in six (6) parts as shown below:

PART I

    a. Elements of Trajectories versus Time of Flight and Elevation for 70°F Propellant Temperature

    b. Sight Angle versus Slant Range and Position Angle for 70°F propellant Temperature

    c. Time of Flight versus Slant Range and Position Angle for 70°F Propellant Temperature

PART II

    a. Drift versus Time of Flight and Position Angle for 70°F Propellant Temperature

    b. Deflection due to Cross Wind versus Time of Flight and Position Angle for 70°F Propellant Temperature

PART III

    a. Effect on Horizontal Range and Altitude due to:

        Change in Initial Velocity
        Change in Air Density
        Change in Air Temperature
        Change in Elevation
        Rear Wind

    for 70°F Propellant Temperature

PART IV

    a. Corrections to Sight Angle and Time of Flight for:

        Change in Initial Velocity
        Change in Air Density
        Change in Air Temperature
        Rear Wind

    for 70°F Propellant Temperature

PART V

    a. Sight Angle versus Slant Range and Position Angle for 30°F Propellant Temperature

    b. Time of Flight versus Slant Range and Position Angle for 30°F Propellant Temperature

PART VI

    a. Sight Angle versus Slant Range and Position Angle for 110°F Propellant Temperature

    b. Time of Flight versus Slant Range and Position Angle for 110°F Propellant Temperature

2. It is to be noted that in these tables the time in all instances is measured from the closing of the ignition circuit. Measurements have shown that at 70°F propellant temperature the interval from the closing of the ignition circuit to the instant the projectile emerges from the muzzle of the launcher is approximately 0.013 second.

3. The ballistic data used in the preparation of these tables were obtained from firings of 52 rounds, 14 of which were fired with a propellant temperature of 30°F, 23 with a temperature of 70°F and 15 with a temperature of 110°F. All rounds were fired from ground launchers. The angles of elevation ranged from 1°30' to 5°30' with times of flight to surface impact of approximately 4, 8, and 12 seconds.

4. The basic trajectories used in the preparation of the tables are solutions of the following system of differential equations in which perfect trailing is assumed:

$$\ddot{x} = \left(\frac{A}{v} - E\right)\dot{x}$$

$$\ddot{y} = \left(\frac{A}{v} - E\right)\dot{y} - g$$

In these equations,
    x is horizontal range (yds);
    y is altitude (yds);
    A is acceleration (yds/sec^2) due to thrust;
    v is velocity of the rocket (yds/sec); and
    $E = \dfrac{\rho \, v K_D(M)}{C}$,

    g is the acceleration of gravity (yds/sec^2);
wherein

    ρ is the atmospheric density,
    $K_D(M)$ is the drag coefficient for the Projectile Type 6.1 expressed as a
        function of the Mach number, M,
and
    C is the ballistic coefficient with respect to the drag function for the
        Projectile Type 6.1.

The functions A and 1/C and the parameters v_o and t_b were chosen as follows:

    a. Thrust Acceleration, A.

Propellant Temperature (°F)	Thrust Acceleration (yd/sec^2)	
30	$A = 3293\ t$	
70	$A = 2302\ t + 345.3$	$0 \leq t \leq t_b$
110	$A = 2739\ t + 410.8$	

For all propellant temperatures, $A = 0$ when $t > t_b$.

In these equations,

    t is time measured from the instant the ignition circuit is closed;

and

    t_b is the chosen value of the time of end of burning.

    b. Reciprocal Ballistic Coefficient, 1/C.

$$1/C = 1.94 \qquad 0 \leq t \leq t_b;$$
$$1/C = 3.11 - 0.257\ M^2, \qquad t > t_b.$$

The reciprocal ballistic coefficient is with respect to the drag function for the Projectile Type 6.1

    c. Burning Time, t_b.

Propellant Temperature (°F)	Burning Time (sec)
30	$t_b = 0.6147$
70	$t_b = 0.6037$
110	$t_b = 0.5450$

    d. Initial Velocity, v_o, (the velocity of the rocket at the instant it leaves the muzzle of the launcher).

Propellant Temperature (°F)	Initial Velocity (yd/sec)
30	$v_o = 370.67$
70	$v_o = 396$
110	$v_o = 411$

5. The drift of the rocket, Z (t), was computed by means of the following equation:

$$Z(t) = C_1 x(t) + C_2 [x(t) \int_{t_b}^{t} \frac{dt}{v^2} - \int_{t_b}^{t} \frac{x(t)dt}{v^2}], \quad t > t_b$$

in which $C_1 = \ddot{Z}(t_b)/\dot{x}(t_b)$. This value of C_1 was chosen for reasons which will be given in a forthcoming Naval Proving Ground report. The constant C_1 was computed by the integration of "rigid body equations" (six degrees of freedom allowed) during the burning period and was thereby determined to be 0.0017 radians. (The "rigid body equations" which were used are quite similar to those given in NPG Report No. 800.) The constant C_2 was determined empirically from observed drift data and was chosen as 286.5 yd2/sec3.

6. The effects of wind may be divided into two parts:

  a. the effects of wind acting on the rocket during the burning period and

  b. the effects of wind acting on the rocket after the burning period.

While a range wind acting during the after-burning period has significant effects only on the range and altitude of the rocket, a range wind acting during the burning period affects the deflection of the rocket as well as its range and altitude. Similarly, a cross wind acting during the after-burning period has significant effects only on the deflection of the rocket, but a cross wind acting during the burning period affects the range and altitude of the rocket as well as its deflection.

7. Part III of the tables of ballistic data contains, in addition to various other effects, the effects on range and altitude of a uniform range wind (tail wind, constant in direction and velocity) acting throughout the trajectory of the rocket. These effects, x_w and y_w, were computed by means of the following equations, derivations of which will be given in the forthcoming Naval Proving Ground Report, referred to in paragraph 5 above:

$$x_W = \frac{6080.2}{180} \left\{ \frac{180}{\pi} x_\phi \left(\frac{1}{v_o} + \frac{108}{6080.2} C_3 \right) \sin\phi - 0.03 \, x_v \cos\phi + t_v \right\}$$

and

$$y_W = \frac{6080.2}{180} \left\{ \frac{180}{\pi} y_\phi \left(\frac{1}{v_o} + \frac{108}{6080.2} C_3 \right) \sin\phi - 0.03 \, y_v \cos\phi \right\}$$

In the preceeding equations,

  x_w, y_w are in yds/100 kts;

ϕ is elevation angle of the launcher;

x_ϕ, y_ϕ are partial derivatives of x and y with respect to ϕ (yds/deg);

x_v, y_v are partial derivatives of x and y with respect to v (yds/100 ft/sec);

and

c_3 is the difference (for $\phi \approx 90°$ and g = 0) between the effect of a 100 knot tail wind on $\dot{x}/v$ at the end of burning, perfect trailing being assumed, and the effect when yawing motion is assumed. (Both effects were computed, the latter by means of the "rigid body equation". The value of c_3 obtained was 0.0041 radians/100 knots.)

8. Part II of the tables of ballistic data contains the deflection due to a uniform cross wind acting throughout the trajectory of the rocket. This effect, z_w, was computed by means of the following equation:

$$z_w = \frac{6080.2}{108}\left\{t - x\left(\frac{1}{v_o} + \frac{108}{6080.2}\ c_3\right)\ \sec\phi\right\};$$

in which

z_w is in yds/100 kts.

9. The tables do not contain the deflection due to a uniform range wind acting during burning nor the effects on range and altitude of a uniform cross wind acting during burning. These effects may be approximated in the following manner:

a. The deflection due to 100 knots of tail wind acting during burning is approximately equivalent to the effect of increasing the azimuth of the launcher (in mils) by: $-1000\ c_4\ \tan\phi$. The constant c_4 is the effect (for $\phi = 90°$ and g = 0) of a 100 knot cross wind on $\dot{x}/v$ at the end of burning, yawing motion being assumed. It was computed by integration of the "rigid body equations". The value of c_4 obtained was 0.0146 radians/100 knots.

b. The effects on x and y of 100 knots of cross wind (blowing from left to right) during burning are approximately equivalent

respectively to the effects of decreasing the elevation angle (in degrees) by $(180/\pi) C_4$. The correction to the sight angle to score a hit is the negative of this quantity.

(A detailed discussion of these methods of computing the effects of wind acting during burning will be given in a forthcoming Naval Proving Ground Report.) As indicated above, the effects on range, altitude and deflection of a uniform wind acting throughout the trajectory of the rocket may be obtained from the tables included in Parts II and III and by the methods described in the preceding subparagraphs "a" and "b".

10. In the event that the rocket trajectory is subjected to a non-uniform wind, it is recommended that the wind effects be obtained from the tables included in Parts II and III using the ballistic wind determined from the wind acting during the after-burning portion of the trajectory. In addition, the following effects must be computed and added to those obtained from the tables of Parts II and III:

a. Using the difference between the range wind acting during burning (assumed to be uniform) and the ballistic range wind, compute the effects on range and altitude as follows: The effects on range and altitude of 100 knots of tail wind during burning is approximately equivalent to the effect of increasing the elevation angle (in degrees) by: $(180/\pi) C_5 \sin\phi$.* The correction to the sight angle to score a hit is the negative of this quantity.

b. Using the difference between the cross wind acting during burning (assumed to be uniform) and the ballistic cross wind, compute the deflection as follows: The deflection resulting from 100 knots of cross wind (blowing from left to right) during burning is approximately equivalent to the effect of decreasing the azimuth of the launcher (in mils) by: $(1000 C_5)/\cos\phi$.*

Since it is assumed that both the range wind and the cross wind, acting during burning, are uniform (even in the case of a non-uniform wind acting throughout the trajectory), the effects on range and altitude of a cross wind acting during burning are computed as described in paragraph 9b, above, while the deflection due to range wind acting during burning is computed as in paragraph 9a above.

11. The following facts concerning the tables of ballistic data should be noted:

a. All the rounds fired for ballistic data were from a single lot, namely, PA-E-11499, with Thiokol propellant T 10E1 mix 1050. All

_____

* where $C_5 = 0.085$ rad/100 kts.

rounds were fired from a T 110 E 2B launcher installed on experimental mounts.

b.

In computing the tables, perfect trailing of the rocket was assumed. In practice, corrections based on the deviations of actual trajectories from the trajectories wherein perfect trailing was assumed should be applied to the data of the tables. In firing from service mounts a mal-launching effect may occur which will result in a disturbance of the trajectory in the lateral as well as in the vertical plane.

c. The wind effects due to wind acting during the burning period are not based on flight observations but are theoretical in nature. Wind tunnel aerodynamic data were used in computing them.

12. A forthcoming Naval Proving Ground Report will contain descriptions of the methods used in obtaining the ballistic data and in the preparation of the tables. The accuracy of the tables, the dispersion of the rocket and other factors will be discussed. Also, a method for obtaining the corrections required for the mal-launching effects of the service launcher (paragraph 11b above) will be described.

PART I

Elements of Trajectories versus Time of Flight and Elevation for
70°F Propellant Temperature

Sight Angle versus Slant Range and Position Angle for
70°F Propellant Temperature

Time of Flight versus Slant Range and Position Angle for
70°F Propellant Temperature

Time of flight	Horizontal range	Altitude	Slant range	Position angle	Sight angle	Horizontal velocity	Vertical velocity
1	2	3	4	5	6	7	8
Seconds	Yards	Yards	Yards	Degrees	Degrees	F. S.	F. S.

ANGLE OF ELEVATION

5°

0	0	0	0	5.00	.00	1183	104
1	706	54	708	4.40	.60	2465	175
2	1405	99	1408	4.04	.96	1750	97
3	1897	122	1900	3.67	1.33	1240	42
4	2263	129	2267	3.26	1.74	1005	4
5	2578	125	2581	2.78	2.22	889	−27
6	2858	112	2861	2.24	2.76	798	−54
7	3112	89	3113	1.64	3.36	723	−80
8	3342	59	3343	1.00	4.00	661	−104
9	3553	20	3553	.33	4.67	607	−126
9.46	3644	0	3644	.00	5.00	585	−163
10	3747	−26	3748	−.39	5.39	560	−147

10°

0	0	0	0	10.00	.00	1170	206
1	698	116	707	9.41	.59	2439	390
2	1391	222	1408	9.05	.95	1739	251
3	1881	287	1902	8.68	1.32	1238	151
4	2246	327	2270	8.28	1.72	1003	93
5	2560	351	2584	7.80	2.20	889	52
6	2841	362	2864	7.26	2.74	799	16
7	3095	362	3116	6.67	3.33	727	−16
8	3327	352	3345	6.03	3.97	665	−45
9	3540	332	3555	5.36	4.64	613	−73
10	3736	303	3749	4.64	5.36	567	−98
11	3919	267	3928	3.89	6.11	527	−122
12	4088	222	4094	3.11	6.89	492	−145
13	4247	170	4250	2.29	7.71	460	−167
14	4395	111	4397	1.44	8.56	431	−188
15	4535	45	4535	.57	9.43	405	−207
15.63	4618	0	4618	.00	10.00	389	−219
16	4665	−27	4665	−.34	10.34	380	−226

Time of flight	Horizontal range	Altitude	Slant range	Position angle	Sight angle	Horizontal velocity	Vertical velocity
1	2	3	4	5	6	7	8
Seconds	Yards	Yards	Yards	Degrees	Degrees	F. S.	F. S.

ANGLE OF ELEVATION

15°

0	0	0	0	15.00	.00	1148	307
1	685	176	707	14.41	.59	2395	601
2	1366	342	1409	14.06	.94	1713	403
3	1850	451	1904	13.71	1.29	1225	261
4	2212	523	2273	13.31	1.69	992	182
5	2523	575	2588	12.84	2.16	881	131
6	2802	611	2868	12.31	2.69	795	87
7	3055	634	3120	11.72	3.28	724	49
8	3286	644	3348	11.09	3.91	665	14
9	3499	644	3557	10.42	4.58	614	-18
10	3696	633	3749	9.71	5.29	570	-48
11	3879	612	3927	8.97	6.03	531	-75
12	4050	583	4092	8.18	6.82	497	-102
13	4211	544	4246	7.37	7.63	466	-127
14	4361	498	4390	6.52	8.48	438	-150
15	4503	445	4525	5.64	9.36	412	-173
16	4636	383	4652	4.73	10.27	389	-194
17	4762	315	4773	3.79	11.21	367	-214
18	4881	241	4887	2.82	12.18	347	-234
19	4994	160	4996	1.83	13.17	327	-252
20	5100	73	5100	.82	14.18	309	-269
20.79	5179	0	5179	.00	15.00	296	-282
21	5200	-20	5200	-.22	15.22	292	-285

Time of flight	Horizontal range	Altitude	Slant range	Position angle	Sight angle	Horizontal velocity	Vertical velocity
1	2	3	4	5	6	7	8
Seconds	Yards	Yards	Yards	Degrees	Degrees	F. S.	F. S.

ANGLE OF ELEVATION

20°

0	0	0	0	20.00	.00	1116	406
1	667	235	707	19.43	.57	2333	809
2	1331	461	1409	19.09	.91	1674	553
3	1805	612	1906	18.74	1.26	1202	370
4	2160	717	2276	18.35	1.65	974	270
5	2466	796	2591	17.89	2.11	866	210
6	2740	857	2871	17.37	2.63	783	159
7	2990	903	3123	16.80	3.20	715	114
8	3218	934	3351	16.19	3.81	658	74
9	3429	953	3559	15.53	4.47	609	38
10	3625	960	3750	14.83	5.17	567	4
11	3808	956	3926	14.09	5.91	530	−27
12	3979	942	4089	13.32	6.68	497	−57
13	4140	918	4240	12.51	7.49	468	−84
14	4291	886	4382	11.66	8.34	441	−111
15	4434	845	4514	10.78	9.22	417	−136
16	4569	795	4638	9.87	10.13	394	−160
17	4697	738	4755	8.93	11.07	373	−183
18	4818	674	4865	7.96	12.04	354	−204
19	4933	602	4970	6.96	13.04	335	−225
20	5042	524	5069	5.93	14.07	318	−245
21	5145	439	5164	4.88	15.12	301	−263
22	5243	348	5254	3.80	16.20	285	−281
23	5335	252	5341	2.71	17.29	270	−297
24	5423	151	5425	1.59	18.41	255	−312
25	5505	44	5506	.46	19.54	241	−326
25.40	5537	0	5537	.00	20.00	236	−332
26	5584	−67	5584	−.69	20.69	228	−339

B-12507

Time of flight	Horizontal range	Altitude	Slant range	Position angle	Sight angle	Horizontal velocity	Vertical velocity
1	2	3	4	5	6	7	8
Seconds	Yards	Yards	Yards	Degrees	Degrees	F. S.	F. S.

ANGLE OF ELEVATION

25°

0	0	0	0	25.00	.00	1077	502
1	643	293	707	24.45	.55	2253	1010
2	1286	576	1409	24.12	.88	1622	700
3	1746	769	1908	23.78	1.22	1170	477
4	2091	905	2279	23.41	1.59	947	357
5	2389	1012	2594	22.96	2.04	844	288
6	2657	1098	2875	22.46	2.54	765	230
7	2900	1166	3126	21.91	3.09	700	180
8	3124	1219	3354	21.31	3.69	646	135
9	3332	1257	3561	20.67	4.33	599	94
10	3525	1282	3750	19.98	5.02	559	57
11	3705	1295	3925	19.26	5.74	524	22
12	3874	1297	4086	18.50	6.50	493	−10
13	4034	1288	4235	17.71	7.29	465	−41
14	4185	1269	4373	16.87	8.13	440	−70
15	4328	1241	4502	16.01	8.99	417	−98
16	4463	1204	4623	15.10	9.90	396	−124
17	4592	1159	4736	14.16	10.84	376	−149
18	4714	1105	4842	13.19	11.81	357	−173
19	4830	1043	4941	12.19	12.81	340	−196
20	4941	974	5036	11.16	13.84	323	−218
21	5046	898	5125	10.09	14.91	307	−239
22	5146	816	5210	9.01	15.99	292	−258
23	5240	726	5291	7.89	17.11	278	−277
24	5331	631	5368	6.75	18.25	264	−294
25	5416	531	5442	5.59	19.41	250	−310
26	5497	425	5514	4.42	20.58	237	−325
27	5574	314	5583	3.22	21.78	224	−339
28	5647	199	5650	2.02	22.98	212	−352
29	5716	80	5716	.80	24.20	200	−364
29.65	5758	0	5758	.00	25.00	193	−371
30	5780	−44	5781	−.43	25.43	189	−374

8-12507

Time of flight	Horizontal range	Altitude	Slant range	Position angle	Sight angle	Horizontal velocity	Vertical velocity
1	2	3	4	5	6	7	8
Seconds	*Yards*	*Yards*	*Yards*	*Degrees*	*Degrees*	*F. S.*	*F. S.*

ANGLE OF ELEVATION

30°

0	0	0	0	30.00	.00	1029	594
1	615	348	707	29.47	.53	2155	1203
2	1231	687	1409	29.16	.84	1556	842
3	1672	921	1909	28.83	1.17	1127	582
4	2006	1088	2282	28.47	1.53	912	442
5	2293	1222	2598	28.05	1.95	815	364
6	2551	1332	2878	27.57	2.43	739	300
7	2787	1422	3129	27.04	2.96	678	244
8	3004	1495	3356	26.46	3.54	627	195
9	3206	1553	3562	25.84	4.16	584	150
10	3394	1596	3750	25.18	4.82	546	109
11	3570	1626	3923	24.48	5.52	513	72
12	3736	1644	4082	23.75	6.25	484	36
13	3893	1650	4229	22.97	7.03	458	3
14	4042	1646	4364	22.16	7.84	434	−28
15	4183	1631	4490	21.31	8.69	413	−58
16	4317	1607	4607	20.42	9.58	393	−87
17	4445	1574	4716	19.49	10.51	375	−114
18	4567	1531	4817	18.53	11.47	357	−140
19	4684	1480	4912	17.54	12.46	341	−165
20	4795	1421	5001	16.51	13.49	325	−189
21	4901	1354	5084	15.45	14.55	311	−212
22	5002	1280	5163	14.35	15.65	296	−234
23	5098	1198	5237	13.23	16.77	283	−254
24	5190	1110	5307	12.08	17.92	269	−274
25	5278	1016	5375	10.90	19.10	256	−292
26	5361	916	5439	9.70	20.30	244	−309
27	5440	810	5500	8.47	21.53	231	−325
28	5515	700	5559	7.23	22.77	220	−339
29	5587	584	5617	5.97	24.03	208	−353
30	5654	464	5673	4.70	25.30	197	−365
31	5718	341	5728	3.41	26.59	186	−377
32	5778	213	5782	2.12	27.88	176	−387
33	5835	83	5836	.81	29.19	166	−396
33.62	5869	0	5869	.00	30.00	160	−401
34	5889	−51	5889	−.49	30.49	156	−404

Time of flight	Horizontal range	Altitude	Slant range	Position angle	Sight angle	Horizontal velocity	Vertical velocity
1	2	3	4	5	6	7	8
Seconds	Yards	Yards	Yards	Degrees	Degrees	F. S.	F. S.

ANGLE OF ELEVATION

35°

0	0	0	0	35.00	.00	973	681
1	582	400	706	34.50	.50	2040	1388
2	1166	792	1409	34.20	.80	1478	978
3	1586	1066	1911	33.90	1.10	1074	683
4	1904	1263	2284	33.55	1.45	870	524
5	2177	1422	2601	33.15	1.85	778	438
6	2424	1556	2881	32.69	2.31	707	368
7	2650	1668	3132	32.19	2.81	650	307
8	2859	1762	3358	31.64	3.36	602	253
9	3053	1838	3563	31.05	3.95	562	205
10	3234	1899	3750	30.42	4.58	527	161
11	3405	1946	3921	29.75	5.25	496	121
12	3565	1980	4078	29.04	5.96	469	83
13	3718	2001	4222	28.29	6.71	445	47
14	3863	2012	4355	27.51	7.49	424	14
15	4000	2011	4477	26.69	8.31	404	−18
16	4132	1999	4590	25.82	9.18	386	−49
17	4258	1978	4695	24.92	10.08	369	−78
18	4378	1947	4792	23.98	11.02	353	−106
19	4493	1907	4881	23.00	12.00	338	−133
20	4603	1859	4964	21.99	13.01	324	−159
21	4709	1801	5042	20.93	14.07	310	−184
22	4810	1736	5114	19.85	15.15	297	−208
23	4907	1663	5181	18.72	16.28	284	−230
24	5000	1583	5244	17.57	17.43	272	−251
25	5088	1496	5303	16.38	18.62	260	−272
26	5173	1402	5359	15.16	19.84	248	−291
27	5253	1302	5412	13.92	21.08	236	−308
28	5330	1197	5463	12.65	22.35	225	−325
29	5403	1086	5511	11.36	23.64	214	−340
30	5473	970	5558	10.05	24.95	203	−355
31	5538	849	5603	8.72	26.28	193	−368
32	5601	725	5648	7.37	27.63	182	−380
33	5660	596	5691	6.01	28.99	173	−390
34	5716	465	5735	4.65	30.35	163	−400
35	5769	330	5778	3.27	31.73	154	−409

B-12507

CONFIDENTIAL

Time of flight	Horizontal range	Altitude	Slant range	Position angle	Sight angle	Horizontal velocity	Vertical velocity
1	2	3	4	5	6	7	8
Seconds	Yards	Yards	Yards	Degrees	Degrees	F. S.	F. S.

ANGLE OF ELEVATION
35

35	5769	330	5778	3.27	31.73	154	−409
36	5819	192	5822	1.89	33.11	145	−416
37	5865	52	5866	.51	34.49	136	−423
37.37	5882	0	5882	.00	35.00	133	−425
38	5909	−90	5910	−.87	35.87	128	−429

B-12507

Time of flight	Horizontal range	Altitude	Slant range	Position angle	Sight angle	Horizontal velocity	Vertical velocity
1	2	3	4	5	6	7	8
Seconds	Yards	Yards	Yards	Degrees	Degrees	F. S.	F. S.

ANGLE OF ELEVATION

40°

0	0	0	0	40.00	.00	910	764
1	545	450	706	39.54	.46	1910	1562
2	1091	892	1409	39.25	.75	1387	1107
3	1487	1202	1912	38.97	1.03	1012	780
4	1786	1428	2287	38.65	1.35	819	602
5	2044	1612	2603	38.27	1.73	734	509
6	2277	1769	2884	37.84	2.16	669	433
7	2491	1902	3134	37.37	2.63	616	368
8	2689	2015	3360	36.85	3.15	572	310
9	2873	2110	3564	36.29	3.71	534	259
10	3046	2188	3750	35.70	4.30	502	212
11	3208	2252	3919	35.06	4.94	474	169
12	3362	2301	4074	34.39	5.61	449	129
13	3508	2338	4216	33.68	6.32	428	91
14	3647	2362	4345	32.93	7.07	408	56
15	3780	2375	4464	32.14	7.86	390	22
16	3907	2377	4574	31.31	8.69	373	−11
17	4029	2368	4674	30.44	9.56	358	−42
18	4146	2349	4766	29.53	10.47	344	−72
19	4259	2321	4850	28.59	11.41	331	−100
20	4367	2283	4927	27.60	12.40	318	−128
21	4471	2235	4998	26.57	13.43	305	−154
22	4570	2180	5064	25.50	14.50	293	−180
23	4666	2116	5124	24.39	15.61	282	−204
24	4758	2044	5179	23.24	16.76	270	−228
25	4847	1964	5229	22.06	17.94	259	−250
26	4931	1877	5276	20.84	19.16	248	−271
27	5012	1784	5320	19.59	20.41	238	−290
28	5090	1684	5361	18.30	21.70	227	−309
29	5164	1578	5399	16.99	23.01	217	−326
30	5234	1466	5436	15.65	24.35	206	−342
31	5301	1350	5471	14.29	25.71	197	−357
32	5365	1229	5504	12.90	27.10	187	−371
33	5426	1103	5537	11.49	28.51	177	−383
34	5483	973	5569	10.07	29.93	168	−394
35	5538	840	5601	8.63	31.37	159	−404

Time of flight	Horizontal range	Altitude	Slant range	Position angle	Sight angle	Horizontal velocity	Vertical velocity
1	2	3	4	5	6	7	8
Seconds	Yards	Yards	Yards	Degrees	Degrees	F. S.	F. S.

ANGLE OF ELEVATION

40°

35	5538	840	5601	8.63	31.37	159	−404
36	5589	704	5634	7.18	32.82	150	−413
37	5638	565	5666	5.72	34.28	142	−421
38	5684	423	5700	4.26	35.74	134	−428
39	5727	279	5734	2.79	37.21	126	−435
40	5768	133	5769	1.32	38.68	118	−440
40.97	5805	0	5805	.00	40.00	111	−444
41	5806	−14	5806	−.14	40.14	111	−444

Time of flight	Horizontal range	Altitude	Slant range	Position angle	Sight angle	Horizontal velocity	Vertical velocity
1	2	3	4	5	6	7	8
Seconds	Yards	Yards	Yards	Degrees	Degrees	F. S.	F. S.

ANGLE OF ELEVATION

45°

0	0	0	0	45.00	.00	840	840
1	503	495	706	44.57	.43	1765	1724
2	1009	985	1410	44.31	.69	1285	1228
3	1375	1330	1913	44.04	.96	940	871
4	1654	1583	2289	43.75	1.25	762	676
5	1894	1791	2606	43.40	1.60	683	576
6	2111	1969	2886	43.00	2.00	623	495
7	2310	2122	3137	42.56	2.44	575	425
8	2495	2253	3362	42.08	2.92	535	365
9	2668	2365	3565	41.56	3.44	501	310
10	2830	2460	3750	41.01	3.99	472	261
11	2983	2540	3917	40.42	4.58	446	216
12	3128	2605	4070	39.79	5.21	424	174
13	3265	2656	4209	39.12	5.88	404	134
14	3397	2694	4336	38.42	6.58	387	97
15	3524	2721	4452	37.67	7.33	371	61
16	3645	2735	4557	36.89	8.11	356	27
17	3761	2739	4653	36.06	8.94	343	−5
18	3873	2732	4740	35.20	9.80	330	−37
19	3981	2715	4819	34.29	10.71	318	−67
20	4085	2687	4890	33.34	11.66	307	−96
21	4186	2651	4955	32.34	12.66	296	−124
22	4283	2605	5013	31.31	13.69	286	−151
23	4376	2550	5065	30.23	14.77	275	−178
24	4467	2486	5112	29.10	15.90	265	−203
25	4553	2415	5154	27.94	17.06	255	−226
26	4637	2336	5192	26.74	18.26	245	−249
27	4717	2249	5226	25.49	19.51	236	−271
28	4794	2155	5256	24.21	20.79	226	−291
29	4867	2055	5283	22.89	22.11	216	−310
30	4938	1949	5308	21.53	23.47	207	−328
31	5005	1836	5332	20.15	24.85	197	−345
32	5070	1719	5353	18.73	26.27	188	−360
33	5131	1596	5374	17.28	27.72	179	−374
34	5189	1470	5393	15.81	29.19	170	−387
35	5245	1339	5413	14.32	30.68	162	−399

Time of flight	Horizontal range	Altitude	Slant range	Position angle	Sight angle	Horizontal velocity	Vertical velocity
1	2	3	4	5	6	7	8
Seconds	Yards	Yards	Yards	Degrees	Degrees	F. S.	F. S.

ANGLE OF ELEVATION

45°

35	5245	1339	5413	14.32	30.68	162	−399
36	5297	1204	5432	12.80	32.20	153	−409
37	5347	1066	5452	11.27	33.73	145	−419
38	5394	925	5473	9.73	35.27	137	−427
39	5438	781	5494	8.17	36.83	130	−434
40	5480	635	5517	6.61	38.39	122	−441
41	5520	487	5541	5.05	39.95	115	−446
42	5557	338	5567	3.48	41.52	108	−451
43	5592	187	5595	1.91	43.09	102	−455
44	5625	35	5625	.35	44.65	95	−458
44.23	5632	0	5632	.00	45.00	94	−458
45	5656	−119	5657	−1.20	46.20	89	−460

Time of flight	Horizontal range	Altitude	Slant range	Position angle	Sight angle	Horizontal velocity	Vertical velocity
1	2	3	4	5	6	7	8
Seconds	Yards	Yards	Yards	Degrees	Degrees	F. S.	F. S.

ANGLE OF ELEVATION

50°

0	0	0	0	50.00	.00	764	910
1	457	538	706	49.61	.39	1605	1872
2	918	1070	1410	49.37	.63	1172	1339
3	1253	1448	1914	49.13	.87	860	955
4	1507	1725	2291	48.86	1.14	697	744
5	1727	1955	2608	48.54	1.46	626	638
6	1926	2153	2889	48.18	1.82	572	552
7	2109	2325	3139	47.78	2.22	528	479
8	2279	2473	3364	47.34	2.66	492	416
9	2438	2602	3566	46.87	3.13	462	359
10	2588	2713	3749	46.36	3.64	436	307
11	2729	2808	3915	45.81	4.19	413	260
12	2863	2887	4066	45.23	4.77	393	216
13	2992	2952	4203	44.62	5.38	376	175
14	3114	3004	4327	43.97	6.03	360	136
15	3232	3043	4439	43.27	6.73	346	99
16	3345	3070	4541	42.55	7.45	334	64
17	3454	3086	4632	41.78	8.22	322	30
18	3560	3091	4714	40.96	9.04	311	−2
19	3662	3085	4788	40.11	9.89	301	−34
20	3761	3068	4854	39.21	10.79	291	−64
21	3856	3042	4912	38.27	11.73	282	−94
22	3949	3006	4963	37.28	12.72	273	−123
23	4038	2960	5007	36.24	13.76	264	−150
24	4125	2906	5046	35.16	14.84	255	−177
25	4209	2843	5079	34.04	15.96	247	−202
26	4289	2771	5107	32.86	17.14	238	−227
27	4367	2691	5130	31.64	18.36	229	−250
28	4442	2604	5149	30.38	19.62	221	−272
29	4514	2510	5165	29.07	20.93	212	−293
30	4584	2409	5178	27.73	22.27	203	−313
31	4650	2302	5188	26.33	23.67	195	−331
32	4714	2188	5197	24.90	25.10	187	−348
33	4774	2070	5204	23.44	26.56	178	−364
34	4832	1946	5209	21.93	28.07	170	−379
35	4888	1817	5215	20.40	29.60	162	−392

Time of flight	Horizontal range	Altitude	Slant range	Position angle	Sight angle	Horizontal velocity	Vertical velocity
1	2	3	4	5	6	7	8
Seconds	Yards	Yards	Yards	Degrees	Degrees	F. S.	F. S.

ANGLE OF ELEVATION

50°

35	4888	1817	5215	20.40	29.60	162	−392
36	4940	1685	5220	18.83	31.17	154	−404
37	4990	1548	5225	17.24	32.76	146	−415
38	5038	1408	5231	15.62	34.38	138	−425
39	5083	1265	5238	13.98	36.02	131	−433
40	5125	1120	5246	12.32	37.68	124	−441
41	5165	972	5256	10.65	39.35	117	−447
42	5203	822	5267	8.97	41.03	110	−453
43	5239	670	5281	7.29	42.71	104	−458
44	5272	516	5297	5.59	44.41	98	−462
45	5304	362	5316	3.90	46.10	92	−465
46	5333	206	5337	2.22	47.78	86	−468
47	5361	50	5361	.54	49.46	81	−469
47.32	5370	0	5370	.00	50.00	79	−470
48	5387	−107	5388	−1.13	51.13	76	−471

CONFIDENTIAL

Time of flight	Horizontal range	Altitude	Slant range	Position angle	Sight angle	Horizontal velocity	Vertical velocity
1	2	3	4	5	6	7	8
Seconds	Yards	Yards	Yards	Degrees	Degrees	F. S.	F. S.

ANGLE OF ELEVATION

55°

0	0	0	0	55.00	.00	681	973
1	408	576	706	54.65	.35	1434	2006
2	820	1147	1410	54.44	.56	1048	1440
3	1120	1554	1915	54.22	.78	772	1032
4	1348	1855	2293	53.98	1.02	625	807
5	1546	2104	2611	53.70	1.30	562	695
6	1725	2320	2891	53.37	1.63	515	605
7	1890	2509	3141	53.01	1.99	476	529
8	2043	2674	3365	52.62	2.38	444	462
9	2186	2818	3567	52.19	2.81	417	403
10	2322	2943	3749	51.74	3.26	394	350
11	2450	3052	3913	51.25	3.75	375	301
12	2572	3144	4062	50.72	4.28	357	256
13	2688	3223	4197	50.17	4.83	342	213
14	2800	3287	4318	49.57	5.43	329	173
15	2907	3338	4427	48.95	6.05	317	136
16	3011	3378	4525	48.28	6.72	306	99
17	3112	3405	4612	47.58	7.42	296	65
18	3209	3421	4690	46.83	8.17	287	31
19	3303	3426	4759	46.04	8.96	279	-2
20	3395	3420	4818	45.21	9.79	271	-33

Time of flight	Horizontal range	Altitude	Slant range	Position angle	Sight angle	Horizontal velocity	Vertical velocity
1	2	3	4	5	6	7	8
Seconds	Yards	Yards	Yards	Degrees	Degrees	F. S.	F. S.

ANGLE OF ELEVATION

60°

0	0	0	0	60.00	.00	594	1029
1	356	609	705	59.69	.31	1230	2125
2	715	1215	1410	59.51	.49	916	1530
3	978	1448	1916	59.32	.68	676	1100
4	1178	1969	2295	59.11	.89	548	862
5	1351	2236	2613	58.86	1.14	493	746
6	1508	2469	2893	58.58	1.42	452	652
7	1653	2673	3143	58.27	1.73	419	573
8	1788	2852	3366	57.92	2.08	391	505
9	1914	3010	3567	57.55	2.45	368	444
10	2033	3149	3748	57.14	2.86	348	389
11	2147	3270	3911	56.72	3.28	331	338
12	2255	3375	4058	56.25	3.75	317	292
13	2358	3465	4191	55.76	4.24	304	248
14	2457	3540	4310	55.24	4.76	292	208
15	2553	3603	4416	54.68	5.32	282	169
16	2645	3653	4510	54.09	5.91	273	132
17	2735	3691	4594	53.46	6.54	265	96
18	2822	3718	4668	52.80	7.20	258	62
19	2907	3733	4731	52.09	7.91	251	29
20	2990	3737	4786	51.34	8.66	245	−4

B-12507

Time of flight	Horizontal range	Altitude	Slant range	Position angle	Sight angle	Horizontal velocity	Vertical velocity
1	2	3	4	5	6	7	8
Seconds	*Yards*	*Yards*	*Yards*	*Degrees*	*Degrees*	*F. S.*	*F. S.*

ANGLE OF ELEVATION

65°

0	0	0	0	65.00	.00	502	1077
1	301	638	705	64.74	.26	1058	2227
2	605	1273	1410	64.59	.41	776	1607
3	828	1729	1917	64.43	.57	574	1160
4	998	2068	2296	64.25	.75	465	911
5	1144	2350	2614	64.04	.96	419	790
6	1278	2597	2895	63.80	1.20	384	694
7	1401	2814	3144	63.53	1.47	356	612
8	1516	3006	3367	63.24	1.76	333	542
9	1624	3176	3567	62.92	2.08	314	479
10	1726	3326	3747	62.58	2.42	298	423
11	1823	3459	3909	62.21	2.79	283	371
12	1915	3574	4055	61.82	3.18	271	324
13	2004	3675	4186	61.40	3.60	261	280
14	2089	3761	4302	60.95	4.05	251	238
15	2171	3834	4406	60.48	4.52	243	199
16	2251	3894	4498	59.97	5.03	236	161
17	2329	3941	4578	59.42	5.58	230	125
18	2404	3977	4647	58.85	6.15	224	90
19	2478	4001	4707	58.23	6.77	218	56
20	2550	4015	4756	57.58	7.42	214	23

B-12507

Time of flight	Horizontal range	Altitude	Slant range	Position angle	Sight angle	Horizontal velocity	Vertical velocity
1	2	3	4	5	6	7	8
Seconds	*Yards*	*Yards*	*Yards*	*Degrees*	*Degrees*	*F. S.*	*F. S.*

ANGLE OF ELEVATION

70°

0	0	0	0	70.00	.00	406	1116
1	244	662	705	69.79	.21	856	2312
2	490	1322	1410	69.67	.33	629	1671
3	671	1797	1918	69.53	.47	466	1209
4	809	2150	2297	69.39	.61	378	951
5	928	2445	2616	69.22	.78	340	827
6	1037	2704	2896	69.03	.97	313	728
7	1137	2933	3145	68.81	1.19	290	645
8	1230	3135	3368	68.57	1.43	272	573
9	1318	3315	3568	68.32	1.68	256	509
10	1401	3475	3747	68.04	1.96	243	451
11	1481	3617	3908	67.74	2.26	232	399
12	1556	3741	4052	67.42	2.58	222	351
13	1629	3851	4181	67.08	2.92	214	306
14	1699	3946	4296	66.71	3.29	206	264
15	1766	4027	4397	66.32	3.68	200	224
16	1832	4095	4486	65.90	4.10	194	186
17	1896	4151	4564	65.45	4.55	189	150
18	1958	4195	4630	64.98	5.02	185	114
19	2019	4228	4685	64.47	5.53	181	80
20	2079	4249	4730	63.92	6.08	178	47

8-12507

CONFIDENTIAL

Time of flight	Horizontal range	Altitude	Slant range	Position angle	Sight angle	Horizontal velocity	Vertical velocity
1	2	3	4	5	6	7	8
Seconds	Yards	Yards	Yards	Degrees	Degrees	F. S.	F. S.

ANGLE OF ELEVATION

75°

0	0	0	0	75.00	.00	307	1148
1	184	681	705	74.84	.16	648	2378
2	371	1360	1410	74.75	.25	477	1722
3	508	1850	1918	74.65	.35	353	1249
4	613	2215	2298	74.54	.46	287	983
5	703	2520	2617	74.41	.59	259	856
6	786	2788	2897	74.26	.74	237	755
7	862	3026	3146	74.10	.90	221	671
8	933	3237	3369	73.92	1.08	207	597
9	1000	3425	3568	73.72	1.28	195	532
10	1063	3592	3747	73.51	1.49	185	474
11	1124	3742	3907	73.28	1.72	177	421
12	1181	3874	4050	73.04	1.96	170	372
13	1237	3990	4177	72.78	2.22	163	327
14	1290	4092	4291	72.50	2.50	158	285
15	1342	4180	4390	72.20	2.80	153	245
16	1393	4255	4477	71.88	3.12	149	206
17	1442	4318	4552	71.54	3.46	146	170
18	1490	4369	4616	71.17	3.83	143	134
19	1537	4408	4668	70.78	4.22	140	100
20	1583	4435	4709	70.36	4.64	138	67

Time of flight	Horizontal range	Altitude	Slant range	Position angle	Sight angle	Horizontal velocity	Vertical velocity
1	2	3	4	5	6	7	8
Seconds	Yards	Yards	Yards	Degrees	Degrees	F. S.	F. S.

ANGLE OF ELEVATION

80°

0	0	0	0	80.00	.00	206	1170
1	124	694	705	79.90	.10	435	2426
2	249	1388	1410	79.83	.17	320	1758
3	341	1888	1918	79.76	.24	238	1277
4	411	2262	2299	79.69	.31	193	1006
5	472	2574	2617	79.60	.40	174	877
6	528	2849	2898	79.51	.49	160	775
7	579	3093	3147	79.40	.60	149	689
8	627	3310	3369	79.27	.73	139	615
9	672	3504	3568	79.14	.86	131	550
10	715	3677	3746	79.00	1.00	125	491
11	756	3832	3906	78.85	1.15	119	437
12	794	3969	4048	78.68	1.32	114	388
13	832	4091	4175	78.51	1.49	110	343
14	868	4198	4287	78.32	1.68	107	300
15	903	4291	4385	78.12	1.88	104	260
16	937	4371	4471	77.90	2.10	101	221
17	971	4439	4544	77.67	2.33	99	185
18	1003	4495	4605	77.42	2.58	97	149
19	1035	4539	4655	77.15	2.85	95	115
20	1067	4571	4694	76.86	3.14	94	81

B-12507

Time of flight	Horizontal range	Altitude	Slant range	Position angle	Sight angle	Horizontal velocity	Vertical velocity
1	2	3	4	5	6	7	8
Seconds	Yards	Yards	Yards	Degrees	Degrees	F. S.	F. S.

ANGLE OF ELEVATION

85°

0	0	0	0	85.00	.00	104	1183
1	62	702	705	84.95	.05	218	2455
2	125	1404	1410	84.91	.09	161	1780
3	171	1911	1919	84.88	.12	119	1294
4	207	2290	2299	84.84	.16	97	1020
5	237	2607	2618	84.80	.20	87	890
6	265	2886	2898	84.75	.25	80	787
7	291	3134	3147	84.70	.30	75	701
8	315	3355	3369	84.64	.36	70	626
9	338	3552	3568	84.57	.43	66	560
10	359	3729	3746	84.50	.50	63	501
11	380	3887	3905	84.42	.58	60	447
12	399	4027	4047	84.34	.66	58	398
13	418	4152	4173	84.25	.75	56	352
14	436	4262	4285	84.15	.85	54	309
15	454	4359	4382	84.05	.95	52	269
16	471	4442	4467	83.94	1.06	51	231
17	488	4512	4539	83.83	1.17	50	194
18	505	4571	4599	83.70	1.30	49	158
19	521	4618	4647	83.56	1.44	48	124
20	537	4654	4685	83.42	1.58	48	91

Time of flight	Horizontal range	Altitude	Slant range	Position angle	Sight angle	Horizontal velocity	Vertical velocity
1	2	3	4	5	6	7	8
Seconds	*Yards*	*Yards*	*Yards*	*Degrees*	*Degrees*	*F. S.*	*F. S.*

ANGLE OF ELEVATION

90°

0	0	0	0	90.00	.00	0	1188
1	0	705	705	90.00	.00	0	2465
2	0	1410	1410	90.00	.00	0	1788
3	0	1919	1919	90.00	.00	0	1300
4	0	2299	2299	90.00	.00	0	1025
5	0	2618	2618	90.00	.00	0	894
6	0	2898	2898	90.00	.00	0	791
7	0	3147	3147	90.00	.00	0	705
8	0	3369	3369	90.00	.00	0	630
9	0	3568	3568	90.00	.00	0	564
10	0	3746	3746	90.00	.00	0	504
11	0	3905	3905	90.00	.00	0	450
12	0	4047	4047	90.00	.00	0	401
13	0	4173	4173	90.00	.00	0	355
14	0	4284	4284	90.00	.00	0	312
15	0	4381	4381	90.00	.00	0	272
16	0	4465	4465	90.00	.00	0	234
17	0	4537	4537	90.00	.00	0	197
18	0	4597	4597	90.00	.00	0	162
19	0	4645	4645	90.00	.00	0	127
20	0	4682	4682	90.00	.00	0	94

Sight angle in degrees

Slant range, yards	Position angle in degrees																		
	0	5	10	15	20	25	30	35	40	45	50	55	60	65	70	75	80	85	90
200	.30	.30	.30	.28	.28	.27	.26	.24	.23	.18	.18	.17	.14	.12	.10	.07	.06	.04	.00
400	.45	.44	.44	.42	.40	.40	.39	.36	.34	.29	.28	.26	.22	.18	.15	.11	.08	.05	.00
600	.56	.55	.54	.53	.51	.50	.48	.45	.42	.38	.35	.32	.28	.23	.19	.14	.10	.05	.00
800	.65	.64	.64	.63	.61	.59	.57	.53	.50	.46	.42	.37	.33	.28	.22	.17	.11	.06	.00
1000	.75	.74	.73	.72	.70	.68	.65	.61	.57	.53	.48	.43	.37	.32	.26	.19	.13	.07	.00
1200	.85	.84	.83	.82	.80	.77	.73	.69	.65	.60	.55	.49	.42	.36	.29	.22	.15	.08	.00
1400	.96	.96	.95	.93	.90	.87	.83	.79	.74	.68	.62	.55	.48	.40	.33	.25	.17	.09	.00
1600	1.09	1.09	1.07	1.05	1.03	.99	.94	.89	.83	.77	.70	.62	.54	.46	.37	.28	.19	.10	.00
1800	1.25	1.24	1.22	1.20	1.17	1.12	1.07	1.01	.95	.87	.79	.71	.62	.52	.42	.32	.21	.11	.00
2000	1.43	1.42	1.40	1.37	1.33	1.29	1.23	1.16	1.08	1.00	.91	.81	.70	.59	.48	.36	.24	.12	.00
2200	1.66	1.65	1.62	1.59	1.54	1.48	1.41	1.34	1.25	1.15	1.04	.93	.81	.68	.55	.42	.28	.14	.00
2400	1.94	1.92	1.89	1.85	1.79	1.72	1.64	1.55	1.45	1.33	1.21	1.08	.94	.79	.64	.48	.32	.16	.00
2600	2.26	2.24	2.21	2.16	2.09	2.01	1.92	1.81	1.68	1.55	1.40	1.25	1.09	.92	.74	.56	.38	.19	.00
2800	2.65	2.62	2.58	2.52	2.44	2.35	2.24	2.11	1.96	1.81	1.64	1.46	1.27	1.07	.86	.65	.44	.22	.00
3000	3.09	3.06	3.01	2.94	2.85	2.74	2.61	2.46	2.29	2.11	1.91	1.70	1.48	1.25	1.01	.76	.51	.26	.00
3200	3.60	3.57	3.51	3.43	3.32	3.19	3.04	2.86	2.67	2.45	2.22	1.98	1.72	1.45	1.17	.89	.60	.30	.00
3400	4.18	4.14	4.08	3.98	3.86	3.71	3.53	3.33	3.11	2.86	2.59	2.31	2.01	1.70	1.37	1.04	.70	.35	.00
3600	4.84	4.80	4.73	4.63	4.49	4.31	4.11	3.88	3.62	3.33	3.02	2.69	2.34	1.98	1.60	1.21	.81	.41	.00
3800	5.60	5.56	5.48	5.36	5.20	5.01	4.78	4.51	4.21	3.88	3.53	3.15	2.74	2.32	1.87	1.42	.95	.48	.00
4000	6.46	6.43	6.34	6.21	6.04	5.82	5.56	5.26	4.92	4.54	4.13	3.69	3.22	2.72	2.20	1.67	1.12	.56	.00
4200	7.45	7.42	7.34	7.20	7.01	6.78	6.49	6.15	5.77	5.34	4.87	4.35	3.81	3.22	2.62	1.98	1.33	.67	.00
4400	8.58	8.56	8.49	8.36	8.17	7.91	7.60	7.23	6.81	6.33	5.79	5.20	4.56	3.88	3.16	2.40	1.62	.81	.00
4600	9.87	9.89	9.84	9.73	9.55	9.30	8.98	8.60	8.15	7.63	7.03	6.37	5.63	4.83	3.96	3.03	2.05	1.04	.00
4800	11.38	11.45	11.45	11.39	11.26	11.06	10.79	10.45	10.04										
5000	13.14	13.31	13.42	13.48															

I – 22

B-11547

Time of flight in seconds

Slant range, yards	Position angle in degrees																		
	0	5	10	15	20	25	30	35	40	45	50	55	60	65	70	75	80	85	90
200	.39	.39	.39	.39	.39	.39	.39	.39	.39	.39	.39	.39	.39	.39	.39	.39	.39	.39	.39
400	.64	.64	.64	.64	.64	.64	.64	.64	.64	.64	.64	.64	.64	.64	.64	.64	.64	.64	.64
600	.87	.87	.87	.87	.87	.87	.87	.87	.87	.87	.87	.87	.87	.87	.87	.87	.87	.87	.87
800	1.11	1.12	1.12	1.12	1.12	1.12	1.12	1.12	1.12	1.12	1.12	1.12	1.12	1.12	1.12	1.12	1.12	1.12	1.12
1000	1.38	1.38	1.38	1.38	1.38	1.38	1.38	1.38	1.38	1.38	1.38	1.38	1.38	1.38	1.38	1.38	1.38	1.38	1.38
1200	1.66	1.67	1.67	1.67	1.67	1.67	1.67	1.67	1.67	1.67	1.67	1.67	1.67	1.67	1.67	1.67	1.67	1.67	1.67
1400	1.99	1.99	1.99	1.99	1.99	1.98	1.98	1.98	1.98	1.98	1.98	1.98	1.98	1.98	1.98	1.98	1.98	1.98	1.98
1600	2.35	2.35	2.35	2.35	2.35	2.34	2.34	2.34	2.34	2.34	2.34	2.34	2.34	2.34	2.34	2.34	2.34	2.34	2.34
1800	2.77	2.77	2.76	2.76	2.76	2.75	2.75	2.75	2.75	2.74	2.74	2.74	2.74	2.74	2.74	2.74	2.74	2.74	2.74
2000	3.25	3.25	3.24	3.24	3.23	3.23	3.22	3.22	3.21	3.21	3.21	3.20	3.20	3.20	3.20	3.20	3.19	3.19	3.19
2200	3.81	3.80	3.79	3.78	3.78	3.77	3.76	3.75	3.75	3.74	3.74	3.73	3.73	3.72	3.72	3.72	3.72	3.72	3.72
2400	4.42	4.41	4.40	4.39	4.38	4.37	4.36	4.35	4.34	4.33	4.33	4.32	4.32	4.31	4.31	4.31	4.30	4.30	4.30
2600	5.07	5.06	5.05	5.04	5.03	5.01	5.00	4.99	4.99	4.98	4.97	4.96	4.96	4.95	4.95	4.94	4.94	4.94	4.94
2800	5.78	5.77	5.75	5.74	5.73	5.72	5.71	5.70	5.69	5.68	5.67	5.66	5.65	5.65	5.64	5.64	5.64	5.64	5.64
3000	6.55	6.53	6.52	6.50	6.49	6.48	6.47	6.46	6.45	6.44	6.43	6.42	6.41	6.41	6.40	6.40	6.40	6.40	6.39
3200	7.37	7.36	7.35	7.33	7.32	7.31	7.30	7.29	7.28	7.27	7.26	7.25	7.24	7.24	7.24	7.23	7.23	7.23	7.23
3400	8.27	8.25	8.24	8.23	8.22	8.21	8.20	8.19	8.18	8.18	8.17	8.16	8.16	8.16	8.15	8.15	8.15	8.15	8.15
3600	9.23	9.23	9.22	9.21	9.20	9.20	9.19	9.19	9.18	9.18	9.18	9.18	9.17	9.17	9.17	9.17	9.17	9.17	9.17
3800	10.28	10.28	10.28	10.28	10.28	10.28	10.28	10.29	10.29	10.29	10.30	10.31	10.31	10.32	10.32	10.32	10.33	10.33	10.33
4000	11.42	11.43	11.44	11.45	11.46	11.48	11.49	11.51	11.53	11.55	11.57	11.59	11.60	11.62	11.63	11.64	11.65	11.66	11.66
4200	12.66	12.68	12.71	12.74	12.78	12.81	12.85	12.90	12.94	12.98	13.03	13.07	13.11	13.14	13.18	13.20	13.22	13.23	13.24
4400	14.01	14.06	14.12	14.18	14.25	14.32	14.40	14.49	14.58	14.67	14.76	14.85	14.93	15.01	15.08	15.13	15.18	15.20	15.21
4600	15.49	15.58	15.69	15.80	15.93	16.07	16.22	16.39	16.56	16.75	16.94	17.14	17.33	17.52	17.70	17.85	17.96	18.04	18.06
4800	17.13	17.28	17.46	17.66	17.89	18.15	18.45	18.79	19.18										
5000	18.95	19.21	19.51	19.87															

I – 23

B-11547

PART II

Drift versus Time of Flight and Position Angle for 70°F Propellant Temperature

Deflection due to Cross Wind versus Time of Flight and Position Angle for 70°F Propellant Temperature

Drift in yards

Time of flight, seconds	| Position angle in degrees																		
	0	5	10	15	20	25	30	35	40	45	50	55	60	65	70	75	80	85	90
0	0	0	0	0	0	0	0	0	0	0	0	0	0	0	0	0	0	0	0
1	1	1	1	1	1	1	1	1	1	1	1	1	1	1	0	0	0	0	0
2	3	3	3	3	3	3	2	2	2	2	2	2	1	1	1	1	1	0	0
3	4	4	4	4	4	4	4	3	3	3	3	3	2	2	2	1	1	0	0
4	6	6	6	6	6	5	5	5	5	4	4	4	3	3	2	2	1	1	0
5	8	8	8	8	8	8	7	7	6	6	5	5	4	4	3	2	1	1	0
6	11	11	11	11	11	10	10	9	9	8	7	6	6	5	4	3	2	1	0
7	15	15	15	14	14	14	13	12	11	11	10	9	7	6	5	4	3	1	0
8	19	19	19	19	18	18	17	16	15	14	13	11	10	9	7	5	4	2	0
9	25	25	25	24	24	23	22	21	19	18	16	15	13	11	9	7	4	2	0
10	31	31	31	30	30	29	28	26	25	23	21	19	16	14	11	8	6	3	0
11	38	38	38	38	37	36	35	33	31	29	26	24	21	18	14	11	7	4	0
12	46	46	46	46	45	44	43	41	38	36	33	30	26	22	18	14	9	5	0
13	55	56	56	55	55	53	52	49	47	44	40	36	32	27	22	17	11	6	0
14	65	66	66	66	65	64	62	60	57	53	49	44	39	34	28	21	14	7	0
15	77	78	78	78	77	76	74	71	68	64	59	54	48	41	34	26	17	9	0
16	89	91	91	91	91	89	88	85	81	77	71	65	58	50	41	31	21	11	0
17	103	105	106	106	106	105	103	100	96	91	85	78	70	61	50	39	26	13	0
18	117	120	121	122	122	121	119	117	113	107	101	93	84	73	61	48	33	17	0
19	133	136	138	140	140	140	138	135	131	126	119	111	101	89	75	59	41	21	0
20	150	153	157	159	160	159	158	156	152	147	140	132	121	108	92	73	52	27	0

B-11547

II – 1

Deflection in yards for a 100-knot cross wind

Time of flight, seconds	Position angle in degrees																		
	0	5	10	15	20	25	30	35	40	45	50	55	60	65	70	75	80	85	90
0	00	00	00	00	00	00	00	00	00	00	00	00	00	00	00	00	00	00	00
1	-47	-47	-47	-47	-47	-48	-48	-48	-48	-48	-48	-48	-48	-48	-48	-48	-48	-48	-48
2	-93	-94	-94	-94	-95	-95	-95	-96	-96	-96	-96	-96	-97	-97	-97	-97	-97	-97	-97
3	-109	-110	-111	-111	-112	-113	-114	-114	-115	-116	-116	-117	-117	-118	-118	-118	-118	-118	-118
4	-106	-108	-109	-110	-111	-113	-114	-115	-116	-117	-118	-119	-120	-120	-121	-121	-121	-122	-122
5	-96	-98	-100	-101	-103	-105	-106	-108	-109	-111	-112	-113	-114	-115	-115	-116	-116	-117	-117
6	-81	-83	-85	-88	-90	-92	-94	-96	-98	-100	-101	-102	-104	-105	-106	-106	-107	-107	-107
7	-62	-65	-67	-70	-73	-76	-78	-80	-83	-85	-87	-88	-90	-91	-92	-93	-94	-94	-94
8	-40	-43	-46	-50	-53	-56	-59	-62	-65	-67	-69	-72	-73	-75	-76	-77	-78	-78	-78
9	-15	-19	-23	-27	-30	-34	-38	-41	-44	-47	-50	-52	-54	-56	-58	-59	-60	-60	-60
10	12	08	03	-1	-6	-10	-14	-18	-22	-25	-28	-31	-33	-35	-37	-38	-39	-40	-40
11	41	36	31	26	21	16	11	07	03	-1	-5	-8	-10	-13	-15	-16	-17	-18	-18
12	72	66	60	54	49	43	38	33	28	24	20	17	14	11	09	07	06	05	05
13	104	97	91	84	78	72	66	61	56	51	47	43	39	36	34	32	31	30	30
14	138	130	123	115	108	102	95	89	84	79	74	70	66	63	60	58	57	56	56
15	172	164	156	148	140	133	126	119	113	107	102	97	93	90	87	85	83	83	83
16	207	198	189	181	172	164	157	149	143	137	131	126	122	118	115	112	111	110	110
17	243	234	224	214	205	197	188	181	173	167	161	155	151	147	143	141	139	138	138
18	280	270	259	249	239	230	221	212	205	198	191	185	180	176	172	169	167	167	167
19	318	306	295	284	274	263	254	245	237	229	222	216	210	206	202	199	196	196	196
20	356	343	331	320	308	298	287	278	269	261	253	247	241	236	232	228	226	225	225

II - 2

8-11547

PART III

Effect on Horizontal Range and Altitude due to:

        Change in Initial Velocity
        Change in Air Density
        Change in Air Temperature
        Change in Elevation
        Rear Wind

    for 70°F Propellant Temperature

PART 3—EFFECTS ON HORIZONTAL RANGE AND ALTITUDE DUE TO VARIATIONS FROM STANDARD CONDITIONS

Effect on horizontal range in yards due to a 100 feet per second increase in initial velocity

Time of flight, seconds	Angle of elevation in degrees																	
	5	10	15	20	25	30	35	40	45	50	55	60	65	70	75	80	85	90
0	0	0	0	0	0	0	0	0	0	0	0	0	0	0	0	0	0	0
1	28	28	27	26	26	24	23	22	20	18	16	14	12	10	7	5	2	0
2	54	54	53	51	50	47	45	42	39	35	32	28	23	19	14	10	5	0
3	73	73	72	70	68	65	62	58	54	49	44	38	33	26	20	13	7	0
4	82	82	81	80	77	74	71	67	62	57	51	44	38	31	23	16	8	0
5	87	87	86	85	82	79	76	71	66	60	54	48	40	33	25	17	8	0
6	91	91	90	89	86	83	79	75	69	64	57	50	43	35	26	18	9	0
7	94	95	94	92	90	87	83	78	72	66	60	52	44	36	28	19	9	0
8	97	97	97	95	93	89	85	81	75	69	62	54	46	38	29	19	10	0
9	99	100	99	98	95	92	88	83	77	71	64	56	48	39	30	20	10	0
10		102	101	100	98	94	90	85	79	73	66	58	49	40	30	21	10	0
11		104	103	102	100	96	92	87	81	75	67	59	50	41	31	21	11	0
12		105	105	104	102	98	94	89	83	76	69	61	52	42	32	22	11	0
13		107	107	106	103	100	96	91	85	78	70	62	53	43	33	22	11	0
14		108	108	107	105	102	98	92	86	79	72	63	54	44	33	23	11	0
15		110	110	109	107	103	99	94	88	81	73	64	55	45	34	23	12	0
16			111	110	108	105	101	95	89	82	74	65	56	46	35	23	12	0
17			112	111	109	106	102	97	91	83	75	66	57	46	35	24	12	0
18			113	113	111	108	103	98	92	85	76	67	58	47	36	24	12	0
19			115	114	112	109	105	99	93	86	78	68	58	48	36	25	12	0
20			116	115	113	110	106	101	94	87	79	69	59	48	37	25	13	0

III – 1

B-11547

Effect on altitude in yards due to 100 feet per second increase in initial velocity

Time of flight, seconds	Angle of elevation in degrees

Time of flight, seconds	5	10	15	20	25	30	35	40	45	50	55	60	65	70	75	80	85	90
0	0	0	0	0	0	0	0	0	0	0	0	0	0	0	0	0	0	0
1	3	5	7	10	12	14	16	18	20	22	23	25	26	27	27	28	28	28
2	5	10	14	19	23	28	32	36	39	43	45	48	50	52	54	55	55	56
3	7	13	20	26	32	38	44	49	54	59	63	67	70	73	75	76	77	78
4	8	15	22	30	37	44	50	57	63	68	73	78	82	85	87	89	90	91
5	9	17	24	32	40	47	54	61	67	73	79	84	88	91	94	96	97	98
6	10	18	26	34	42	50	57	64	71	78	83	88	93	97	100	102	103	104
7	11	19	27	36	44	52	60	68	75	81	87	93	98	102	105	107	109	109
8	11	20	29	37	46	54	63	70	78	85	91	97	102	106	109	112	113	114
9	12	21	30	39	48	56	65	73	81	88	95	100	106	110	114	116	118	118
10		22	31	40	49	58	67	75	83	91	98	104	109	114	117	120	122	122
11		23	32	42	51	60	69	78	86	93	101	107	113	117	121	124	126	126
12		23	33	43	52	62	71	80	88	96	103	110	116	121	125	127	129	130
13		24	34	44	54	63	73	82	90	98	106	113	119	124	128	131	132	133
14		25	35	45	55	65	74	84	92	101	108	115	122	127	131	134	136	136
15		26	36	46	56	66	76	85	94	103	111	118	124	130	134	137	139	140
16			36	47	57	67	77	87	96	105	113	120	127	132	137	140	142	143
17			37	48	58	69	79	89	98	107	115	123	129	135	139	143	145	145
18			38	49	59	70	80	90	100	109	117	125	132	138	142	146	148	148
19			39	49	60	71	81	92	101	111	119	127	134	140	145	148	150	151
20			39	50	61	72	83	93	103	113	122	130	137	143	147	151	153	154

Effect on horizontal range in yards due to a 10 percent increase in air density

Time of flight, seconds	Angle of elevation in degrees																	
	5	10	15	20	25	30	35	40	45	50	55	60	65	70	75	80	85	90
0	0	0	0	0	0	0	0	0	0	0	0	0	0	0	0	0	0	0
1	-8	-8	-8	-8	-7	-7	-7	-6	-6	-5	-5	-4	-3	-3	-2	-1	-1	0
2	-39	-38	-37	-36	-35	-33	-31	-29	-27	-25	-22	-19	-16	-13	-10	-7	-3	0
3	-77	-77	-75	-73	-70	-67	-64	-60	-55	-50	-44	-39	-33	-26	-20	-14	-7	0
4	-104	-103	-102	-100	-96	-93	-88	-82	-76	-70	-62	-54	-46	-37	-28	-19	-10	0
5	-122	-122	-120	-118	-114	-109	-104	-97	-90	-82	-74	-64	-55	-44	-34	-23	-11	0
6	-140	-139	-138	-135	-131	-125	-119	-112	-104	-95	-85	-74	-63	-51	-39	-26	-13	0
7	-156	-156	-154	-151	-147	-141	-134	-126	-117	-106	-95	-83	-71	-57	-44	-29	-15	0
8	-172	-172	-170	-167	-162	-156	-148	-139	-129	-118	-106	-93	-79	-64	-48	-32	-16	0
9	-188	-188	-186	-182	-177	-170	-162	-152	-141	-129	-116	-101	-86	-70	-53	-36	-18	0
10		-203	-201	-197	-192	-184	-176	-165	-153	-140	-126	-110	-93	-76	-58	-39	-19	0
11		-217	-215	-211	-206	-198	-189	-178	-165	-151	-135	-118	-101	-82	-62	-42	-21	0
12		-231	-229	-225	-219	-211	-201	-190	-176	-161	-145	-127	-108	-87	-66	-45	-22	0
13		-244	-243	-239	-233	-224	-214	-201	-187	-171	-154	-135	-114	-93	-71	-47	-24	0
14		-257	-256	-252	-245	-237	-226	-213	-198	-181	-163	-143	-121	-98	-75	-50	-25	0
15		-270	-268	-264	-258	-249	-238	-224	-208	-191	-171	-150	-128	-104	-79	-53	-27	0
16			-281	-277	-270	-261	-249	-235	-219	-200	-180	-158	-134	-109	-83	-56	-28	0
17			-292	-289	-282	-272	-260	-246	-229	-210	-188	-165	-140	-114	-86	-58	-29	0
18			-304	-300	-293	-284	-271	-256	-239	-219	-196	-172	-146	-119	-90	-61	-30	0
19			315	-312	-305	-295	-282	-267	-248	-228	-204	-179	-152	-123	-94	-63	-32	0
20			-326	-323	-316	-306	-293	-277	-258	-236	-212	-186	-158	-128	-97	-65	-33	0

B-11547

Effect on altitude in yards due to a 10 percent increase in air density

Time of flight, seconds	Angle of elevation in degrees																	
	5	10	15	20	25	30	35	40	45	50	55	60	65	70	75	80	85	90
0	0	0	0	0	0	0	0	0	0	0	0	0	0	0	0	0	0	0
1	-1	-1	-2	-3	-3	-4	-5	-5	-6	-6	-6	-7	-7	-7	-8	-8	-8	-8
2	-3	-6	-10	-13	-16	-19	-21	-24	-27	-29	-31	-32	-34	-35	-36	-37	-37	-37
3	-5	-12	-19	-25	-31	-38	-43	-49	-54	-58	-62	-66	-69	-71	-73	-75	-76	-76
4	-7	-17	-25	-34	-43	-52	-60	-67	-74	-81	-87	-92	-97	-100	-104	-106	-107	-107
5	-9	-20	-30	-41	-51	-61	-71	-80	-88	-96	-103	-110	-115	-120	-123	-126	-127	-128
6	-10	-23	-35	-47	-59	-70	-81	-92	-101	-110	-119	-126	-132	-138	-142	-145	-147	-147
7	-11	-25	-39	-53	-66	-79	-91	-103	-114	-124	-134	-142	-149	-155	-160	-163	-165	-166
8	-12	-28	-43	-58	-73	-87	-101	-114	-126	-138	-148	-157	-165	-172	-177	-181	-183	-184
9	-13	-30	-46	-63	-79	-95	-110	-124	-138	-151	-162	-172	-181	-188	-194	-198	-201	-202
10		-32	-50	-68	-85	-102	-119	-134	-149	-163	-175	-187	-196	-204	-211	-215	-218	-219
11		-33	-53	-72	-91	-109	-127	-144	-160	-175	-188	-200	-211	-220	-226	-232	-235	-236
12		-35	-55	-76	-96	-116	-135	-153	-170	-186	-201	-214	-225	-234	-242	-247	-251	-252
13		-36	-58	-80	-101	-122	-143	-162	-180	-197	-213	-227	-239	-249	-257	-263	-266	-267
14		-37	-60	-83	-106	-129	-150	-171	-190	-208	-225	-239	-252	-263	-271	-277	-281	-282
15		-38	-62	-87	-111	-134	-157	-179	-199	-218	-236	-251	-265	-276	-285	-292	-296	-297
16			-64	-89	-115	-140	-164	-187	-208	-228	-247	-263	-278	-290	-299	-306	-310	-311
17			-65	-92	-119	-145	-170	-194	-217	-238	-257	-275	-290	-302	-312	-319	-324	-325
18			-67	-94	-122	-149	-176	-201	-225	-247	-268	-286	-302	-315	-325	-333	-337	-339
19			-67	-96	-125	-154	-181	-208	-233	-256	-278	-297	-313	-327	-338	-346	-350	-352
20			-68	-98	-128	-158	-187	-214	-241	-265	-287	-307	-325	-339	-350	-358	-363	-365

Effect on horizontal range in yards due to a 100° F increase in air temperature

Time of flight, seconds	Angle of elevation in degrees																	
	5	10	15	20	25	30	35	40	45	50	55	60	65	70	75	80	85	90
0	0	0	0	0	0	0	0	0	0	0	0	0	0	0	0	0	0	0
1	-8	-8	-7	-7	-7	-7	-6	-6	-5	-5	-4	-4	-3	-3	-2	-1	-1	0
2	-56	-56	-54	-53	-51	-48	-46	-43	-40	-36	-32	-28	-24	-19	-14	-10	-5	0
3	-109	-108	-106	-103	-100	-96	-91	-85	-79	-72	-64	-56	-47	-38	-29	-19	-10	0
4	-129	-129	-128	-126	-122	-118	-112	-106	-99	-90	-81	-71	-60	-49	-37	-25	-13	0
5	-131	-132	-131	-129	-126	-122	-116	-110	-102	-94	-84	-74	-63	-51	-39	-26	-13	0
6	-133	-134	-133	-131	-128	-124	-119	-112	-105	-96	-86	-76	-65	-53	-40	-27	-13	0
7	-134	-135	-135	-134	-131	-127	-121	-115	-107	-98	-88	-78	-66	-54	-41	-28	-14	0
8	-135	-137	-137	-136	-133	-129	-123	-117	-109	-100	-90	-79	-68	-55	-42	-28	-14	0
9	-137	-139	-139	-138	-135	-131	-126	-119	-111	-102	-92	-81	-69	-56	-43	-29	-15	0
10		-140	-141	-140	-137	-133	-128	-121	-113	-104	-94	-83	-70	-57	-44	-30	-15	0
11		-142	-143	-142	-139	-135	-130	-123	-115	-106	-96	-84	-72	-59	-45	-30	-15	0
12		-144	-144	-143	-141	-137	-132	-125	-117	-108	-97	-86	-73	-60	-46	-31	-16	0
13		-145	-146	-145	-143	-139	-134	-127	-119	-110	-99	-87	-75	-61	-46	-31	-16	0
14		-147	-148	-147	-145	-141	-136	-129	-121	-111	-101	-89	-76	-62	-47	-32	-16	0
15		-149	-150	-149	-147	-143	-138	-131	-123	-113	-102	-90	-77	-63	-48	-32	-16	0
16			-152	-151	-149	-145	-140	-133	-125	-115	-104	-92	-78	-64	-49	-33	-16	0
17			-153	-153	-151	-147	-142	-135	-127	-117	-106	-93	-80	-65	-49	-33	-17	0
18			-155	-155	-153	-149	-144	-137	-128	-118	-107	-95	-81	-66	-50	-34	-17	0
19			-157	-157	-155	-151	-146	-139	-130	-120	-109	-96	-82	-67	-51	-34	-17	0
20			-158	-158	-157	-153	-148	-141	-132	-122	-110	-97	-83	-68	-52	-35	-17	0

III – 5

B-11547

Effect on altitude in yards due to 100° F increase in air temperature

Time of flight second	5	10	15	20	25	30	35	40	45	50	55	60	65	70	75	80	85	90
0	0	0	0	0	0	0	0	0	0	0	0	0	0	0	0	0	0	0
1	-1	-1	-2	-2	-3	-4	-4	-5	-5	-6	-6	-7	-7	-7	-7	-7	-7	-7
2	-4	-9	-14	-18	-23	-27	-31	-35	-39	-42	-45	-47	-50	-51	-53	-54	-55	-55
3	-8	-17	-26	-36	-44	-53	-61	-69	-77	-83	-89	-95	-99	-103	-106	-108	-109	-110
4	-10	-21	-33	-44	-55	-66	-77	-87	-96	-105	-113	-121	-127	-132	-136	-140	-141	-142
5	-11	-23	-35	-47	-58	-70	-81	-92	-101	-111	-120	-127	-134	-140	-144	-147	-149	-150
6	-13	-25	-37	-49	-61	-73	-84	-95	-105	-115	-124	-132	-139	-145	-150	-153	-155	-156
7	-14	-26	-38	-51	-63	-75	-87	-98	-109	-119	-128	-136	-144	-150	-155	-158	-160	-161
8	-15	-28	-40	-53	-65	-77	-90	-101	-112	-122	-132	-141	-148	-154	-160	-163	-165	-166
9	-16	-29	-41	-54	-67	-80	-92	-104	-115	-126	-136	-145	-152	-159	-164	-168	-170	-171
10		-30	-43	-56	-69	-82	-95	-107	-118	-129	-139	-148	-156	-163	-169	-172	-175	-175
11		-31	-44	-57	-71	-84	-97	-109	-121	-132	-143	-152	-160	-167	-173	-177	-179	-180
12		-32	-45	-59	-72	-86	-99	-112	-124	-135	-146	-156	-164	-171	-177	-181	-184	-184
13		-33	-46	-60	-74	-88	-101	-114	-127	-138	-149	-159	-168	-175	-181	-185	-188	-189
14		-33	-47	-61	-75	-89	-103	-116	-129	-141	-152	-162	-171	-179	-185	-189	-192	-193
15		-34	-48	-62	-77	-91	-105	-119	-132	-144	-155	-166	-175	-182	-189	-193	-196	-197
16			-49	-63	-78	-93	-107	-121	-134	-147	-158	-169	-178	-186	-192	-197	-199	-200
17			-50	-64	-79	-94	-108	-123	-136	-149	-161	-172	-181	-189	-196	-200	-203	-204
18			-50	-65	-80	-95	-110	-125	-138	-151	-164	-175	-184	-193	-199	-204	-207	-208
19			-51	-66	-81	-97	-112	-126	-141	-154	-166	-178	-188	-196	-203	-207	-210	-211
20			-51	-67	-82	-98	-113	-128	-142	-156	-169	-181	-191	-199	-206	-211	-214	-215

III – 6

Effect on horizontal range in yards due to 1 degree increase in angle of elevation

Time of flight, seconds	Angle of elevation in degrees																	
	5	10	15	20	25	30	35	40	45	50	55	60	65	70	75	80	85	90
0	0	0	0	0	0	0	0	0	0	0	0	0	0	0	0	0	0	0
1	-1	-2	-3	-4	-5	-6	-7	-8	-9	-10	-10	-11	-11	-12	-12	-12	-12	-12
2	-2	-4	-6	-8	-10	-12	-14	-16	-17	-19	-20	-22	-23	-23	-24	-25	-25	-25
3	-2	-5	-8	-10	-13	-16	-19	-21	-23	-26	-28	-29	-31	-32	-33	-34	-34	-34
4	-2	-5	-9	-12	-16	-19	-22	-25	-28	-31	-33	-35	-37	-39	-40	-41	-41	-41
5	-2	-6	-10	-13	-17	-21	-25	-28	-32	-35	-38	-40	-42	-44	-46	-47	-47	-47
6	-1	-6	-10	-15	-19	-23	-27	-31	-35	-39	-42	-45	-47	-49	-51	-52	-53	-53
7	-1	-6	-11	-15	-20	-25	-30	-34	-38	-42	-46	-49	-52	-54	-56	-57	-58	-58
8	0	-6	-11	-16	-21	-27	-32	-36	-41	-45	-49	-53	-56	-58	-60	-62	-63	-63
9	0	-6	-11	-17	-22	-28	-33	-39	-44	-48	-52	-56	-60	-62	-65	-66	-67	-68
10		-5	-11	-17	-23	-29	-35	-41	-46	-51	-55	-60	-63	-66	-69	-70	-72	-72
11		-5	-11	-17	-24	-30	-36	-42	-48	-53	-58	-63	-67	-70	-73	-74	-76	-76
12		-4	-11	-18	-24	-31	-37	-44	-50	-56	-61	-66	-70	-73	-76	-78	-79	-80
13		-4	-11	-18	-25	-32	-39	-45	-52	-58	-63	-69	-73	-77	-80	-82	-83	-84
14		-3	-10	-18	-25	-32	-40	-47	-53	-60	-66	-71	-76	-80	-83	-85	-87	-87
15		-3	-10	-18	-25	-33	-40	-48	-55	-62	-68	-74	-79	-83	-86	-89	-90	-91
16			-10	-17	-25	-33	-41	-49	-56	-63	-70	-76	-81	-86	-90	-92	-94	-94
17			-9	-17	-25	-33	-42	-50	-58	-65	-72	-78	-84	-89	-93	-95	-97	-98
18			-9	-17	-25	-34	-42	-51	-59	-67	-74	-81	-86	-92	-96	-99	-100	-101
19			-8	-16	-25	-34	-43	-51	-60	-68	-76	-83	-89	-94	-98	-102	-104	-104
20			-7	-16	-25	-34	-43	-52	-61	-69	-77	-85	-91	-97	-101	-105	-107	-107

8-11547

Effect on altitude in yards due to 1 degree increase in angle of elevation

Time of flight, seconds	Angle of elevation in degrees																	
	5	10	15	20	25	30	35	40	45	50	55	60	65	70	75	80	85	90
0	0	0	0	0	0	0	0	0	0	0	0	0	0	0	0	0	0	0
1	12	12	12	12	11	11	10	10	9	8	7	6	5	4	3	2	1	0
2	25	24	24	23	23	22	21	19	18	16	15	13	11	9	7	4	2	0
3	33	33	33	32	31	30	28	26	25	22	20	18	15	12	9	6	3	0
4	40	39	39	38	37	36	34	32	30	27	24	21	18	15	11	7	4	0
5	45	45	45	44	43	41	39	37	34	31	28	25	21	17	13	9	4	0
6	50	50	50	49	47	46	44	41	38	35	32	28	24	19	15	10	5	0
7	54	54	54	53	52	50	48	45	42	39	35	31	26	21	16	11	5	0
8	58	59	58	57	56	54	52	49	46	42	38	33	28	23	18	12	6	0
9	62	62	62	61	60	58	56	53	49	45	41	36	31	25	19	13	6	0
10		66	66	65	64	62	59	56	53	48	44	38	33	27	20	14	7	0
11		69	69	68	67	65	63	59	56	51	46	41	35	28	22	15	7	0
12		72	72	71	70	68	66	62	59	54	49	43	37	30	23	15	8	0
13		75	75	74	73	71	69	65	61	57	51	45	39	32	24	16	8	0
14		77	78	77	76	74	72	68	64	59	54	47	41	33	25	17	9	0
15		80	80	80	79	77	74	71	67	62	56	50	42	35	26	18	9	0
16			82	82	81	80	77	74	69	64	58	52	44	36	28	19	9	0
17			84	84	84	82	79	76	72	67	61	54	46	38	29	19	10	0
18			86	86	86	84	82	78	74	69	63	56	48	39	30	20	10	0
19			88	88	88	86	84	81	76	71	65	58	50	41	31	21	11	0
20			90	90	90	88	86	83	79	73	67	59	51	42	32	22	11	0

B-11547

Effect on horizontal range in yards due to a 100 knot rear wind

Time of flight, seconds	Angle of elevation in degrees																	
	5	10	15	20	25	30	35	40	45	50	55	60	65	70	75	80	85	90
0	0	0	0	0	0	0	0	0	0	0	0	0	0	0	0	0	0	0
1	9	7	5	2	-1	-5	-10	-14	-19	-24	-29	-33	-37	-41	-44	-46	-48	-48
2	20	18	14	8	1	-7	-16	-26	-37	-47	-57	-67	-75	-83	-89	-93	-96	-97
3	45	41	36	28	19	7	-6	-20	-34	-49	-62	-75	-88	-98	-107	-113	-117	-118
4	86	81	74	64	52	38	22	4	-14	-32	-50	-67	-82	-96	-106	-115	-119	-121
5	134	129	120	109	94	77	57	37	15	-8	-29	-50	-69	-85	-99	-108	-114	-116
6	184	178	169	156	139	119	96	72	47	21	-5	-29	-51	-70	-86	-97	-104	-106
7	235	229	218	204	185	163	138	110	81	52	23	-4	-30	-51	-70	-83	-91	-94
8	287	281	269	253	233	209	181	150	118	86	53	22	-6	-31	-50	-65	-75	-78
9	340	333	321	304	282	255	225	192	157	121	85	52	20	-7	-29	-46	-56	-59
10		386	374	355	332	304	271	235	197	158	119	82	48	19	-6	-24	-36	-39
11		440	427	407	383	353	318	279	238	196	154	114	78	45	19	-1	-13	-17
12		494	480	460	434	402	366	325	281	236	191	148	108	73	45	24	11	6
13		548	534	513	486	453	414	371	324	277	229	183	141	103	72	50	36	31
14		603	589	568	539	504	463	416	369	319	268	219	173	134	101	77	62	57
15		658	643	622	593	556	514	466	415	361	308	256	208	166	131	105	89	84
16			699	676	646	609	565	515	461	405	348	294	244	198	161	134	117	111
17			754	731	701	662	616	564	508	449	391	333	279	232	193	163	145	139
18			810	787	755	715	668	615	557	495	433	372	316	266	225	193	174	168
19			866	842	810	769	721	665	605	541	476	413	354	301	257	224	204	196
20			921	898	866	824	774	717	654	588	521	454	393	337	290	255	233	226

III – 9

Effect on altitude in yards due to a 100 knot rear wind

	Angle of elevation in degrees																	
Time of flight, seconds	5	10	15	20	25	30	35	40	45	50	55	60	65	70	75	80	85	90
0	0	0	0	0	0	0	0	0	0	0	0	0	0	0	0	0	0	0
1	5	9	14	18	21	25	27	28	28	28	27	24	22	19	14	10	5	0
2	10	19	28	37	44	50	55	58	59	58	56	52	45	38	30	20	10	0
3	13	26	39	50	60	69	75	79	81	80	76	71	63	53	41	28	15	0
4	16	32	48	63	75	86	94	99	101	101	97	89	79	67	53	36	18	0
5	18	38	57	74	90	103	113	120	123	122	117	109	96	81	63	44	22	0
6	20	43	65	86	104	119	131	139	143	142	136	126	112	95	74	51	26	0
7	22	48	73	96	117	134	148	157	161	160	154	144	128	108	85	58	29	0
8	24	52	80	105	128	148	163	174	179	178	172	160	142	120	94	65	33	0
9	25	56	86	114	140	161	178	190	196	196	189	175	156	133	103	71	36	0
10		60	92	122	150	173	192	205	212	212	204	190	170	144	112	77	40	0
11		63	97	130	160	185	206	220	227	227	220	205	183	155	121	83	43	0
12		66	103	137	169	196	218	234	242	243	235	219	196	166	130	90	45	0
13		69	107	144	177	207	230	247	256	257	250	233	209	177	139	95	49	0
14		71	112	150	185	216	242	260	270	272	264	247	221	188	147	101	52	0
15		73	115	156	193	226	253	272	283	285	277	260	233	199	155	107	55	0
16			119	161	200	235	263	284	296	298	291	273	245	209	164	113	58	0
17			123	166	207	243	273	295	308	311	304	285	257	219	172	118	61	0
18			125	171	213	251	282	306	320	324	317	298	269	229	180	124	63	0
19			128	175	219	259	291	316	332	336	329	311	280	239	189	130	66	0
20			131	179	224	265	300	326	343	348	342	323	291	249	197	137	69	0

III – 10

PART IV

Corrections to Sight Angle and Time of Flight for:

Change in Initial Velocity
Change in Air Density
Change in Air Temperature
Rear Wind

for 70°F Propellant Temperature

PART 4—CORRECTIONS TO SIGHT ANGLE AND TIME OF FLIGHT FOR VARIATIONS FROM STANDARD CONDITIONS

Correction to sight angle in degrees for 100 feet per second increase in initial velocity

Time of flight, seconds	Position angle in degrees
	0	5	10	15	20	25	30	35	40	45	50	55	60	65	70	75	80	85	90
0	.00	.00	.00	.00	.00	.00	.00	.00	.00	.00	.00	.00	.00	.00	.00	.00	.00	.00	.00
1	-.05	-.05	-.05	-.05	-.05	-.05	-.04	-.04	-.04	-.03	-.03	-.03	-.03	-.03	-.03	-.02	-.01	-.01	.00
2	-.08	-.08	-.08	-.08	-.07	-.07	-.07	-.07	-.06	-.06	-.05	-.05	-.04	-.03	-.03	-.02	-.01	-.01	.00
3	-.13	-.13	-.13	-.12	-.12	-.12	-.11	-.11	-.10	-.09	-.08	-.07	-.06	-.05	-.04	-.03	-.02	-.01	.00
4	-.19	-.19	-.19	-.18	-.18	-.18	-.17	-.16	-.15	-.14	-.12	-.11	-.10	-.08	-.07	-.05	-.03	-.02	.00
5	-.25	-.25	-.25	-.25	-.24	-.23	-.22	-.21	-.20	-.19	-.17	-.15	-.13	-.11	-.09	-.07	-.05	-.02	.00
6	-.32	-.32	-.32	-.31	-.31	-.30	-.28	-.27	-.25	-.24	-.21	-.19	-.17	-.14	-.11	-.09	-.06	-.03	.00
7	-.38	-.39	-.38	-.38	-.37	-.36	-.33	-.33	-.31	-.29	-.26	-.24	-.21	-.18	-.14	-.11	-.07	-.04	.00
8	-.45	-.46	-.46	-.45	-.44	-.43	-.40	-.40	-.37	-.35	-.32	-.28	-.25	-.21	-.17	-.13	-.09	-.05	.00
9	-.52	-.53	-.53	-.53	-.52	-.50	-.49	-.47	-.44	-.41	-.38	-.34	-.30	-.25	-.20	-.15	-.10	-.05	.00
10	-.60	-.61	-.61	-.61	-.60	-.58	-.57	-.54	-.51	-.48	-.44	-.40	-.35	-.30	-.24	-.18	-.12	-.06	.00
11	-.68	-.69	-.69	-.69	-.68	-.67	-.65	-.62	-.59	-.56	-.51	-.46	-.41	-.35	-.28	-.22	-.15	-.08	.00
12	-.76	-.78	-.78	-.78	-.78	-.77	-.75	-.72	-.68	-.64	-.59	-.54	-.47	-.41	-.33	-.25	-.17	-.09	.00
13	-.85	-.87	-.88	-.88	-.88	-.87	-.85	-.82	-.78	-.74	-.68	-.62	-.55	-.47	-.39	-.30	-.20	-.10	.00
14	-.94	-.97	-.98	-.99	-.99	-.98	-.96	-.94	-.90	-.85	-.79	-.72	-.64	-.55	-.46	-.35	-.24	-.12	.00
15	-1.04	-1.07	-1.10	-1.11	-1.11	-1.11	-1.10	-1.07	-1.03	-.98	-.92	-.84	-.75	-.65	-.54	-.41	-.28	-.14	.00
16	-1.15	-1.19	-1.22	-1.24	-1.25	-1.26	-1.25	-1.22	-1.19	-1.14	-1.07	-.99	-.89	-.77	-.64	-.49	-.33	-.17	.00
17	-1.26	-1.31	-1.35	-1.38	-1.41	-1.42	-1.42	-1.41	-1.38	-1.33	-1.26	-1.17	-1.06	-.93	-.77	-.60	-.41	-.21	.00
18	-1.38	-1.45	-1.50	-1.55	-1.59	-1.61	-1.63	-1.63	-1.61	-1.57	-1.50	-1.41	-1.29	-1.13	-.95	-.74	-.51	-.26	.00
19	-1.51	-1.59	-1.67	-1.73	-1.79	-1.84	-1.88	-1.90	-1.90	-1.87	-1.82	-1.73	-1.60	-1.43	-1.21	-.95	-.66	-.34	.00
20	-1.66	-1.76	-1.86	-1.95	-2.04	-2.12	-2.19	-2.24	-2.28	-2.29	-2.26	-2.19	-2.06	-1.87	-1.61	-1.29	-.90	-.46	.00

Correction to time of flight in seconds for 100 feet per second increase in initial velocity

Time of flight, seconds	\	\	\	\	\	\	\	\	Position angle in degrees	\	\	\	\	\	\	\	\	\	\
	0	5	10	15	20	25	30	35	40	45	50	55	60	65	70	75	80	85	90
0	.00	.00	.00	.00	.00	.00	.00	.00	.00	.00	.00	.00	.00	.00	.00	.00	.00	.00	.00
1	-.03	-.03	-.03	-.03	-.03	-.03	-.03	-.03	-.03	-.03	-.03	-.03	-.03	-.03	-.03	-.03	-.03	-.03	-.03
2	-.09	-.09	-.09	-.09	-.09	-.09	-.09	-.09	-.09	-.09	-.09	-.09	-.09	-.09	-.09	-.09	-.09	-.09	-.09
3	-.18	-.18	-.18	-.18	-.18	-.18	-.18	-.18	-.18	-.18	-.18	-.18	-.18	-.18	-.18	-.18	-.18	-.18	-.18
4	-.25	-.25	-.25	-.25	-.25	-.25	-.26	-.26	-.26	-.26	-.26	-.26	-.26	-.26	-.26	-.26	-.26	-.27	-.27
5	-.29	-.30	-.30	-.30	-.31	-.31	-.31	-.31	-.32	-.32	-.32	-.32	-.32	-.32	-.33	-.33	-.33	-.33	-.33
6	-.34	-.35	-.35	-.36	-.36	-.36	-.37	-.37	-.37	-.38	-.38	-.38	-.39	-.39	-.39	-.39	-.39	-.39	-.39
7	-.39	-.40	-.40	-.41	-.41	-.42	-.43	-.43	-.43	-.44	-.44	-.45	-.45	-.46	-.46	-.46	-.46	-.46	-.46
8	-.44	-.45	-.46	-.46	-.47	-.48	-.49	-.49	-.50	-.51	-.51	-.52	-.52	-.53	-.53	-.54	-.54	-.54	-.54
9	-.49	-.50	-.51	-.52	-.53	-.54	-.55	-.56	-.57	-.58	-.59	-.60	-.61	-.61	-.62	-.62	-.63	-.63	-.63
10	-.54	-.56	-.57	-.58	-.60	-.61	-.62	-.64	-.65	-.66	-.67	-.68	-.70	-.70	-.71	-.72	-.72	-.73	-.73
11	-.59	-.61	-.63	-.65	-.67	-.68	-.70	-.72	-.74	-.75	-.77	-.78	-.80	-.81	-.82	-.83	-.83	-.84	-.84
12	-.65	-.67	-.70	-.72	-.74	-.76	-.78	-.81	-.83	-.85	-.87	-.89	-.91	-.93	-.94	-.95	-.96	-.97	-.97
13	-.71	-.74	-.76	-.79	-.82	-.85	-.88	-.91	-.94	-.97	-.99	-1.02	-1.05	-1.07	-1.09	-1.10	-1.11	-1.12	-1.12
14	-.77	-.80	-.84	-.87	-.91	-.94	-.98	-1.02	-1.06	-1.10	-1.14	-1.17	-1.20	-1.24	-1.26	-1.28	-1.30	-1.31	-1.?
15	-.83	-.87	-.91	-.96	-1.00	-1.05	-1.10	-1.15	-1.20	-1.25	-1.30	-1.35	-1.40	-1.43	-1.47	-1.50	-1.52	-1.53	-1.54
16	-.90	-.95	-1.00	-1.05	-1.11	-1.17	-1.23	-1.30	-1.37	-1.43	-1.50	-1.57	-1.63	-1.69	-1.74	-1.78	-1.81	-1.82	-1.83
17	-.97	-1.03	-1.09	-1.16	-1.24	-1.31	-1.39	-1.48	-1.57	-1.66	-1.75	-1.84	-1.93	-2.01	-2.08	-2.14	-2.18	-2.21	-2.21
18	-1.05	-1.12	-1.20	-1.28	-1.38	-1.47	-1.58	-1.69	-1.82	-1.94	-2.07	-2.20	-2.33	-2.44	-2.55	-2.63	-2.70	-2.74	-2.75
19	-1.13	-1.22	-1.32	-1.42	-1.54	-1.67	-1.81	-1.97	-2.13	-2.31	-2.50	-2.69	-2.88	-3.06	-3.22	-3.36	-3.47	-3.53	-3.56
20	-1.23	-1.33	-1.45	-1.58	-1.74	-1.91	-2.10	-2.31	-2.55	-2.81	-3.10	-3.40	-3.71	-4.01	-4.30	-4.55	-4.74	-4.87	-4.91

B–115u7

Correction to time of flight in seconds for 10 percent increase in air density

Time of flight, seconds	Position angle in degrees																		
	0	5	10	15	20	25	30	35	40	45	50	55	60	65	70	75	80	85	90
0	.00	.00	.00	.00	.00	.00	.00	.00	.00	.00	.00	.00	.00	.00	.00	.00	.00	.00	.00
1	.01	.01	.01	.01	.01	.01	.01	.01	.01	.01	.01	.01	.01	.01	.01	.01	.01	.01	.01
2	.07	.07	.07	.07	.07	.06	.06	.06	.06	.06	.06	.06	.06	.06	.06	.06	.06	.06	.06
3	.19	.19	.19	.19	.18	.18	.18	.18	.18	.18	.18	.18	.18	.18	.18	.18	.18	.18	.18
4	.31	.31	.31	.31	.31	.31	.31	.31	.31	.31	.31	.31	.31	.31	.31	.31	.31	.31	.31
5	.41	.41	.42	.42	.42	.42	.42	.42	.42	.42	.43	.43	.43	.43	.43	.43	.43	.43	.43
6	.52	.53	.53	.54	.54	.54	.54	.54	.55	.55	.55	.55	.55	.55	.56	.56	.56	.56	.56
7	.65	.65	.66	.66	.67	.67	.68	.68	.68	.69	.69	.69	.70	.70	.70	.70	.71	.71	.71
8	.78	.79	.80	.81	.81	.82	.83	.83	.84	.85	.85	.86	.86	.87	.87	.87	.88	.88	.88
9	.93	.94	.95	.96	.97	.99	1.00	1.01	1.02	1.02	1.03	1.04	1.05	1.06	1.06	1.07	1.07	1.07	1.07
10	1.08	1.10	1.12	1.13	1.15	1.17	1.18	1.20	1.21	1.23	1.24	1.25	1.27	1.28	1.29	1.29	1.30	1.30	1.30
11	1.25	1.27	1.30	1.32	1.34	1.37	1.39	1.41	1.43	1.46	1.48	1.50	1.51	1.53	1.54	1.55	1.56	1.57	1.57
12	1.43	1.46	1.49	1.52	1.56	1.59	1.62	1.66	1.69	1.72	1.75	1.78	1.80	1.83	1.85	1.86	1.87	1.88	1.88
13	1.62	1.66	1.70	1.75	1.79	1.84	1.88	1.93	1.97	2.02	2.06	2.10	2.14	2.17	2.20	2.22	2.24	2.25	2.26
14	1.82	1.88	1.93	1.99	2.05	2.11	2.18	2.24	2.30	2.37	2.43	2.49	2.54	2.59	2.63	2.67	2.69	2.71	2.71
15	2.04	2.11	2.18	2.26	2.34	2.43	2.51	2.60	2.69	2.78	2.87	2.95	3.03	3.10	3.16	3.21	3.25	3.27	3.27
16	2.27	2.36	2.46	2.56	2.67	2.79	2.90	3.03	3.15	3.28	3.40	3.52	3.63	3.74	3.83	3.90	3.95	3.98	4.00
17	2.52	2.64	2.77	2.90	3.05	3.20	3.36	3.53	3.71	3.88	4.06	4.24	4.40	4.56	4.69	4.80	4.88	4.94	4.95
18	2.80	2.95	3.11	3.29	3.48	3.68	3.91	4.14	4.39	4.65	4.91	5.17	5.42	5.66	5.87	6.05	6.18	6.26	6.29
19	3.10	3.29	3.50	3.73	3.98	4.26	4.57	4.90	5.26	5.65	6.04	6.45	6.85	7.24	7.59	7.88	8.10	8.24	8.29
20	3.43	3.67	3.93	4.24	4.58	4.96	5.39	5.88	6.42	7.00	7.64	8.31	9.00	9.67	10.31	10.86	11.29	11.57	11.66

Correction to sight angle in degrees for 10 percent increase in air density

Time of flight, seconds	Position angle in degrees																		
	0	5	10	15	20	25	30	35	40	45	50	55	60	65	70	75	80	85	90
0	.00	.00	.00	.00	.00	.00	.00	.00	.00	.00	.00	.00	.00	.00	.00	.00	.00	.00	.00
1	.00	.01	.01	.01	.00	.00	.00	.01	.01	.01	.00	.00	.00	.01	.00	.01	.00	.01	.00
2	.03	.03	.03	.03	.03	.02	.03	.02	.02	.02	.02	.02	.02	.01	.01	.01	.01	.00	.00
3	.08	.08	.08	.08	.08	.07	.07	.07	.06	.06	.05	.05	.04	.03	.03	.02	.01	.01	.00
4	.17	.17	.17	.17	.15	.16	.15	.14	.13	.12	.11	.10	.08	.07	.06	.05	.03	.02	.00
5	.28	.28	.27	.27	.26	.25	.24	.23	.21	.20	.18	.16	.14	.12	.09	.07	.05	.02	.00
6	.39	.39	.39	.38	.37	.36	.34	.32	.30	.28	.26	.23	.20	.17	.14	.10	.07	.03	.00
7	.53	.53	.52	.52	.50	.48	.46	.44	.41	.38	.35	.31	.27	.23	.19	.14	.09	.05	.00
8	.67	.68	.67	.66	.65	.63	.60	.57	.53	.50	.45	.40	.35	.30	.24	.18	.12	.06	.00
9	.84	.84	.84	.83	.81	.79	.76	.72	.68	.63	.57	.51	.45	.38	.31	.23	.16	.08	.00
10	1.02	1.03	1.03	1.02	1.00	.97	.93	.89	.84	.78	.71	.64	.56	.48	.39	.29	.20	.10	.00
11	1.22	1.23	1.24	1.23	1.21	1.18	1.14	1.09	1.03	.96	.88	.79	.69	.59	.48	.37	.25	.12	.00
12	1.44	1.46	1.47	1.46	1.44	1.41	1.37	1.31	1.24	1.16	1.07	.96	.85	.72	.59	.45	.30	.15	.00
13	1.69	1.71	1.72	1.72	1.71	1.67	1.63	1.57	1.49	1.40	1.29	1.17	1.03	.88	.72	.55	.37	.19	.00
14	1.95	1.99	2.01	2.02	2.01	1.98	1.93	1.87	1.78	1.68	1.56	1.42	1.26	1.08	.88	.67	.46	.23	.00
15	2.25	2.30	2.33	2.35	2.35	2.32	2.28	2.22	2.13	2.02	1.88	1.72	1.53	1.31	1.08	.83	.56	.28	.00
16	2.56	2.63	2.69	2.72	2.73	2.72	2.69	2.63	2.54	2.42	2.27	2.09	1.87	1.61	1.33	1.02	.70	.35	.00
17	2.91	3.01	3.08	3.14	3.18	3.18	3.17	3.12	3.04	2.92	2.76	2.55	2.30	2.00	1.66	1.28	.87	.44	.00
18	3.30	3.42	3.53	3.62	3.69	3.73	3.75	3.72	3.65	3.54	3.38	3.16	2.87	2.52	2.11	1.64	1.12	.57	.00
19	3.72	3.89	4.04	4.18	4.29	4.39	4.44	4.47	4.44	4.36	4.21	3.98	3.67	3.26	2.76	2.16	1.49	.76	.00
20	4.19	4.41	4.62	4.82	5.00	5.17	5.31	5.42	5.48	5.46	5.38	5.19	4.87	4.40	3.78	3.01	2.10	1.08	.00

IV – 4

Correction to time of flight in seconds for 100° F increase in air temperature

Time of flight, seconds	Position angle in degrees																		
	0	5	10	15	20	25	30	35	40	45	50	55	60	65	70	75	80	85	90
0	.00	.00	.00	.00	.00	.00	.00	.00	.00	.00	.00	.00	.00	.00	.00	.00	.00	.00	.00
1	.01	.01	.01	.01	.01	.01	.01	.01	.01	.01	.01	.01	.01	.01	.01	.01	.01	.01	.01
2	.10	.10	.10	.10	.10	.09	.09	.09	.09	.09	.09	.09	.09	.09	.09	.09	.09	.09	.09
3	.26	.26	.26	.26	.26	.26	.26	.26	.26	.26	.26	.26	.25	.25	.25	.25	.25	.25	.25
4	.38	.39	.39	.39	.40	.40	.40	.40	.41	.41	.41	.41	.41	.41	.41	.41	.42	.42	.42
5	.44	.45	.45	.46	.46	.47	.47	.48	.48	.48	.49	.49	.49	.50	.50	.50	.50	.50	.50
6	.50	.51	.52	.52	.53	.54	.54	.55	.56	.56	.57	.57	.58	.58	.58	.59	.59	.59	.59
7	.55	.57	.58	.59	.60	.61	.62	.63	.64	.65	.65	.66	.67	.67	.68	.68	.68	.69	.69
8	.61	.63	.65	.66	.68	.69	.70	.71	.72	.74	.75	.76	.76	.77	.78	.79	.79	.79	.79
9	.67	.70	.72	.74	.75	.77	.79	.80	.82	.84	.85	.86	.87	.89	.89	.90	.91	.91	.91
10	.74	.77	.79	.82	.84	.86	.88	.90	.92	.94	.96	.98	1.00	1.01	1.02	1.03	1.04	1.04	1.04
11	.81	.84	.87	.90	.93	.96	.98	1.01	1.04	1.07	1.09	1.11	1.13	1.15	1.17	1.18	1.19	1.20	1.20
12	.88	.92	.96	.99	1.03	1.06	1.10	1.13	1.17	1.20	1.24	1.27	1.29	1.32	1.34	1.36	1.37	1.38	1.38
13	.96	1.00	1.05	1.09	1.14	1.18	1.23	1.27	1.32	1.36	1.40	1.44	1.48	1.51	1.54	1.56	1.58	1.59	1.59
14	1.04	1.09	1.15	1.20	1.26	1.31	1.37	1.43	1.48	1.54	1.60	1.65	1.70	1.74	1.78	1.81	1.83	1.85	1.85
15	1.12	1.19	1.25	1.32	1.39	1.46	1.53	1.60	1.68	1.75	1.83	1.90	1.96	2.02	2.07	2.11	2.14	2.16	2.17
16	1.22	1.29	1.37	1.45	1.54	1.63	1.72	1.81	1.91	2.01	2.11	2.20	2.29	2.37	2.44	2.49	2.54	2.56	2.57
17	1.31	1.40	1.50	1.60	1.71	1.82	1.94	2.06	2.19	2.32	2.45	2.59	2.71	2.82	2.92	3.00	3.06	3.10	3.11
18	1.42	1.53	1.65	1.77	1.90	2.05	2.20	2.36	2.53	2.72	2.90	3.08	3.26	3.42	3.57	3.69	3.78	3.84	3.86
19	1.54	1.67	1.81	1.96	2.13	2.32	2.52	2.74	2.98	3.23	3.49	3.76	4.03	4.28	4.51	4.71	4.86	4.95	4.98
20	1.68	1.83	2.00	2.19	2.41	2.63	2.90	3.22	3.56	3.93	4.33	4.75	5.19	5.61	6.01	6.36	6.63	6.81	6.87

IV – 5

Correction to sight angle in degrees for 100° F increase in air temperature

Time of flight, seconds	Position angle in degrees																		
	0	5	10	15	20	25	30	35	40	45	50	55	60	65	70	75	80	85	90
0	.00	.00	.00	.00	.00	.00	.00	.00	.00	.00	.00	.00	.00	.00	.00	.00	.00	.00	.00
1	.00	.00	.00	.00	.00	.00	.00	.00	.00	.00	.00	.00	.00	.00	.00	.00	.00	.00	.00
2	.03	.03	.03	.03	.03	.03	.03	.03	.03	.02	.02	.02	.01	.01	.01	.01	.01	.00	.00
3	.12	.12	.11	.11	.11	.10	.10	.09	.09	.08	.07	.07	.06	.05	.04	.03	.02	.01	.00
4	.23	.23	.23	.22	.22	.21	.20	.19	.18	.16	.15	.13	.11	.10	.08	.06	.04	.02	.00
5	.34	.34	.33	.33	.32	.31	.30	.29	.27	.25	.23	.20	.18	.15	.12	.09	.06	.03	.00
6	.44	.44	.44	.43	.42	.41	.39	.38	.35	.33	.30	.27	.23	.20	.16	.12	.08	.04	.00
7	.53	.54	.53	.53	.52	.51	.49	.46	.44	.41	.37	.33	.29	.25	.20	.15	.10	.05	.00
8	.62	.63	.63	.63	.62	.61	.59	.56	.53	.49	.45	.41	.36	.30	.24	.19	.13	.06	.00
9	.72	.73	.74	.74	.72	.71	.69	.66	.62	.58	.53	.48	.42	.36	.29	.22	.15	.07	.00
10	.82	.83	.84	.85	.84	.82	.80	.76	.73	.68	.63	.57	.50	.43	.35	.26	.18	.09	.00
11	.92	.94	.96	.96	.95	.94	.91	.88	.83	.78	.73	.66	.58	.49	.41	.31	.21	.10	.00
12	1.03	1.06	1.06	1.08	1.08	1.07	1.04	1.00	.96	.90	.84	.76	.67	.58	.47	.36	.24	.12	.00
13	1.15	1.18	1.20	1.22	1.22	1.21	1.18	1.15	1.10	1.04	.96	.88	.78	.67	.55	.42	.28	.14	.00
14	1.27	1.31	1.34	1.36	1.37	1.36	1.34	1.31	1.26	1.19	1.12	1.02	.91	.78	.64	.49	.33	.17	.00
15	1.40	1.45	1.50	1.52	1.54	1.53	1.52	1.49	1.44	1.38	1.29	1.19	1.06	.92	.76	.58	.39	.20	.00
16	1.54	1.61	1.66	1.70	1.73	1.73	1.73	1.70	1.66	1.59	1.50	1.39	1.25	1.09	.90	.69	.47	.24	.00
17	1.69	1.78	1.84	1.90	1.94	1.96	1.97	1.95	1.92	1.86	1.76	1.64	1.48	1.30	1.08	.84	.57	.29	.00
18	1.86	1.96	2.05	2.12	2.18	2.23	2.26	2.26	2.23	2.18	2.10	1.97	1.80	1.59	1.33	1.04	.71	.36	.00
19	2.05	2.17	2.28	2.38	2.47	2.54	2.60	2.63	2.64	2.61	2.54	2.41	2.23	1.99	1.69	1.33	.92	.47	.00
20	2.25	2.39	2.54	2.67	2.81	2.88	2.98	3.11	3.17	3.18	3.15	3.06	2.88	2.62	2.26	1.80	1.26	.65	.00

8-11547

Correction to time of flight in seconds for a 100 knot rear wind

Position angle in degrees

Time of flight, seconds	0	5	10	15	20	25	30	35	40	45	50	55	60	65	70	75	80	85	90
0	.00	.00	.00	.00	.00	.00	.00	.00	.00	.00	.00	.00	.00	.00	.00	.00	.00	.00	.00
1	-.01	-.01	-.01	-.01	-.01	-.01	-.01	-.01	-.01	-.01	-.01	-.01	-.01	.00	.00	.00	.00	.00	.00
2	-.04	-.04	-.04	-.03	-.03	-.03	-.03	-.03	-.03	-.02	-.02	-.02	-.02	-.01	-.01	-.01	-.01	-.01	.00
3	-.11	-.11	-.11	-.10	-.10	-.10	-.09	-.08	-.08	-.07	-.07	-.06	-.05	-.04	-.03	-.02	-.02	-.01	.00
4	-.26	-.26	-.25	-.24	-.23	-.22	-.21	-.20	-.19	-.17	-.15	-.14	-.12	-.10	-.08	-.06	-.04	-.02	.00
5	-.46	-.45	-.44	-.43	-.42	-.40	-.38	-.36	-.33	-.31	-.28	-.25	-.22	-.18	-.15	-.11	-.07	-.04	.00
6	-.70	-.69	-.68	-.66	-.64	-.62	-.59	-.55	-.52	-.48	-.43	-.38	-.33	-.28	-.23	-.17	-.12	-.06	.00
7	-.98	-.97	-.96	-.94	-.91	-.88	-.84	-.79	-.74	-.68	-.62	-.55	-.48	-.41	-.33	-.25	-.17	-.08	.00
8	-1.31	-1.30	-1.28	-1.26	-1.22	-1.18	-1.13	-1.07	-1.00	-.92	-.84	-.75	-.65	-.55	-.45	-.34	-.23	-.11	.00
9	-1.68	-1.67	-1.65	-1.63	-1.58	-1.53	-1.47	-1.39	-1.30	-1.21	-1.10	-.98	-.86	-.73	-.59	-.45	-.30	-.15	.00
10	-2.10	-2.09	-2.08	-2.04	-2.00	-1.94	-1.86	-1.77	-1.66	-1.54	-1.40	-1.26	-1.10	-.93	-.76	-.57	-.38	-.20	.00
11	-2.57	-2.57	-2.55	-2.52	-2.47	-2.40	-2.31	-2.20	-2.07	-1.92	-1.76	-1.58	-1.38	-1.18	-.95	-.72	-.49	-.24	.00
12	-3.08	-3.09	-3.08	-3.05	-3.00	-2.92	-2.82	-2.70	-2.55	-2.37	-2.18	-1.96	-1.72	-1.46	-1.19	-.91	-.61	-.30	.00
13	-3.66	-3.68	-3.68	-3.65	-3.60	-3.52	-3.41	-3.27	-3.10	-2.90	-2.67	-2.40	-2.12	-1.80	-1.47	-1.12	-.76	-.38	.00
14	-4.29	-4.33	-4.34	-4.33	-4.28	-4.20	-4.09	-3.94	-3.75	-3.52	-3.25	-2.94	-2.60	-2.22	-1.81	-1.38	-.93	-.47	.00
15	-4.98	-5.05	-5.08	-5.09	-5.06	-4.99	-4.87	-4.72	-4.51	-4.25	-3.94	-3.59	-3.18	-2.74	-2.24	-1.71	-1.16	-.59	.00
16	-5.74	-5.84	-5.91	-5.95	-5.94	-5.89	-5.79	-5.63	-5.42	-5.14	-4.79	-4.39	-3.91	-3.37	-2.78	-2.13	-1.44	-.73	.00
17	-6.58	-6.73	-6.85	-6.93	-6.96	-6.94	-6.87	-6.73	-6.52	-6.23	-5.85	-5.39	-4.84	-4.20	-3.48	-2.67	-1.81	-.92	.00
18	-7.51	-7.72	-7.90	-8.04	-8.14	-8.19	-8.17	-8.07	-7.88	-7.60	-7.21	-6.70	-6.07	-5.31	-4.42	-3.42	-2.33	-1.19	.00
19	-8.53	-8.83	-9.11	-9.34	-9.53	-9.67	-9.74	-9.73	-9.62	-9.39	-9.02	-8.49	-7.77	-6.88	-5.79	-4.52	-3.10	-1.58	.00
20	-9.67	-10.08	-10.48	-10.85	-11.19	-11.48	-11.72	-11.87	-11.92	-11.82	-11.56	-11.08	-10.34	-9.31	-7.97	-6.32	-4.38	-2.24	.00

IV – 7

CONFIDENTIAL

Correction to sight angle in degrees for s▪▪ knot rear wind

Position angle in degrees

Time of flight, seconds	0	5	10	15	20	25	30	35	40	45	50	55	60	65	70	75	80	85	90
0	.00	.00	.00	.00	.00	.00	.00	.00	.00	.00	.00	.00	.00	.00	.00	.00	.00	.00	.00
1	-.03	-.36	-.70	-1.03	-1.34	-1.63	-1.95	-2.23	-2.48	-2.73	-2.96	-3.15	-3.32	-3.48	-3.63	-3.72	-3.78	-3.84	-3.84
2	-.07	-.40	-.73	-1.05	-1.38	-1.68	-1.96	-2.24	-2.52	-2.76	-2.99	-3.19	-3.37	-3.52	-3.65	-3.75	-3.82	-3.86	-3.88
3	-.13	-.41	-.70	-.98	-1.26	-1.52	-1.78	-2.03	-2.26	-2.47	-2.67	-2.84	-3.00	-3.14	-3.25	-3.34	-3.40	-3.44	-3.44
4	-.23	-.46	-.70	-.93	-1.15	-1.36	-1.57	-1.77	-1.96	-2.13	-2.29	-2.44	-2.56	-2.67	-2.77	-2.84	-2.89	-2.92	-2.93
5	-.39	-.57	-.75	-.92	-1.09	-1.26	-1.43	-1.58	-1.72	-1.85	-1.97	-2.08	-2.18	-2.25	-2.32	-2.38	-2.42	-2.44	-2.44
6	-.60	-.73	-.86	-.99	-1.11	-1.23	-1.34	-1.44	-1.54	-1.62	-1.71	-1.77	-1.84	-1.89	-1.93	-1.97	-2.00	-2.01	-2.01
7	-.85	-.94	-1.03	-1.11	-1.18	-1.25	-1.31	-1.36	-1.41	-1.45	-1.48	-1.51	-1.54	-1.56	-1.58	-1.60	-1.60	-1.60	-1.61
8	-1.17	-1.22	-1.26	-1.29	-1.31	-1.33	-1.34	-1.34	-1.33	-1.32	-1.32	-1.31	-1.29	-1.27	-1.26	-1.24	-1.24	-1.23	-1.23
9	-1.54	-1.55	-1.54	-1.53	-1.50	-1.47	-1.42	-1.37	-1.31	-1.25	-1.19	-1.12	-1.06	-1.02	-.97	-.93	-.90	-.88	-.87
10	-1.98	-1.94	-1.90	-1.84	-1.76	-1.67	-1.57	-1.46	-1.34	-1.23	-1.10	-.99	-.89	-.79	-.70	-.64	-.58	-.56	-.54
11	-2.48	-2.41	-2.32	-2.22	-2.09	-1.95	-1.79	-1.62	-1.44	-1.26	-1.08	-.90	-.74	-.59	-.47	-.36	-.29	-.24	-.22
12	-3.06	-2.95	-2.83	-2.67	-2.50	-2.30	-2.08	-1.84	-1.60	-1.35	-1.10	-.86	-.64	-.43	-.26	-.11	-.01	.06	.08
13	-3.71	-3.57	-3.41	-3.22	-2.99	-2.74	-2.46	-2.15	-1.83	-1.51	-1.19	-.87	-.57	-.31	-.08	.11	.25	.34	.37
14	-4.44	-4.29	-4.10	-3.86	-3.59	-3.28	-2.93	-2.56	-2.17	-1.76	-1.35	-.95	-.57	-.23	.07	.32	.50	.61	.65
15	-5.27	-5.10	-4.89	-4.62	-4.30	-3.94	-3.53	-3.08	-2.61	-2.11	-1.60	-1.11	-.64	-.21	.18	.49	.73	.87	.92
16	-6.19	-6.02	-5.79	-5.50	-5.15	-4.74	-4.27	-3.75	-3.18	-2.59	-1.98	-1.37	-.79	-.25	.23	.63	.93	1.11	1.17
17	-7.23	-7.07	-6.84	-6.54	-6.16	-5.71	-5.19	-4.59	-3.94	-3.24	-2.51	-1.78	-1.06	-.39	.22	.72	1.10	1.34	1.43
18	-8.40	-8.27	-8.05	-7.75	-7.37	-6.89	-6.33	-5.67	-4.94	-4.13	-3.28	-2.39	-1.52	-.68	.10	.75	1.24	1.56	1.66
19	-9.71	-9.63	-9.46	-9.19	-8.83	-8.36	-7.77	-7.08	-6.27	-5.36	-4.37	-3.31	-2.23	-1.17	-.19	.66	1.33	1.74	1.88
20	-11.19	-11.18	-11.09	-10.90	-10.60	-10.18	-9.62	-8.93	-8.10	-7.11	-5.99	-4.75	-3.43	-2.09	-.79	.37	1.30	1.90	2.10

B-11547

IV - 8

CONFIDENTIAL

PART V

Sight Angle versus Slant Range and Position Angle for
30°F Propellant Temperature

Time of Flight versus Slant Range and Position Angle for
30°F Propellant Temperature

Sight angle in degrees

Position angle in degrees

Slant range, yards	0	5	10	15	20	25	30	35	40	45	50	55	60	65	70	75	80	85	90
600	.63	.62	.62	.61	.59	.57	.54	.51	.47	.44	.41	.36	.31	.27	.22	.16	.11	.06	.00
800	.75	.75	.74	.73	.71	.68	.65	.62	.57	.54	.48	.44	.38	.32	.26	.19	.13	.07	.00
1000	.86	.85	.85	.83	.81	.78	.74	.70	.65	.61	.55	.50	.43	.36	.29	.22	.15	.08	.00
1200	.97	.96	.95	.93	.91	.88	.84	.79	.74	.69	.63	.56	.49	.41	.33	.25	.17	.09	.00
1400	1.10	1.09	1.08	1.05	1.03	.99	.95	.89	.84	.77	.70	.63	.55	.46	.37	.28	.19	.10	.00
1600	1.24	1.23	1.22	1.19	1.16	1.12	1.07	1.01	.94	.87	.79	.71	.61	.52	.42	.32	.21	.11	.00
1800	1.41	1.40	1.39	1.36	1.32	1.27	1.21	1.15	1.07	.99	.90	.80	.70	.59	.48	.36	.24	.12	.00
2000	1.62	1.61	1.59	1.55	1.51	1.45	1.39	1.31	1.22	1.13	1.02	.91	.80	.67	.54	.41	.28	.14	.00
2200	1.87	1.86	1.84	1.80	1.74	1.68	1.60	1.51	1.41	1.30	1.18	1.05	.92	.77	.63	.47	.32	.16	.00
2400	2.18	2.17	2.13	2.09	2.03	1.95	1.86	1.75	1.63	1.51	1.37	1.22	1.06	.89	.72	.55	.37	.18	.00
2600	2.54	2.52	2.49	2.43	2.36	2.27	2.16	2.04	1.90	1.75	1.59	1.41	1.23	1.04	.84	.63	.43	.21	.00
2800	2.96	2.94	2.90	2.83	2.74	2.64	2.51	2.37	2.21	2.03	1.84	1.64	1.43	1.21	.98	.74	.49	.25	.00
3000	3.44	3.42	3.37	3.29	3.19	3.07	2.92	2.75	2.57	2.37	2.15	1.91	1.66	1.40	1.14	.86	.58	.29	.00
3200	3.99	3.97	3.91	3.82	3.70	3.56	3.39	3.20	2.99	2.75	2.50	2.22	1.94	1.63	1.32	1.00	.67	.34	.00
3400	4.62	4.59	4.53	4.43	4.30	4.13	3.94	3.72	3.47	3.20	2.91	2.59	2.25	1.90	1.54	1.16	.78	.39	.00
3600	5.34	5.31	5.24	5.13	4.98	4.80	4.58	4.32	4.04	3.72	3.38	3.02	2.63	2.22	1.80	1.36	.91	.46	.00
3800	6.16	6.13	6.06	5.93	5.77	5.56	5.32	5.03	4.70	4.34	3.95	3.53	3.08	2.60	2.11	1.60	1.07	.54	.00
4000	7.10	7.07	7.00	6.87	6.69	6.46	6.19	5.86	5.50	5.09	4.64	4.15	3.62	3.07	2.49	1.89	1.27	.64	.00
4200	8.17	8.15	8.08	7.96	7.77	7.53	7.23	6.87	6.46	6.00	5.49	4.92	4.31	3.66	2.98	2.26	1.52	.77	.00
4400	9.39	9.41	9.36	9.24	9.06	8.81	8.50	8.12	7.68	7.17	6.59	5.95	5.25	4.48	3.66	2.79	1.89	.95	.00
4600	10.81	10.87	10.86	10.78	10.63	10.41	10.12	9.75	9.32	8.80	8.20	7.52	6.75						
4800	12.46	12.60	12.67	12.68	12.63	12.52													

V – 1

Time of flight in seconds

Slant range, yards	Position angle in degrees																		
	0	5	10	15	20	25	30	35	40	45	50	55	60	65	70	75	80	85	90
600	.91	.91	.91	.91	.91	.91	.91	.91	.91	.91	.91	.91	.91	.91	.91	.91	.91	.91	.91
800	1.17	1.17	1.17	1.17	1.17	1.17	1.17	1.17	1.17	1.17	1.17	1.17	1.17	1.18	1.18	1.18	1.18	1.18	1.18
1000	1.44	1.45	1.45	1.45	1.45	1.45	1.45	1.45	1.45	1.45	1.45	1.45	1.45	1.45	1.45	1.45	1.45	1.45	1.45
1200	1.75	1.75	1.75	1.75	1.75	1.75	1.75	1.75	1.75	1.75	1.75	1.75	1.75	1.75	1.75	1.75	1.75	1.75	1.75
1400	2.09	2.09	2.09	2.09	2.09	2.09	2.09	2.09	2.09	2.09	2.09	2.09	2.09	2.09	2.09	2.09	2.09	2.09	2.09
1600	2.48	2.47	2.47	2.47	2.47	2.47	2.47	2.47	2.47	2.47	2.47	2.46	2.46	2.46	2.46	2.46	2.46	2.46	2.46
1800	2.92	2.92	2.92	2.91	2.91	2.91	2.91	2.90	2.90	2.90	2.90	2.90	2.90	2.89	2.89	2.89	2.89	2.89	2.89
2000	3.44	3.44	3.43	3.43	3.42	3.42	3.41	3.41	3.40	3.40	3.40	3.39	3.39	3.39	3.39	3.39	3.38	3.38	3.38
2200	4.02	4.02	4.01	4.00	3.99	3.99	3.98	3.98	3.97	3.97	3.96	3.96	3.95	3.95	3.95	3.95	3.94	3.94	3.94
2400	4.65	4.64	4.64	4.63	4.62	4.61	4.60	4.60	4.59	4.59	4.58	4.58	4.57	4.57	4.56	4.56	4.56	4.56	4.56
2600	5.33	5.32	5.31	5.30	5.30	5.29	5.28	5.27	5.27	5.26	5.25	5.25	5.24	5.24	5.24	5.23	5.23	5.23	5.23
2800	6.07	6.06	6.05	6.04	6.03	6.02	6.01	6.00	6.00	5.99	5.98	5.98	5.97	5.97	5.97	5.96	5.96	5.96	5.96
3000	6.86	6.85	6.84	6.83	6.82	6.82	6.81	6.80	6.79	6.79	6.78	6.78	6.77	6.77	6.77	6.77	6.76	6.76	6.76
3200	7.72	7.71	7.70	7.70	7.69	7.68	7.68	7.67	7.67	7.66	7.66	7.65	7.65	7.65	7.65	7.65	7.65	7.65	7.64
3400	8.65	8.64	8.64	8.63	8.63	8.63	8.63	8.62	8.62	8.62	8.62	8.62	8.62	8.62	8.62	8.62	8.62	8.62	8.63
3600	9.65	9.65	9.65	9.66	9.66	9.66	9.67	9.67	9.68	9.69	9.69	9.70	9.71	9.71	9.72	9.72	9.72	9.72	9.73
3800	10.74	10.75	10.76	10.78	10.79	10.81	10.82	10.84	10.86	10.88	10.90	10.91	10.93	10.95	10.96	10.97	10.98	10.98	10.98
4000	11.93	11.95	11.98	12.01	12.04	12.08	12.12	12.15	12.19	12.23	12.27	12.31	12.34	12.37	12.40	12.42	12.44	12.45	12.45
4200	13.22	13.27	13.32	13.38	13.44	13.51	13.58	13.65	13.73	13.80	13.88	13.95	14.02	14.09	14.14	14.19	14.22	14.24	14.25
4400	14.63	14.72	14.81	14.91	15.02	15.14	15.27	15.41	15.55	15.70	15.85	16.00	16.15	16.29	16.41	16.51	16.59	16.64	16.66
4600	16.19	16.33	16.48	16.65	16.85	17.06	17.30	17.56	17.85	18.17	18.52	18.90	19.32						
4800	17.92	18.14	18.40	18.69	19.04	19.44													

V – 2

B–11547

PART VI

Sight Angle versus Slant Range and Position Angle for
110°F Propellant Temperature

Time of Flight versus Slant Range and Position Angle for
110°F Propellant Temperature

Sight angle in degrees

Slant range, yards	Position angle in degrees																		
	0	5	10	15	20	25	30	35	40	45	50	55	60	65	70	75	80	85	90
600	.47	.46	.46	.45	.44	.42	.40	.38	.35	.33	.30	.26	.24	.20	.16	.13	.09	.04	.00
800	.59	.58	.58	.57	.55	.53	.51	.48	.45	.42	.38	.34	.29	.25	.20	.15	.10	.05	.00
1000	.68	.67	.67	.65	.64	.61	.59	.56	.52	.48	.44	.39	.34	.29	.23	.18	.12	.06	.00
1200	.77	.77	.76	.75	.73	.70	.67	.64	.60	.55	.50	.44	.39	.33	.27	.20	.13	.07	.00
1400	.88	.88	.87	.85	.83	.80	.76	.72	.67	.62	.57	.50	.44	.37	.30	.23	.15	.08	.00
1600	1.00	1.00	.99	.97	.94	.91	.87	.82	.77	.71	.64	.57	.50	.42	.34	.26	.17	.09	.00
1800	1.15	1.14	1.13	1.10	1.07	1.03	.99	.93	.87	.80	.73	.65	.57	.48	.39	.29	.20	.10	.00
2000	1.32	1.31	1.29	1.26	1.23	1.18	1.13	1.06	.99	.92	.83	.74	.65	.55	.44	.33	.22	.11	.00
2200	1.52	1.51	1.49	1.46	1.42	1.36	1.30	1.23	1.15	1.05	.96	.85	.74	.63	.51	.38	.26	.13	.00
2400	1.78	1.76	1.74	1.70	1.65	1.58	1.51	1.42	1.33	1.22	1.11	.99	.86	.72	.59	.44	.30	.15	.00
2600	2.08	2.06	2.03	1.98	1.92	1.85	1.76	1.66	1.54	1.42	1.29	1.15	1.00	.84	.68	.51	.34	.17	.00
2800	2.44	2.42	2.38	2.32	2.25	2.16	2.05	1.94	1.80	1.66	1.50	1.34	1.16	.98	.79	.60	.40	.20	.00
3000	2.85	2.83	2.78	2.71	2.63	2.52	2.40	2.26	2.11	1.94	1.76	1.56	1.36	1.15	.92	.70	.47	.24	.00
3200	3.33	3.30	3.25	3.17	3.07	2.94	2.80	2.64	2.46	2.26	2.05	1.82	1.58	1.34	1.08	.82	.55	.27	.00
3400	3.88	3.84	3.78	3.69	3.57	3.43	3.26	3.07	2.86	2.63	2.39	2.12	1.85	1.56	1.26	.95	.64	.32	.00
3600	4.50	4.47	4.39	4.29	4.16	3.99	3.80	3.58	3.34	3.07	2.78	2.48	2.16	1.82	1.47	1.11	.75	.37	.00
3800	5.22	5.18	5.10	4.98	4.83	4.64	4.42	4.17	3.89	3.58	3.25	2.90	2.52	2.13	1.72	1.30	.87	.44	.00
4000	6.03	5.99	5.90	5.78	5.61	5.39	5.15	4.86	4.54	4.19	3.80	3.39	2.95	2.50	2.02	1.53	1.03	.52	.00
4200	6.96	6.92	6.83	6.70	6.51	6.28	6.00	5.68	5.31	4.91	4.47	3.99	3.48	2.95	2.39	1.81	1.21	.61	.00
4400	8.02	8.00	7.91	7.77	7.57	7.32	7.02	6.66	6.25	5.79	5.29	4.74	4.15	3.52	2.86	2.17	1.46	.73	.00
4600	9.24	9.24	9.17	9.04	8.84	8.58	8.26	7.88	7.43	6.92	6.36	5.73	5.04	4.30	3.50	2.67	1.80	.91	.00
4800	10.65	10.68	10.65	10.55	10.39	10.15	9.84	9.47	9.02	8.49	7.89	7.21	6.45						
5000	12.29	12.40	12.44	12.42	12.34														

Time of flight in seconds

Slant range, yards	\-	\-	\-	\-	\-	\-	\-	\-	Position angle in degrees										
	0	5	10	15	20	25	30	35	40	45	50	55	60	65	70	75	80	85	90
600	.81	.81	.81	.81	.81	.81	.81	.81	.81	.81	.81	.81	.81	.81	.82	.82	.82	.82	.82
800	1.07	1.07	1.07	1.07	1.07	1.07	1.07	1.07	1.07	1.07	1.07	1.07	1.07	1.07	1.07	1.07	1.07	1.07	1.07
1000	1.32	1.32	1.33	1.33	1.33	1.33	1.33	1.33	1.33	1.33	1.33	1.33	1.33	1.33	1.33	1.33	1.33	1.33	1.33
1200	1.60	1.60	1.60	1.60	1.60	1.60	1.60	1.60	1.60	1.60	1.60	1.60	1.60	1.60	1.60	1.60	1.60	1.60	1.60
1400	1.91	1.91	1.91	1.91	1.91	1.91	1.91	1.91	1.91	1.91	1.91	1.91	1.91	1.91	1.91	1.91	1.91	1.91	1.91
1600	2.26	2.26	2.26	2.26	2.26	2.25	2.25	2.25	2.25	2.25	2.25	2.25	2.25	2.25	2.25	2.25	2.25	2.25	2.25
1800	2.66	2.66	2.65	2.65	2.65	2.64	2.64	2.64	2.64	2.64	2.63	2.63	2.63	2.63	2.63	2.63	2.63	2.63	2.63
2000	3.12	3.11	3.11	3.10	3.10	3.09	3.09	3.08	3.08	3.08	3.07	3.07	3.07	3.06	3.06	3.06	3.06	3.06	3.06
2200	3.65	3.64	3.63	3.63	3.62	3.61	3.60	3.59	3.59	3.58	3.58	3.57	3.57	3.56	3.56	3.56	3.56	3.56	3.55
2400	4.24	4.23	4.22	4.21	4.20	4.19	4.18	4.17	4.16	4.15	4.14	4.14	4.13	4.13	4.12	4.12	4.12	4.12	4.12
2600	4.88	4.87	4.86	4.84	4.83	4.82	4.81	4.79	4.78	4.77	4.77	4.76	4.75	4.75	4.74	4.74	4.73	4.73	4.73
2800	5.57	5.56	5.54	5.53	5.51	5.50	5.49	5.47	5.46	5.45	5.44	5.43	5.42	5.42	5.41	5.41	5.40	5.40	5.40
3000	6.32	6.30	6.28	6.27	6.25	6.24	6.22	6.21	6.20	6.18	6.17	6.16	6.16	6.15	6.14	6.14	6.14	6.13	6.13
3200	7.12	7.10	7.09	7.07	7.05	7.04	7.02	7.01	7.00	6.99	6.97	6.96	6.96	6.95	6.94	6.94	6.94	6.93	6.93
3400	7.99	7.97	7.96	7.94	7.93	7.91	7.90	7.88	7.87	7.86	7.85	7.84	7.83	7.83	7.82	7.82	7.81	7.81	7.81
3600	8.93	8.92	8.90	8.89	8.87	8.86	8.85	8.84	8.83	8.82	8.81	8.81	8.80	8.80	8.79	8.79	8.79	8.79	8.79
3800	9.95	9.94	9.93	9.92	9.91	9.90	9.90	9.89	9.89	9.89	9.88	9.88	9.88	9.88	9.88	9.88	9.88	9.88	9.88
4000	11.06	11.05	11.05	11.05	11.05	11.05	11.06	11.06	11.07	11.08	11.08	11.09	11.10	11.11	11.11	11.12	11.12	11.12	11.12
4200	12.26	12.27	12.28	12.29	12.31	12.33	12.35	12.38	12.40	12.43	12.45	12.48	12.50	12.52	12.54	12.56	12.57	12.57	12.58
4400	13.56	13.59	13.63	13.67	13.71	13.76	13.82	13.87	13.93	13.99	14.05	14.11	14.16	14.21	14.26	14.29	14.32	14.33	14.34
4600	14.99	15.06	15.13	15.21	15.30	15.40	15.51	15.62	15.74	15.87	16.00	16.12	16.25	16.36	16.47	16.55	16.62	16.66	16.68
4800	16.57	16.68	16.81	16.96	17.13	17.32	17.53	17.76	18.02	18.30	18.60	18.94	19.29						
5000	18.31	18.51	18.74	19.01	19.32														

APPENDIX H

DISTRIBUTION

No. of Copies

Bureau of Ordnance:

Ad3	1
Ad6	5
Re2d	1
Re3	1
Re3d	2
Re4e	1
Ree	1

Armed Services Technical Information Agency
Document Service Center
Knott Building
Dayton 2, Ohio   5

Commanding General
Aberdeen Proving Ground
Aberdeen, Maryland
Attn: Technical Information Section
        Development and Proof Services   1
Attn: Ballistic Research Laboratories   1

Commander, Operational Development Force
U. S. Atlantic Fleet, U. S. Naval Base
Norfolk 11, Virginia   1

Commander
U. S. Naval Ordnance Test Station
Inyokern, China Lake, California
Attn: Code 503   2

Commander
Naval Ordnance Laboratory
White Oak, Silver Spring, Maryland
Attn: Aerodynamics Dept.   1